



INSTITUTO POLITÉCNICO NACIONAL



**CENTRO DE INVESTIGACIÓN EN CIENCIA APLICADA Y
TECNOLOGÍA AVANZADA - UNIDAD QUERETARO**

POSTGRADUATE IN ADVANCED TECHNOLOGY

**COLD PLASMA TREATMENT EFFECT ON STRUCTURAL AND
FUNCTIONAL PROPERTIES OF FILMS MADE WITH HIGH
AMYLOSE STARCHES**

**THESIS TO OBTAIN THE DEGREE OF
DOCTOR IN ADVANCED TECHNOLOGY**

**PRESENTED BY:
M. ISRAEL SIFUENTES NIEVES**

DIRECTED BY:

Dr. MA. GUADALUPE MÉNDEZ MONTEALVO Dr. GONZALO VELAZQUEZ DE LA CRUZ

November 2019



**INSTITUTO POLITÉCNICO NACIONAL
SECRETARÍA DE INVESTIGACIÓN Y POSGRADO**

SIP-13
REP 2017

**ACTA DE REGISTRO DE TEMA DE TESIS
Y DESIGNACIÓN DE DIRECTOR DE TESIS**

Ciudad de México, a 27 de noviembre del 2019

El Colegio de Profesores de Posgrado de **CICATA Unidad Querétaro** en su Sesión ordinaria No. 160516 celebrada el día 6 del mes mayo de 2017, conoció la solicitud presentada por el alumno:

Apellido Paterno:	Sifuentes	Apellido Materno:	Nieves	Nombre (s):	Israel
-------------------	-----------	-------------------	--------	-------------	--------

Número de registro:

A	1	6	0	9	6	9
---	---	---	---	---	---	---

del Programa Académico de Posgrado:

Doctorado en Tecnología Avanzada

Referente al registro de su tema de tesis; acordando lo siguiente:

1.- Se designa al aspirante el tema de tesis titulado:

Cold plasma treatment effect on structural and functional properties of films made with high amylose starches

Objetivo general del trabajo de tesis:

Estudiar los cambios provocados por el plasma frío sobre la matriz polimérica y la superficie de películas elaboradas con almidones altos en amilosa.

2.- Se designa como Directores de Tesis a los profesores:

Director:

Dra. Ma. Guadalupe del Carmen Méndez Montealvo
--

 2° Director:

Dr. Gonzalo Velázquez de la Cruz

No aplica:

3.- El Trabajo de investigación base para el desarrollo de la tesis será elaborado por el alumno en:

CICATA-IPN Querétaro

que cuenta con los recursos e infraestructura necesarios.

4.- El interesado deberá asistir a los seminarios desarrollados en el área de adscripción del trabajo desde la fecha en que se suscribe la presente, hasta la aprobación de la versión completa de la tesis por parte de la Comisión Revisora correspondiente.

Director de Tesis

Dr. Ma. Guadalupe del Carmen Méndez Montealvo

2° Director de Tesis

Dr. Gonzalo Velázquez de la Cruz

Aspirante

Israel Sifuentes Nieves

Presidente del Colegio

Dr. Alejandro Alfredo Lozano Guzmán

DIRECCIÓN



INSTITUTO POLITÉCNICO NACIONAL
SECRETARÍA DE INVESTIGACIÓN Y POSGRADO

SIP-14
REP 2017

ACTA DE REVISIÓN DE TESIS

En la Ciudad de siendo las horas del día del mes de del se reunieron los miembros de la Comisión Revisora de la Tesis, designada por el Colegio de Profesores de Posgrado de: para examinar la tesis titulada: por el (la) alumno (a):

Apellido Paterno:	Sifuentes	Apellido Materno:	Nieves	Nombre (s):	Israel
-------------------	-----------	-------------------	--------	-------------	--------

Número de registro:

Aspirante del Programa Académico de Posgrado:

Después de la lectura y revisión individual, así como el análisis e intercambio de opiniones, los miembros de la Comisión manifestaron **APROBAR** **NO APROBAR** la tesis, en virtud de los motivos siguientes:

El trabajo desarrollado, así como la comprensión y discusión de la información obtenida se considera que se cumple con los requisitos para proceder a sustentar el examen de grado al cual aspira.

Comisión Revisora de Tesis

Director de Tesis
Dra. Ma. Guadalupe del Carmen Méndez Montealvo
COLEGIADO-13993-EH-18

Dr. Martín de Jesús Nieto Pérez
COLEGIADO-11853-ED-16

Dr. Jorge Adalberto Huerta Ruelas
COLEGIADO-13448-EF-186

2° Director de Tesis
Dr. Gonzalo Velázquez e la Cruz
COLEGIADO-14571-ED-19

Dra. Ma. Cristina Arina Pérez Pérez
EXTERNO

Presidente del Colegio de Profesores
INSTITUTO POLITÉCNICO NACIONAL
SECRETARÍA DE INVESTIGACIÓN Y POSGRADO
CIENCIA APLICADA Y TECNOLOGÍA AVANZADA
UNIDAD QUERETARO
DIRECCIÓN



INSTITUTO POLITÉCNICO NACIONAL
SECRETARÍA DE INVESTIGACIÓN Y POSGRADO

CARTA CESION DE DERECHOS

En la Ciudad de México, el día 27 del mes de noviembre del año 2019, el que suscribe **Israel Sifuentes Nieves** alumno (a) del Programa de **Doctorado en Tecnología Avanzada** con número de registro **A160969**, adscrito al **Centro de Investigación en Ciencia Avanzada y Tecnología Aplicada Unidad Queretaro**, manifiesta que es autor intelectual del presente trabajo de Tesis bajo la dirección de **Dra. Ma. Guadalupe del Carmen Méndez Montealvo y Dr. Gonzalo Velázquez de la Cruz** y cede los derechos del trabajo intitulado **Cold plasma treatment effect on structural and functional properties of films made with high amylose starches**, al Instituto Politécnico Nacional para su difusión, con fines académicos y de investigación.

Los usuarios de la información no deben reproducir el contenido textual, gráficas o datos del trabajo sin el permiso expreso del autor y/o director del trabajo. Este puede ser obtenido escribiendo a las siguientes direcciones: cmendez@ipn.mx, gvelazquezd@ipn.mx y sifuentes_01@hotmail.com. Si el permiso se otorga, el usuario deberá dar el agradecimiento correspondiente y citar la fuente del mismo.

Israel Sifuentes Nieves

DEDICATORY

*I would like to dedicate this goal to **GOD** for giving me the opportunity to do my PhD and to share this moment with my beautiful wife **Pam** and our wonderful children **Ian** and **Sebastian**, without their support, I may never have completed this thesis. This achievement is possible thanks to the invaluable support of all my lovely **family**; **mom** and **dad**, without you I would not have been where I am today and what I am today.*

“Make each day your masterpiece”

John Wooden

ACKNOWLEDGMENTS

I would like to begin by thanking my thesis advisers: Dra. Lupita and Dr. Gonzalo without their consistent guidance, tutelage, support, unparalleled knowledge, and encouragement, this thesis would never have existed.

Also, I would like to thank my thesis committee: Dra. Cristina, Dr. Martin and Dr. Jorge for their valuable comments and observations to enrich this thesis project.

A special acknowledgement to my friends (Adrian, Gerardo, Julio, Israel, Miguel, Cecilia, Rodrigo and Baruc) for amusing my time in CICATA and for giving me someone to moan at when work wasn't progressing according to plan.

Finally, I want to express my gratitude to the CONACTY for the financial support in the form of a scholarship.

INDEX

INTRODUCTION	20
1. Chapter 1. Literature review.....	21
1.1 Biodegradable films	21
1.2 Starch films	21
1.2.1 Starch	21
1.2.1.1 Chemical composition, structure and organization.....	21
1.2.1.2 Gelatinization and gelation	25
1.2.2 Films.....	26
1.3 Plasticizers.....	27
1.4 Modification of starch	27
1.4.1 Chemical and physical modification	27
1.5 Plasma.....	28
1.5.1 Plasma treatment on starch granules and starch films	29
1.6 Analysis techniques in films	31
1.6.1 Morphology	31
1.6.1.1 Scanning electronic microscopy (SEM)	31
1.6.1.2 Atomic force microscopy (AFM).....	31
1.6.2 Structural	32
1.6.2.1 Fourier transform infrared (FTIR)	32
1.6.2.2 X-ray diffraction (XRD).....	33
1.6.2.3 X-ray photoelectron spectroscopy (XPS)	34
1.6.3 Thermal properties.....	34
1.6.3.1 Differential scanning calorimetry (DSC)	34
1.6.3.2 Thermogravimetric analysis (TGA)	35
1.6.4 Physical properties	36
1.6.4.1 Water vapor permeability (WVP)	36
1.6.4.2 Water sorption isotherms (WSI).....	36
1.6.4.3 Water contact angle (WCA)	37
1.6.5 Mechanical properties.....	38
2. Chapter 2. Research approach	39
2.1 Justification	39

2.2 Objectives	40
2.2.1 General.....	40
2.2.2 Specifics	40
2.3 Hypothesis	40
2.4 Experimental design	41
Chapter 3. Materials and methods	43
3.1. Materials	43
3.2 Modification of starch and films	43
3.2.1 HMDSO plasma treatment on starches.....	43
3.2.2 Preparation of starch-based films	43
3.2.3 HMDSO plasma treatment on native films	44
3.3 Analysis techniques	44
3.3.1 Film thickness	44
3.3.2 Morphology	44
3.3.2.1 Scanning electronic microscopy	44
3.3.2.2 Atomic force microscopy.....	45
3.3.3 Structural properties	45
3.3.3.1 FTIR spectroscopy	45
3.3.3.2 X ray diffraction.....	46
3.3.3.3 X-ray photoelectron spectroscopy	46
3.3.3.4 Differential scanning calorimetry.....	46
3.3.3.5 TGA analysis	47
3.3.4 Physical properties	47
3.3.4.1 Wettability.....	47
3.3.4.2 Water vapor permeability	47
3.3.4.3 Water vapor adsorption isotherms	48
3.3.5 Mechanical properties.....	48
3.3.6 Statistical analysis	49
Chapter 4. Hexamethyldisiloxane cold plasma treatment and amylose content determine the structural, barrier and mechanical properties of starch-based films.	51
4.1 Introduction	52
4.2 Results and discussion	53

4.2.1 Morphology	53
4.2.2 FTIR spectroscopy.....	56
4.2.3 Wettability	60
4.2.4 Water vapor adsorption isotherms (WVI)	62
4.3.5 Mechanical properties.....	65
4.4 Conclusions	68
Chapter 5. Influence of gelatinization process and HMDSO plasma treatment on the chemical changes and water vapor permeability of corn starch film .	69
5.1 Introduction	70
5.2 Results and discussion	71
5.2.1 Topography	71
5.2.2 X-ray photoelectron spectroscopy.....	74
5.2.3 X-ray diffraction.....	79
5.2.4 Differential scanning calorimetry	81
5.2.5. Water vapor permeability	83
5.3. Conclusions	85
Chapter 6. HMDSO plasma treatment as alternative to modify structural properties of granular starch	86
6.1. Introduction	87
6.2 Results and discussion	88
6.2.1 Thermal behavior (TGA)	88
6.2.2 Crystalline structure	89
6.2.3 Double helices and order degree	92
6.2.4 XPS analysis	96
6.2.5 Thermal properties (DSC).....	99
6.2.6 Final remarks.....	100
Chapter 7. Films made from plasma-modified corn starch: Chemical, mechanical and barrier properties.....	103
7.1 Introduction	104
7.2 Results and discussion	105
7.2.1 X-ray photoelectron spectroscopy.....	105
7.2.2 Thermogravimetric analysis	109
7.2.3 Mechanical properties.....	110

7.2.4 Water vapor permeability	112
7.3 Conclusions	114
8. General conclusions	115
9. References.....	117
Appendix	125

LIST OF TABLES

Table 1.	Granule sizes of starch from different botanical source (Singh et al., 2003 & Hoover, 2001).	22
Table 2.	Variation of the 1047/1022 ratio of starch films from normal and high amylose starch before and after HMDSO plasma treatment.	60
Table 3.	C1s peaks of starch films observed before and after plasma treatment.	78
Table 4.	Deconvolution of Si 2p peak for HMDSO plasma-treated films.	78
Table 5.	Thermal properties of starch films from normal and high amylose starches before and after HMDSO plasma treatment.....	83
Table 6.	Intensity 1047/1022 and 995/1022 ratio of native and modified corn starches with different amylose content.	94
Table 7.	O/C atomic ratio and C1s peaks of native and modified maize starches with different amylose content.	97
Table 8.	Thermal transitions of native and modified corn starches with a different amylose content.	100
Table 9.	C1s peaks of films made from native and plasma-modified starch containing 30, 50, and 70 % amylose.	107

LIST OF FIGURES

Figure 1.	Starch granules morphology from different sources a) wheat, b) rye, c) barley, d) oats, e) corn, f) rice, g) potato and h) cassava. (Singh et al., 2003 & Hoover, 2001).	22
Figure 2.	Amylose a) and amylopectin b) molecule (Perez et al., 2009)	23
Figure 3.	Lamellar structure of starch granule. a) Microcrystalline lamellae separated by amorphous growth rings. b) Crystalline and amorphous region. c) Double helical structure and branching points given rise to crystalline lamellae and amorphous region, respectively (Donald et al., 1997).	24
Figure 4.	Amylopectin structure showing B chains (Hizokuri., 1986).....	24
Figure 5.	A- and B- type polymorphic forms of starch. (Tester et al., 2004)	25
Figure 6.	Gelatinization process: a) native granules, b) swelling granules and c) amylose leaching and partial granule disruption. Adapted from Goesaert et al. (2005).	25
Figure 7.	Chemical formula of glycerol	27
Figure 8.	Proposed mechanism of starch modification after plasma treatment: CL, crosslinking and DP, depolymerization (Wongsagonsup et al., 2014)..	29
Figure 9.	SEM diagram and image obtained.....	31
Figure 10.	Representation of atomic interaction records between the tip and the surface; and example of AFM image obtained.....	32
Figure 11.	Example of IR spectrum	33
Figure 12.	Typical X-ray diffractogram of semi crystalline material	33
Figure 13.	Principle of XPS analysis.....	34
Figure 14.	Typical DSC thermogram of films	35
Figure 15.	Typical TGA curves: 1) No change, 2) Desorption/drying, 3) Single stage decomposition, 4) and 5) Multistage decomposition, 6) and 7) Atmospheric reaction.....	35
Figure 16.	Representation of water permeation through the film	36
Figure 17.	Typical sigmoid sorption isotherm.....	37
Figure 18.	Contact angles formed on solid surfaces	38
Figure 19.	Example of stress-strain curve of films.	38
Figure 20.	Experimental diagram.....	42
Figure 21.	Appearance of the obtained films (a) and a sample of the film fixed with the grips during the tension test (b).	54
Figure 22.	SEM images of films from starch (90° angle), F30: film- 30% amylose a), F50: film- 50% amylose b) and F70: film- 70% amylose c). SEM images of films from starch before and after treatment (45° angle), F30 d), F50 e), F70 f), TF30: treated film- 30% amylose g), TF50: treated film- 50% amylose h) and TF70: treated film- 70% amylose i). All micrographs correspond to 1500x.	55

Figure 23.	FTIR spectra of starch films from normal and high amylose starches before and after HMDSO plasma treatment. F30: film- 30% amylose, F50: film- 50% amylose, F70: film- 70% amylose, TF30: treated film- 30% amylose, TF50: treated film- 50% amylose and TF70: treated film- 70% amylose.....	58
Figure 24.	Deconvoluted FTIR peaks of films made of starch with different amylose content before and after HMDSO plasma treatment. F30: film- 30% amylose, F50: film- 50% amylose, F70: film- 70% amylose, TF30: treated film- 30% amylose, TF50: treated film- 50% amylose and TF70: treated film- 70% amylose.	59
Figure 25.	Evolution of water contact angle of films from normal and high amylose starch before and after plasma treatment. F30: film- 30% amylose, F50: film- 50% amylose, F70: film- 70% amylose, TF30: treated film- 30% amylose, TF50: treated film- 50% amylose and TF70: treated film- 70% amylose.....	61
Figure 26.	Adsorption isotherms of starch-based films from 30% a), 50% b) and 70% amylose c) before and after plasma treatment. Symbols are experimental data and the solid lines indicate the fitting using the GAB model. F30: film- 30% amylose, F50: film- 50% amylose, F70: film- 70% amylose, TF30: treated film- 30% amylose, TF50: treated film- 50% amylose and TF70: treated film- 70% amylose.	64
Figure 27.	Xm values estimated from GAB model fitted to adsorption isotherms of starch-based films before and after plasma treatment. Error bars with different letters indicate significant differences ($P \leq 0.05$).	65
Figure 28.	Mechanical properties of 30%, 50%, and 70% amylose starch-based films a) tensile strength, b) Young's modulus, and c) elongation at break. Error bars with different letters indicate significant differences ($P \leq 0.05$).	67
Figure 29.	AFM images of starch films before and after treatment F30: film- 30% amylose a), F50: film- 50% amylose b), F70: film- 70% amylose c), TF30: treated film- 30% amylose d), TF50: treated film- 50% amylose e) and TF70: treated film- 70% amylose f).....	73
Figure 30.	Roughness of starch films made from normal and high amylose starches before and after HMDSO plasma treatment. Error bars with different letters indicate significant differences ($P \leq 0.05$). F30: film- 30% amylose, F50: film- 50% amylose, F70: film- 70% amylose.	74
Figure 31.	XPS spectra of starch films made from normal and high amylose starches before and after HMDSO plasma treatment. F30: film- 30% amylose, F50: film- 50% amylose, F70: film- 70% amylose, TF30: treated film- 30% amylose, TF50: treated film- 50% amylose and TF70: treated film- 70% amylose.....	76
Figure 32.	Example of deconvoluted XPS spectrum a) C1s and b) Si 2p	77
Figure 33.	XRD spectra of starch films made from normal and high amylose starches before and after HMDSO plasma treatment. F30: film- 30% amylose,	

	F50: film- 50% amylose, F70: film- 70% amylose, TF30: treated film- 30% amylose, TF50: treated film- 50% amylose and TF70: treated film- 70% amylose.....	80
Figure 34.	Relative crystallinity of starch films from normal and high amylose starches before and after HMDSO plasma treatment. F30: film- 30% amylose, F50: film- 50% amylose, F70: film- 70% amylose.	80
Figure 35.	DSC thermograms of starch films from normal and high amylose starches before and after HMDSO plasma treatment. F30: film- 30% amylose, F50: film- 50% amylose, F70: film- 70% amylose, TF30: treated film- 30% amylose, TF50: treated film- 50% amylose and TF70: treated film- 70% amylose.....	82
Figure 36.	Water vapor permeability of starch films from normal and high amylose starches before and after HMDSO plasma treatment. Error bars with different letters indicate significant differences ($P \leq 0.05$). F30: film- 30% amylose, F50: film- 50% amylose, F70: film- 70% amylose.	84
Figure 37.	Drying curves from TGA analysis of native and modified corn starches with different amylose content. S30: starch- 30% amylose, S50: starch- 50% amylose, S70: starch- 70% amylose, TS30: treated starch- 30% amylose, TS50: treated starch- 50% amylose and TS70: treated starch- 70% amylose.....	89
Figure 38.	X ray diffraction spectra of native and modified corn starches with different amylose content. RC= Relative crystallinity. S30: starch- 30% amylose, S50: starch- 50% amylose, S70: starch- 70% amylose, TS30: treated starch- 30% amylose, TS50: treated starch- 50% amylose and TS70: treated starch- 70% amylose.	91
Figure 39.	FTIR spectra of native and modified corn starches with different amylose content. S30: starch- 30% amylose, S50: starch- 50% amylose, S70: starch- 70% amylose, TS30: treated starch- 30% amylose, TS50: treated starch- 50% amylose and TS70: treated starch- 70% amylose.....	93
Figure 40.	Deconvoluted peaks at 1047, 1022 and 995 cm^{-1} of native and modified corn starches with different amylose content. S30: starch- 30% amylose, S50: starch- 50% amylose, S70: starch- 70% amylose, TS30: treated starch- 30% amylose, TS50: treated starch- 50% amylose and TS70: treated starch- 70% amylose	95
Figure 41.	Deconvoluted C1s peaks of native and modified corn starches with different amylose content. S30: starch- 30% amylose, S50: starch- 50% amylose, S70: starch- 70% amylose, TS30: treated starch- 30% amylose, TS50: treated starch- 50% amylose and TS70: treated starch- 70% amylose.....	98
Figure 42.	Possible mechanism of starch modification after HMDSO plasma treatment.	102
Figure 43.	Deconvoluted C1s peaks of films made from native and plasma-modified starch containing 30, 50, and 70 % amylose. SF30: starch film- 30%	

amylose, SF50: starch film- 50% amylose, SF70: starch film- 70% amylose, MSF30: modified starch film- 30% amylose, MSF50: modified starch film- 50% amylose and MSF70: modified starch film- 70% amylose..... 108

Figure 44. TGA thermograms and % weight loss (WL) of films made from native and plasma-modified starch containing 30, 50, and 70 % amylose. *WL= % W.L at 250 °C – % WL at 100°C.SF30: starch film- 30% amylose, SF50: starch film- 50% amylose, SF70: starch film- 70% amylose, MSF30: modified starch film- 30% amylose, MSF50: modified starch film- 50% amylose and MSF70: modified starch film- 70% amylose..... 109

Figure 45. Mechanical properties of films made from native and plasma-modified starch containing 30, 50, and 70% amylose; (a) tensile strength, (b) Young's modulus, and (c) elongation at break. Error bars with different letters indicate significant differences ($P \leq 0.05$)..... 111

Figure 46. Water vapor permeability of films made from native and plasma-modified starch containing 30, 50, and 70% amylose. Error bars with different letters indicate significant differences ($P \leq 0.05$).SF30: starch film- 30% amylose, SF50: starch film- 50% amylose and SF70: starch film- 70% amylose..... 113

ABSTRACT

In this study, the effect of amylose content, gelatinization extent and hexamethyldisiloxane (HMDSO) cold plasma treatment on the functional properties of starch films from normal (30%) and high amylose (50 and 70%) were investigated. Morphological, structural, chemical, mechanical and barrier properties of the films were evaluated. The amount of remnant starch granules (RSG) in the films depended on the extent of gelatinization. The loss of RSG resulted in films with poor barrier properties and high hydrophilicity. However, the HMDSO plasma treatment resulted in hydrophobic films as the treatment promoted the substitution within the starch molecule, incorporating hydrophobic blocking groups (C-Si), which improved the barrier properties and favoring the helix ordering. Furthermore, the crosslinking and ordering of the structures reinforced the surface of the films, improving the mechanical properties.

Moreover, starch modification is another important factor to consider during the elaboration of starch-films; thus, the effect of HMDSO plasma treatment on the structural properties of granular corn starches with different proportion of amylose was also investigated. Thermal, structural and chemical properties were modified after plasma treatment, which promoted the partial evaporation of water molecules changing the organization level of the double helices in the crystalline lamellae. Moreover, XRD results suggested a decrease of the long-range crystallinity and changes in amylose chains after treatments. The crosslinking of modified amylose chains measured by XPS analysis resulted in important modifications in the gelatinization parameters as well as in its heterogeneous crystalline structure. Furthermore, the plasma-modified starches were gelatinized to obtain films (MSF), and its chemical, mechanical and barrier properties were assessed. XPS analysis suggested an oxidation process in all MSF as the atomic proportion of hydroxyl, carbonyl and carboxyl groups was changed. Also, the increase of C-C proportions suggested a crosslinking in the films with higher amylose content. TGA analysis indicated low interaction between starch and the plasticizer as the tensile strength and elongation at break diminished in the MSF50 and MSF70. However, the

crosslinking of MSF70 showed characteristics of rigid films. Cold plasma acted as a precursor of oxidized and crosslinked starch films reducing the WVP.

This research describes the main modification-mechanisms (crosslinking, etching, depolymerization and substitution) of cold plasma on starch molecules as a function of its amylose content, which modified and improved the structural and functional properties of starch granules and films. The results suggest that the HMDSO plasma treatment is a suitable method to produce modified starches and modified films.

RESUMEN

En este estudio se describe el efecto del tratamiento con plasma frío de hexametildisiloxano (HMDSO) sobre las propiedades funcionales de películas de almidón considerando el contenido de amilosa y el grado de gelatinización. El efecto del tratamiento se evaluó a través de las propiedades morfológicas, estructurales, químicas, mecánicas y de barrera de las películas. Se observó que la proporción de gránulos remanentes de almidón (RSG) en las películas depende del grado de gelatinización del almidón, y que la disminución de los RSG generaba películas con características hidrofílicas y propiedades de barrera limitadas. Sin embargo, el tratamiento con plasma HMDSO promovió la incorporación de grupos hidrofóbicos (C-Si) en la molécula de almidón, lo que mejoró las propiedades de barrera y favoreció el ordenamiento de las dobles hélices del almidón dando lugar a películas con características hidrofóbicas. Además, se mejoraron las propiedades mecánicas de las películas debido al entrecruzamiento y ordenamiento de las estructuras, que reforzaron la superficie de las películas después del tratamiento.

Durante la elaboración de películas de almidón, es también importante considerar las modificaciones del almidón; por ello, se investigó el efecto del tratamiento con plasma HMDSO sobre las propiedades estructurales de almidones con diferente proporción de amilosa. En este sentido, se observó que las propiedades térmicas, estructurales y químicas se modificaron después del tratamiento, lo que promovió la evaporación parcial de las moléculas de agua cambiando el nivel de organización de las dobles hélices en las laminillas cristalinas del almidón. Además, los resultados de XRD sugirieron una disminución de la cristalinidad y cambios en las cadenas de amilosa después del tratamiento. Los resultados del análisis de XPS mostraron entrecruzamiento de las cadenas de amilosa que provocó variaciones en los parámetros de gelatinización, así como también en la heterogeneidad de la estructura cristalina.

Posteriormente, los almidones modificados con plasma se llevaron a un proceso de gelatinización para obtener películas (MSF), a las que se evaluó las propiedades químicas, mecánicas y de barrera. El análisis XPS sugirió que se produjo un

mecanismo de oxidación en todas las MSF ya que la proporción atómica de los grupos hidroxilo, carbonilo y carboxilo cambió. El análisis de TGA indicó una baja interacción entre el almidón y el plastificante ya que los valores de tensión a la fractura y porcentaje de elongación disminuyeron en las películas MSF50 y MSF70. Por otro lado, en las películas con mayor contenido de amilosa, el aumento de las proporciones de C-C sugirió entrecruzamiento dando lugar a películas rígidas. El plasma frío actuó como precursor de películas de almidón oxidadas y entrecruzadas, lo que redujo los valores de permeabilidad al vapor de agua (WVP). Esta investigación describe los principales mecanismos (entrecruzamiento, erosión, despolimerización y sustitución) que sucedieron debido al tratamiento con plasma frío en la molécula de almidón en función del contenido de amilosa. Estos mecanismos modificaron y mejoraron las propiedades estructurales y funcionales del almidón y de las películas. Los resultados sugieren que el tratamiento con plasma de HMDSO es un método adecuado para modificar almidones, los cuales, pueden emplearse para elaborar películas y ser aplicadas como material de empaque.

INTRODUCTION

The introduction of the sustainable concept has led to the development of new packaging materials from biopolymers. Starch is an important raw material to this purpose as it is renewable, biodegradable, abundant and of low cost. Also, starch has good film forming properties. However, the hydrophilicity of starch-based films limits their technological application. To overcome such drawbacks, physical modifications like cold plasma have been employed to reduce the hydrophilicity of films surface.

Cold plasma, a friendly process with no chemical residues, is a feasible alternative to improve the film properties as this treatment can modify starch by different mechanisms including crosslinking, depolymerization, etching or by the inclusion of functional groups (S, F, Si, O) (Pankaj et al., 2017; Wiacek & Dul, 2015).

The amylose content is other important factor which determines the structural and functional properties of starch-based films (Mali et al., 2004). Films made from high amylose (>50%) starch are stronger compared to those obtained from normal starch (Lawton, 1996). However, the high amylose films form stronger hydrogen bonds with water resulting in films with limited barrier properties (Muscat et al., 2012). According to the above mentioned, the amylose content and HMDSO plasma have the capability to modify the mechanical and barrier properties of starch-based films, respectively, thus, the elucidation of the main mechanisms of plasma on starch molecules is important to understand the effects of HMDSO plasma treatment on the chemical structure and on the physicochemical properties of starch-based films.

Moreover, the structural properties of starch have been modified to obtain films with adequate functional properties. Therefore, the changes in structure and functionality of plasma-treated starch granules as a function of amylose and amylopectin content, and their organization within granules is an important issue to understand.

Therefore, the aim of this study was to evaluate the effect of HMDSO cold plasma on structural and functional properties of starches and starch-based films with low and high amylose content and to inspect the effects due to the gelatinization extent.

1. Chapter 1. Literature review

This section gives an overview of starch molecule and the main modification methods. Moreover, starch films characteristics and the fundamentals of the principal techniques of characterization are described.

1.1 Biodegradable films

The packaging materials used in the protection and preservation of food have evolved radically until synthetic plastics. These have a very high demand (i.e. by the year 2000, the world production of plastics reached 160 million tons and in Mexico by 2006 exceeded 4 million tons), which has resulted in an accumulation issue since the materials are not degradable. Therefore, there is a currently growing interest in the development of materials (films) with biodegradable characteristics.

Biodegradable films are classified as biopolymers that maintain mechanical and barrier performance during their use and afterward, they are degraded to low molecular weight compounds such as H₂O, CO₂ and other non-toxic products. As an alternative, bioplastic made from macromolecules such as starch are being developed and studied to replace conventional plastics like polyethylene, polypropylene and polystyrene.

1.2 Starch films

1.2.1 Starch

1.2.1.1 Chemical composition, structure and organization

Starch is an important carbohydrate, which is formed of granules of variable forms. The size and morphology of starch granules depend on the botanical source like cereals (i.e. corn, wheat, rice) and tubers (i.e. potato, cassava). Starch granules can be round, elliptical, oval, lenticular, polyhedral, polygonal or even irregularly (Figure

1). The size of the starch granules ranges from 1 to 100 μm and they are classified as large ($>25 \mu\text{m}$), medium (10 to 25 μm), small (5 to 10 μm) and very small ($<5 \mu\text{m}$) (Lindeboom et al., 2004).

In this regard, rice (1-3 μm) and amaranth (3-8 μm) are the smallest granules, meanwhile the largest granules are found in potato starch (50-100 μm) (Table 1).

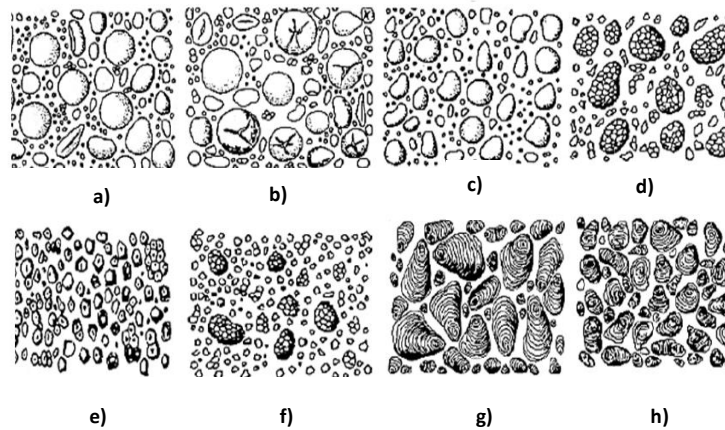


Figure 1. Starch granules morphology from different sources a) wheat, b) rye, c) barley, d) oats, e) corn, f) rice, g) potato and h) cassava. (Singh et al., 2003 & Hoover, 2001).

Table 1. Granule sizes of starch from different botanical source (Singh et al., 2003 & Hoover, 2001).

Source	Size (μm)	Form
Amaranth	1--3	Polygonal
Mango	8--20	Elliptical
Banana	10--50	Irregular
Rice	3--8	Polyhedral
Potato	50--100	Elliptical
Oats	19--24	Elliptical
Barley	2--35	Round
Normal maize	5--25	Round
Waxy maize	5--15	Round
Amylomaize	2--30	Round
Sorghum	5--25	Round
Cassava	5--35	Round
Wheat	2--35	Round
Sweet potato	5--35	Elliptical

Chemically, the starch granules consist of two main components: amylose and amylopectin. Amylose is a linear macromolecule with α -1,4 linked glucopyranosyl units with molecular weight of $1 \times 10^6 \text{ g mol}^{-1}$ and a degree of polymerization (DP) of 250-1000 D-glucose units (Figure 2a). Amylopectin is a highly branched macromolecule with (1-4)- linked α -D- glucopyranosyl units in chains joined by α -1,6 linkages with molecular weight of 1×10^7 to $1 \times 10^9 \text{ g mol}^{-1}$ and a DP of 5000-50000 D-glucose units (Figure 2b) (Perez et al., 2009).

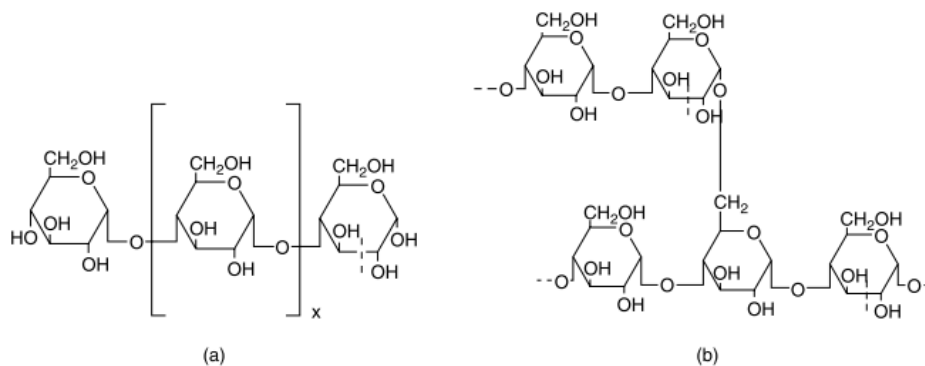


Figure 2. Amylose a) and amylopectin b) molecule (Perez et al., 2009)

The internal structure (Figure 3) of starch granules is characterized by concentric grown rings originated from the hilum of starch granule. Each growth ring varies from 120 to 400 nm length and is composed by blocklets (20-50 nm). The blocklets consists of semi-crystalline lamellae of 9 nm length containing amylopectin and amylose chains (0.1-1 nm) (Le Corre et al., 2010). These lamellae have crystalline and amorphous regions. The crystalline lamellae are formed from amylopectin chains packed into a crystalline lattice, while the amorphous lamellae contain branching points between amylose and amylopectin in disordered conformation (Naguleswaran et al., 2014). Moreover, according to chain length or the degree of polymerization (DP), the crystalline lamellae are formed by short A-chains (chains not substituted and DP (6-12)) and external segments of B-chains (chains substituted) (Figure 4), which are classified as short (B_1 , DP (13-24)) and long chains (B_2 , DP (25-36) and B_3 , DP (>37)) (Bertoft et al., 2012; Kennedy & Mistry, 2003).

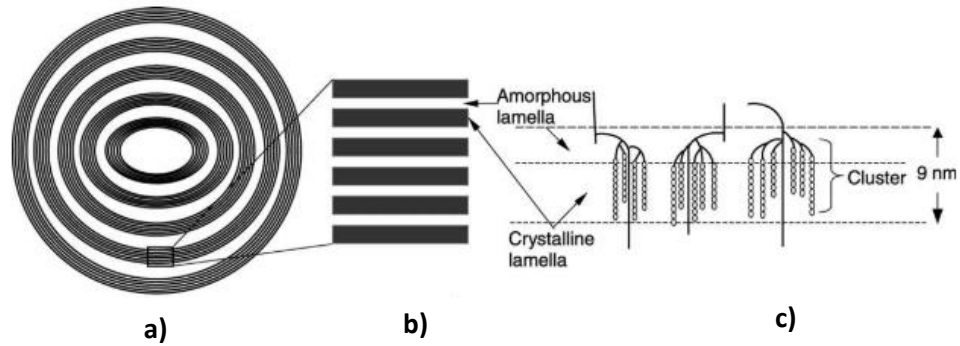


Figure 3. Lamellar structure of starch granule. a) Microcrystalline lamellae separated by amorphous growth rings. b) Crystalline and amorphous region. c) Double helical structure and branching points given rise to crystalline lamellae and amorphous region, respectively (Donald et al., 1997).



Figure 4. Amylopectin structure showing B chains (Hizokuri., 1986)

The crystalline regions of starch lamellae are formed of double helices of amylopectin side chains packed in different polymorphic form (A and B type) (Figure 5). These polymorphs have the same double helical conformation in different packing arrangements and inter-helical water contents (Vermeulen et al., 2004). The A-type crystal is formed by double-helices closely packed into a monoclinic unit cell containing 8 water molecules, meanwhile the B-type crystal contains double-helices packed in a hexagonal unit cell with 36 water molecules (Bertoft, 2017). The A-type crystalline structure is found in cereal starches, while B-type structures are obtained from tubers and high amylose cereal starches (Gernat et al., 1990).

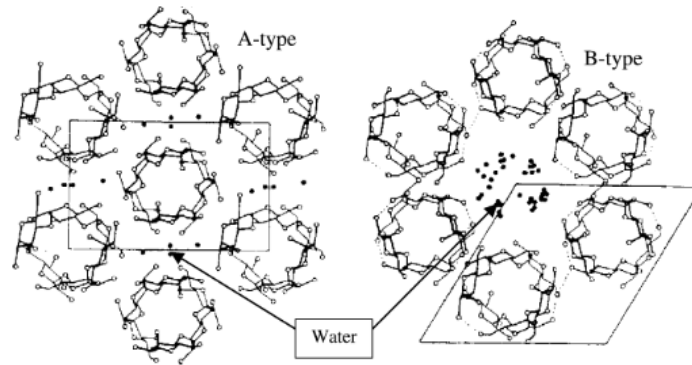


Figure 5. A- and B- type polymorphic forms of starch. (Tester et al., 2004)

1.2.1.2 Gelatinization and gelation

The starch has different extent of organization/disorganization once it is used in aqueous dispersions, which changes its molecular mobility under cooling and heating conditions. In this regard, starch gelatinization is an endothermic process where the double helices of semi-crystalline structure of starch granules change to an amorphous conformation with loss of granular structure (Jane, 2004). The gelatinization is an irreversible process where the starch granules swell in excess of water, and the presence of temperature results in starch molecule disorganization, leaching of amylose and partial granule disruption (Figure 6).

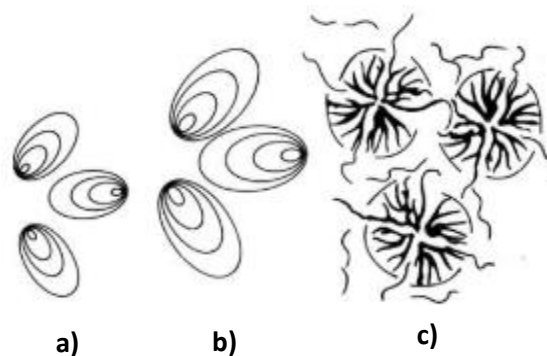


Figure 6. Gelatinization process: a) native granules, b) swelling granules and c) amylose leaching and partial granule disruption. Adapted from Goesaert et al. (2005).

Once the swelling and disruption of starch granules occurs, the amylose chains are leached from the granules and form double helices between them, which allows forming a three-dimensional network with fragmented and swollen granules. Therefore, the amylose and amylopectin chains are transformed in a viscoelastic gel, where the molecular association involves the hydrogen bonds between the chains (Biliaderis, 1991; Hagenimana et al., 2005).

The gel formation or gelation depends on the degree of swelling, granule disintegration and leaching of amylose, which are a function of the type of starch, concentration, temperature and shear applied during heating. Moreover, the amylose and amylopectin reordering increased the stiffness between them and in the swollen granules (Tecante and Doublier, 2002; Hagenimana et al., 2005). Thus, the starch gelation provides important characteristics to develop biodegradable materials like starch-based films.

1.2.2 Films

Biodegradable starch films are obtained from the gelatinized starches by two main techniques: solution casting and subsequent drying (wet method) or thermoplastic processing (dry method) (Paes et al. 2008).

When preparing starch-based films the botanical source, granule size, amylose content and gelatinization extent of starch granule must be considered as determinant of the functional properties of these materials.

In this regard, films made from high amylose starches (>50% amylose) have shown to be stronger than those made from normal starches (25-30% amylose) as its lineal amylose chains interact by hydrogen bonds more easily compared with amylopectin chains (Rindlav et al., 1998). Moreover, films made from high amylose starch (70%) show excellent oxygen barrier properties, low water solubility, low retrogradation temperature and more stable mechanical properties at high relative humidity compared to those made from normal starches (Rindlav-Westking, 1998; Stading et al., 2001). However, the high amylose starch films form stronger hydrogen bonds with water resulting in films with limited barrier properties (Muscat et al., 2012).

Therefore, the starch modification and the use of additives are still been investigated to develop films with adequate mechanical and barrier properties.

1.3 Plasticizers

Plasticizers like glycerol (Figure 7) are additives that increase the plasticity or fluidity of starch films as these are fragile and brittle. According to Muscat et al. (2012), glycerol acting as a plasticizer, reduces the intermolecular forces and increases the mobility of polymeric chains, which modify the mechanical properties of biopolymeric films resulting in a flexible material. In this regard, the plasticizer decreases the interaction between biopolymer chains, such as amylose and amylopectin. However, the high hydrophilic character of the plasticizer also results in films with poor barrier properties.

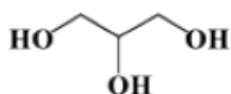


Figure 7. Chemical formula of glycerol

1.4 Modification of starch

Native starch granules have own unique properties useful to elaborate films. However, the mechanical and barrier properties of these materials are deficient. Thus, the modified starch has grabbed much attention to develop films with improved mechanical and barrier properties. To this purpose, chemical and physical modification methods are the most used as described below.

1.4.1 -Chemical and physical modification

Chemical modification is employed to introduce a functional group in the starch molecule modifying several physicochemical characteristics of the starch films, such as solubility in water, gelatinization, pasting properties and retrogradation as a function of the treatment and chemical reagent employed (BeMiller, 1997). In this

regard, chemical modifications such as acid hydrolysis, acetylation, oxidation and crosslinking are the most employed. However, this type of starch modification is limited due to environment and safety concerns. Thus, physical modification methods such as pre-gelatinization, hydrothermal treatments (annealing and high moisture treatment) and non-thermal physical modification (ultrasonication, hydrostatic pressure, pulse electric field and cold plasma) are an alternative to starch modification without using any chemical reagent, and have shown to improve the physicochemical and functional properties of starch granules(Zia-ud- Din et al., 2015).

1.5 Plasma

Plasma is known as the fourth state of matter and it is a partially or fully ionized gas, which contains free charged particles (ions, electrons, atoms and molecules) and neutral particles moving in random directions. The plasma state is produced when molecules of specific gas are subjected to high energy (radiation, electric fields and caloric energy), which ionize the gas and increases the energy levels of the molecules releasing electrons.

Based on temperature, plasmas are classified in thermal (hot) and nonthermal (cold). In near-equilibrium or hot plasmas, most of its constituents are at thermal equilibrium, where the electrons and particles are at high temperature and close to 100% of degrees of ionization.

Nonthermal or cold plasma is not in thermal equilibrium and particles like ions, atoms and molecules are composed by low-temperature particles with charge and neutral molecular species. Moreover, the electrons in this state are at relatively high temperature and they are associated with low degrees (10%) of ionization (Kim, 2004). Nonthermal plasma has shown high performance in different applications such as chemistry, physics, environmental issues and medical sciences (Attri et al., 2013).

Various plasma reactors for cold plasma generations includes the radio frequency (RF), dielectric barrier discharges (DBD), atmospheric glow discharges inductively

coupled plasma (ICP), corona glow discharge, microwave induced plasma (MIP) and gliding arc discharge (Thirumdas et al., 2017); which as well as the type gas fed (i.e; Ar, He, HMDSO), treatment time, input power and substrate determine the mechanism and extent of modification of the starch molecule.

1.5.1 Plasma treatment on starch granules and starch films

Cold plasma technology is an excellent alternative for the treatment of industrial materials. Cold plasma is suited for polymeric matrix modification, particularly as a novel non-conventional technique to modify native starches and films made from starch, altering its structural and functional properties (Bie et al., 2016 a; Wiacek 2015). Cold plasma can modify starch mainly by two mechanisms: crosslinking and depolymerization (Figure 8).

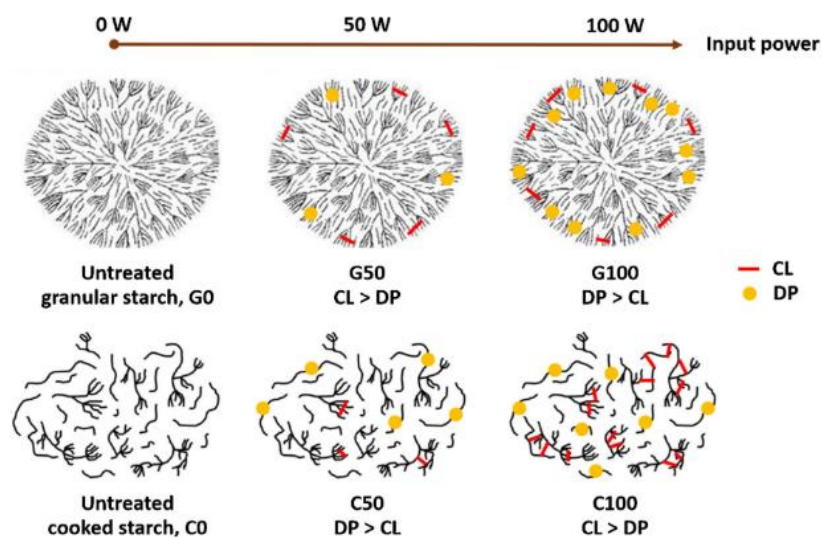


Figure 8. Proposed mechanism of starch modification after plasma treatment: CL, crosslinking and DP, depolymerization (Wongsagonsup et al., 2014).

During plasma treatment, the starch molecules can be crosslinked by free radicals and energetic electrons as proposed by Zou et al. (2004). In this mechanism, the crosslinking takes place between the reducing ends of two starch chains (C-OH) and results in C-O-C linkage between two starch molecules with removal of water molecules, where the C-2 site is the most susceptible for crosslinking among the

three carbons present in the glucose molecule. This mechanism was suggested after ^1H NMR measurement as intensity of OH groups decreased, thus, the crosslinking of starch after plasma treatment resulted in the loss of OH groups (Deeyai et al., 2013).

However, under specific conditions, the active species of plasma cause the depolymerization of the starch molecule, resulting in small fragments of amylose and amylopectin chains. Reactive species of oxygen and nitrogen are reported as the most responsible for polysaccharides fragmentation (Duan et al., 2011). In this regard, Wongsagonsup et al. (2014) reported that plasma treatment can induce the breakdown of C-O bonds in the starch molecule and provoke its depolymerization. Similar behavior was reported by Banura et al. (2018), they found that the amylopectin and amylose depolymerization affects the peak temperature and pasting properties. Thus, during the plasma treatment there is a competition between crosslinking and starch depolymerization as a function of plasma conditions.

The effect of cold plasma treatment on native starch films has been also studied. Bastos et al. (2009) reported that the sulfur hexafluoride (SF_6) plasma promoted the polymerization and crosslinking on the starch-films surface, improving its hydrophobicity. Furthermore, the combination of two plasma sources (SF_6 and HMDSO) allows obtaining super-hydrophobic starch films due to the incorporation of methyl and methylene groups from the HMDSO plasma (Bastos et al., 2013). In addition, the HMDSO plasma treatment resulted in a high atomic concentration of Si (%) changing the barrier performance of the films.

The effect of air plasma on films with different proportion in amylose has been also studied (Pankaj et al., 2015). Pankaj et al. (2017) reported that the films with low-amylose content were most susceptible to high surface oxygenation by increasing of C-O-H bonds. Moreover, after plasma treatment, the high amylose starch films showed an increase in surface roughness by etching mechanism with no changes in its barrier properties.

However, the effect of cold plasma on films with different amylose content remains unclear; therefore, is of importance to study the effect of HMDSO cold plasma as an ecological alternative to modify the starch films properties.

1.6 Analysis techniques

1.6.1 Morphology

1.6.1.1 Scanning electronic microscopy (SEM)

The scanning electron microscope (SEM) is widely used to explore the morphology of polymeric matrices. The SEM principle consist in the use of a focused beam of electrons to create a magnified image of a sample. The electron beam is scanned in a regular pattern across the surface of the sample and the electrons that come out of the sample are used to create the image and once obtained, the morphology of the film can be assessed (Figure 9).

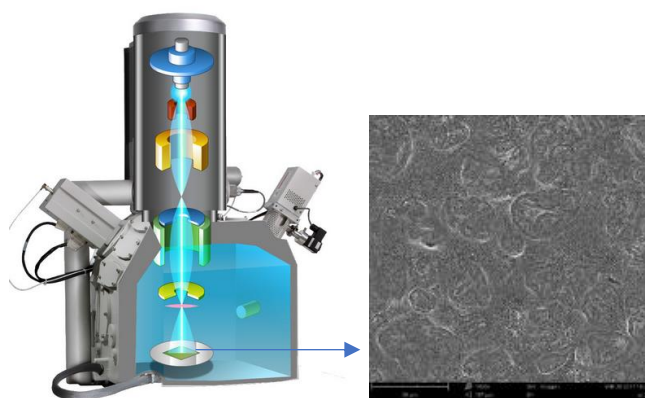


Figure 9. SEM diagram and image obtained

1.6.1.2 Atomic force microscopy (AFM)

Atomic force microscopy (AFM) is a microscopic technique that presents a lateral and vertical resolution at the typical distance between atoms (0.2 \AA), allowing obtaining images covering a range of microns up to a few angstroms (1×10^{-10}). This microscopic technique is employed to analyze polymeric surfaces and to obtain three-dimensional images of their topography and structural defects. AFM records the information of the surface through the movement of a very thin and sharp probe

tip on the sample. The tip is located at the end of a small plank arm (cantilever); when moving the tip on the surface of the sample to be examined, the arm bends in response to the force of atomic interaction between the tip and the surface of an area close to 2 nm (Figure 10).

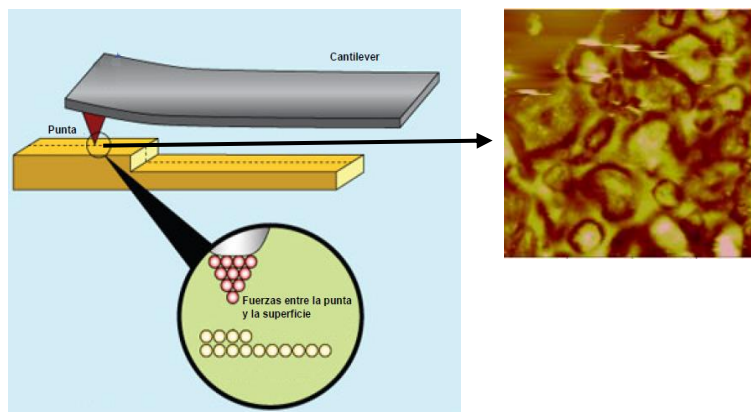


Figure 10.Representation of atomic interaction records between the tip and the surface; and example of AFM image obtained.

1.6.2 Structural

1.6.2.1 Fourier transform infrared (FTIR)

The principle of infrared spectroscopy (IR) involves the use of light to probe the vibrational behavior of molecular systems at a wave number between 0 to 500 cm^{-1} . Once the vibrational movement is generated in the molecule bonds, an IR spectrum is obtained creating a footprint of the films; which permits to identify the functional groups at specific frequencies or wavelength (Figure 11).

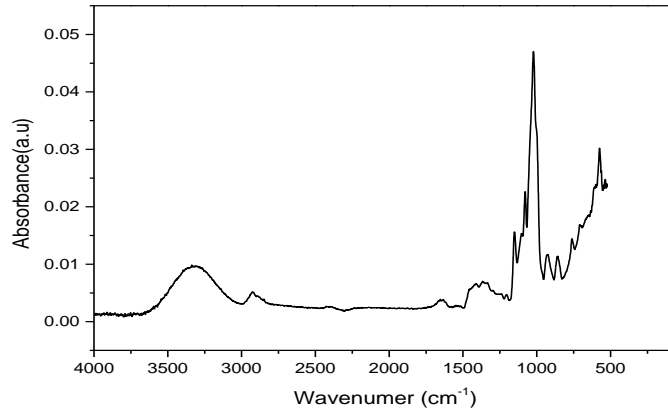


Figure 11.Example of IR spectrum

1.6.2.2 X-ray diffraction (XRD)

X-rays are the form of electromagnetic radiation with a typical wavelength between 0.1 and 1.0 nm, which is comparable to the inter molecular space in crystalline bodies. When an X-ray beam collides with the crystal placed on the surface, it allows the crystal to be rotated with respect to the incident flash and then the diffraction occurs. The diffracted ray is the measure to obtain information on the structure of the crystal and the molecules that form it. Thus, the semi crystalline bodies as starches can diffract X-rays allowing to obtain information on their structure (Figure 12) (Jovanovich et al., 1992).

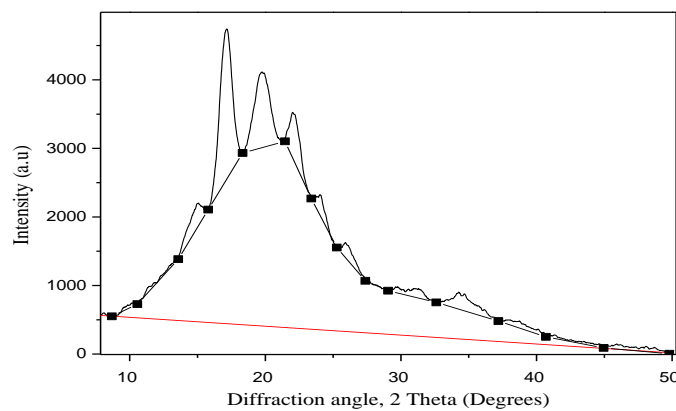


Figure 12.Typical X-ray diffractogram of semi crystalline material

1.6.2.3 X-ray photoelectron spectroscopy (XPS)

X-ray photoelectron spectroscopy (XPS) is widely used in polymeric matrix. X-ray reveals which chemical elements constitute the sample surface, its composition and chemical bonding state by irradiating x-rays on the surface; and also measure the kinetic energy of the photoelectron emitted from the sample. Moreover, any change in the bond energy caused by the electron state surrounding the atoms can be analyzed (Figure 13).

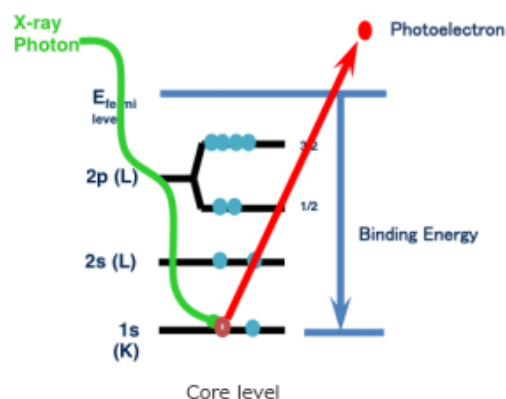


Figure 13. Principle of XPS analysis

1.6.3 Thermal properties

1.6.3.1 Differential scanning calorimetry (DSC)

Differential scanning calorimetry (DSC) is commonly used in the determination of phase transitions (melting, glass transition and crystallization) in polymeric matrices, such as plastics and foods. DSC analysis measures the amount of heat required to increase the temperature of the sample and a reference at the same conditions. Enthalpy changes are recorded as endotherms or exotherms, depending on the process undergone by the sample. Thermograms obtained in films show the endotherm formed by starting (T_s), peak (T_m) and end (T_e) temperatures ($^{\circ}\text{C}$); additionally, the area under the curve indicates the enthalpy (ΔH ; J/g) (Figure 14).

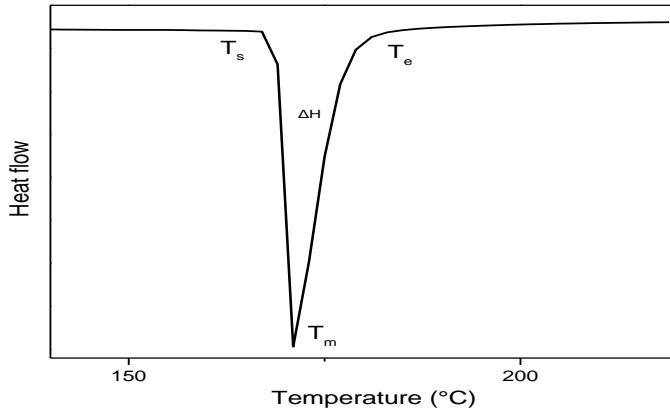


Figure 14. Typical DSC thermogram of films

1.6.3.2 Thermogravimetric analysis (TGA)

Thermogravimetric analysis (TGA) is a method of thermal analysis that measures changes in physical and chemical properties of materials as a function of increasing temperature at a constant heating rate. Changes in the mass of the sample can be due to thermal events such as desorption, absorption, vaporization, oxidation and decomposition (Figure 15).

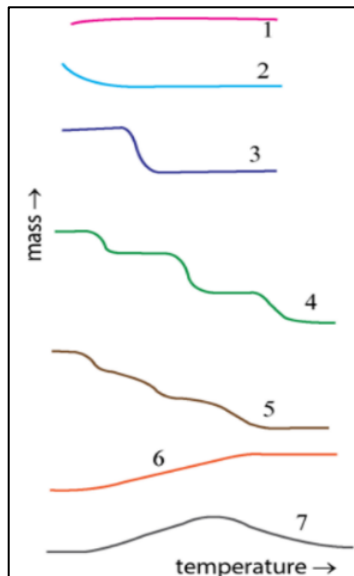


Figure 15. Typical TGA curves: 1) No change, 2) Desorption/drying, 3) Single stage decomposition, 4) and 5) Multistage decomposition, 6) and 7) Atmospheric reaction.

1.6.4 Physical properties

1.6.4.1 Water vapor permeability (WVP)

The barrier properties of films are important because they can be employed as a packaging to protect products against water vapor molecules, which can penetrate through the pores or cracks of the films. According to Figure 16, the permeating molecule is condensated on the film surface, and it is solubilizing inside of the film. Finally, the diffusion of the water molecule is carried out through the film until leaves the system.

The American Society for Testing and Materials (ASTM, 1995) defines the water vapor permeability (WVP) as the rate of water vapor transmission by unit of surface of a flat area per unit of thickness, induced by a unit of vapor pressure difference between two surfaces at specific temperature and relative humidity (RH) conditions.

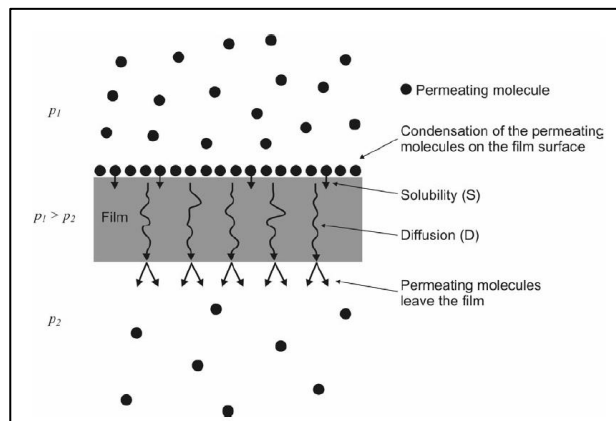


Figure 16.Representation of water permeation through the film

1.6.4.2 Water sorption isotherms (WSI)

Water sorption is a property of biomaterials like films. Depending on its composition, the water may affect their physical state and stability. Sorption isotherms are useful because they indicate the interactions between water activity (a_w) and moisture content in the equilibrium of a sample at a constant temperature and pressure. Thus,

the distribution of water in the material is relevant to quantify the available water and the bound water. Water sorption of the films is modeled using sorption isotherms (Figure 17) and GAB model is the most used since it correlates the a_w with the moisture content (equation 1). This model postulates that the state of sorbate molecules in the second layer is identical to the one in superior layers, but different from those of the liquid state.

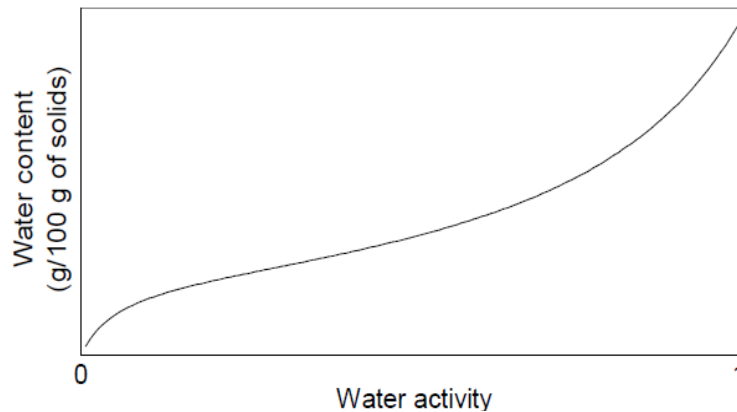


Figure 17. Typical sigmoid sorption isotherm

$$X = \frac{X_m C k a_w}{((1 - k a_w)(1 - k a_w + C k a_w))}$$

Equation 1. GAB model

Where **X_m** is the monolayer moisture content; **C** and **K** are the adsorption constants and **a_w** is the water activity.

1.6.4.3 Water contact angle (WCA)

The water contact angle (WCA) or wettability measurements are used as an indicator of the hydrophilic or hydrophobic behavior of biopolymeric surfaces. Wettability studies indicate the wetting extend when a solid and liquid interact forming an angle at the intersection of the liquid-solid and the liquid-vapor interface (Yuan et al., 2013). Small WCA (<90°) correspond to high hydrophilicity, while large WCA (>90°) correspond to high hydrophobicity (Figure 18). The widest used technique of contact

angle measurement is a direct measurement by telescope-goniometer, where a drop of water is placed on the solid surface and the average of asymmetric angles formed is reported as a WCA.

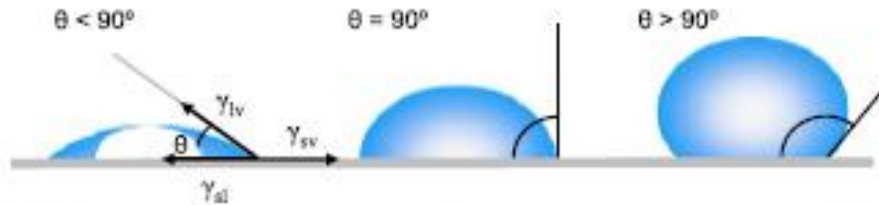


Figure 18.Contact angles formed on solid surfaces

1.6.5 Mechanical properties

The measurement of mechanical properties of biopolymers is important for packaging design. Usually, the mechanical testing of the films consists in stretching a film sample at a constant rate until its breaks. The stress-strain curve obtained can be used to determine, tensile strength (TS), elongation at break (EB) and Young's modulus (YM) (Figure 19); TS is calculated as the ratio of the maximum force at the breaking point and the cross-sectional area (thickness by width), EB is calculated dividing the length achieved at breaking by the original length of the film and YM is calculated from the slope of the linear region in the stress-strain curve.

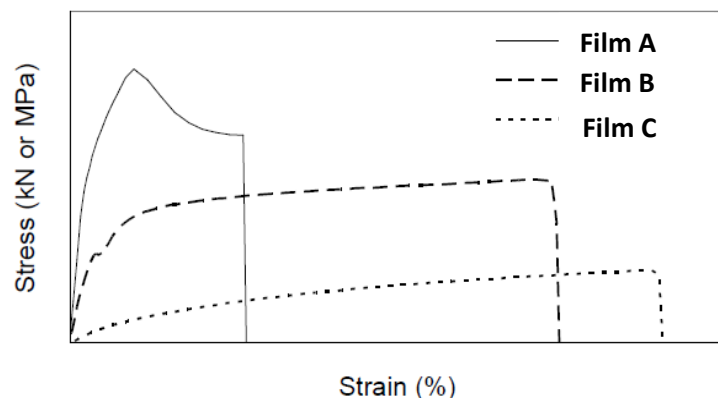


Figure 19.Example of stress-strain curve of films.

2. Chapter 2. Research approach

2.1 Justification

The interest in developing plastic materials from renewable sources has increased considerably due to the need to reduce problems caused by waste accumulation. Starch is one the most promising biopolymers for this purpose because of its availability, low cost and biodegradability. However, it has been observed that films made from this source show high water susceptibility and poor mechanical properties that limit their technological application. Cold plasma treatment has emerged as a promising technique to develop biodegradable films with improved characteristics, since it can improve the hydrophobicity of the surface of polymeric materials. Therefore, the aim of this study is to develop high amylose starch films, because they provided superior mechanical properties compared with those obtained by normal starches. Additionally, HMDSO plasma treatment of the granular starch and films allow to obtain hydrophobic materials that may be used in the food industry.

2.2 Objectives

2.2.1 General

To study the effect of cold plasma treatment on the structural and functional properties of biodegradable films from high amylose starches.

2.2.2 Specifics

- To study the effect of amylose content and HMDSO cold plasma treatment on the structural, mechanical and barrier properties of starch films.
- To evaluate the influence of gelatinization extent and HMDSO cold plasma treatment on the topography, chemical, physicochemical and barrier properties of films from starch with low and high amylose content.
- To evaluate the effect of HMDSO plasma treatment on the structure of starches with different amylose content.
- To study the performance of plasma-modified starches as a film, evaluating its chemical, mechanical and barrier properties.

2.3 Hypothesis

Cold plasma treatments cause structural changes in the polymer matrix and the surface of the films made with high amylose starch, improving its mechanical and barrier properties.

2.4 Experimental design

As shown in the experimental diagram (Figure 20), native starches with different amylose content (30, 50 and 70 %) were used to elaborate films, which were subjected to HMDSO plasma treatment and the first objective was to study the effect of amylose content and HMDSO plasma treatment on the structural (SEM & FTIR), mechanical (TS, YM & EB) and barrier properties (WCA & WSI) of corn starch-based films; as is described in chapter 4. The second objective was to determine the effect of HMDSO plasma on the topography (AFM), chemical (XPS) physicochemical (DSC) and barrier properties (WVP) of films from corn starch with low and high amylose content and to inspect the effect to the gelatinization extent (chapter 5). Also, the effect of the low-pressure HMDSO plasma on the polymeric matrix of corn starches with different amylose content was analyzed, employing analytical techniques such as TGA/DSC, XRD, FTIR and XPS to inspect the changes in the thermal, structural and chemical properties after treatment (chapter 6). In addition, the chapter 7 shows the performance of these plasma-modified starches during the gelatinization process applied to obtain films, studying its chemical, mechanical and barrier properties.

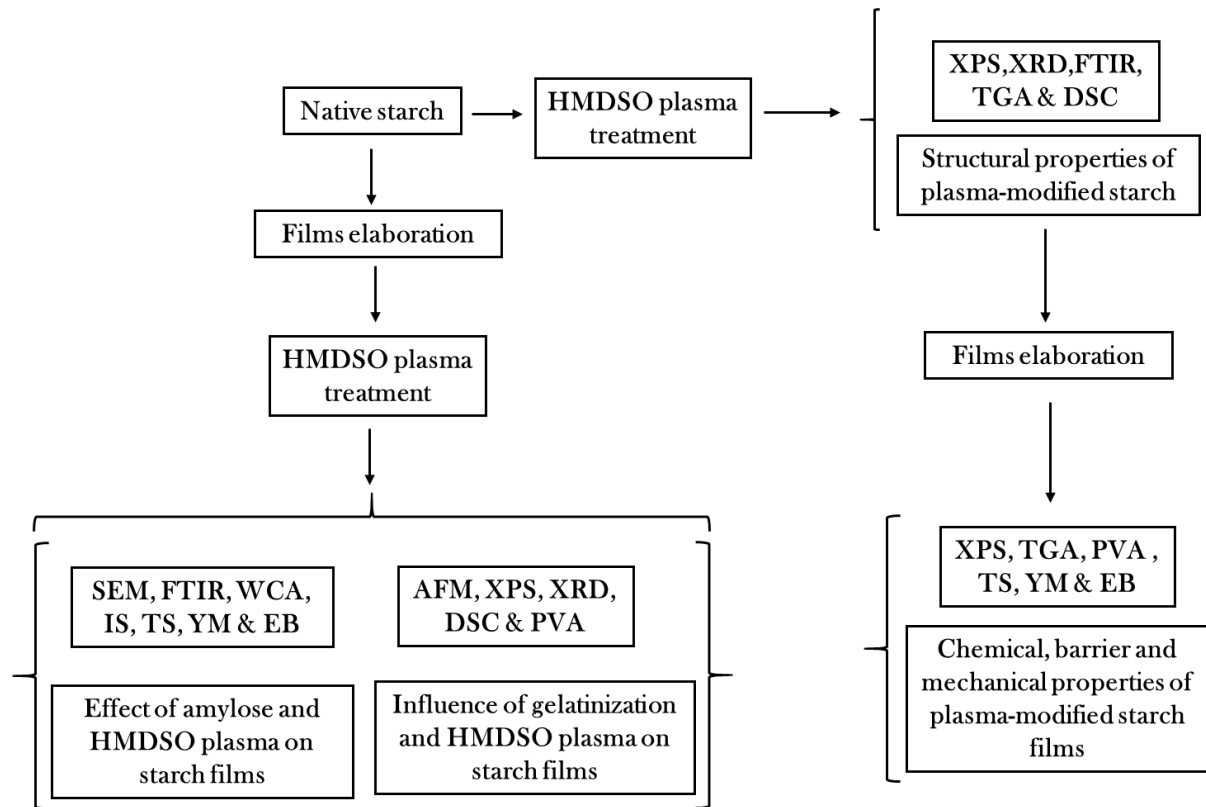


Figure 20. Experimental diagram

Chapter 3. Materials and methods

This section describes the materials and methods used in this research, covering the characteristics of the material, the methods employed, and the procedures followed which are carefully described below.

3.1. Materials

Normal (30% amylose) and high amylose (Hylon V and VII, 50 and 70% amylose, respectively) corn starches were purchased from National Starch (Toluca, Mexico). Glycerol (67757) and hexamethyldisiloxane (HMDSO, 205389) were acquired from Sigma-Aldrich (Saint Louis, MO, USA).

3.2 Modification of starch and films

3.2.1 HMDSO plasma treatment on starches

Normal and high amylose corn starches were placed in a rotatory cylindrical glass reactor (0.5 L), which was connected to a vacuum pump and a radio frequency (RF) power generator operating at 13.56 MHz. Low pressure was generated into the reactor (0.40 mbar) and constant flux of monomer (HMDSO) was injected (0.35 sccm) increasing the pressure to 0.45 mbar. To induce homogeneous modification and high reactivity of HMDSO-plasma species in the starch granules, these were stirred at 20 rpm during all the inductive plasma treatment for 30 min at an input power of 90 W.

3.2.2 Preparation of starch-based films

The film-forming solutions were prepared by incorporating 4 g of native and plasma-modified starch, 30% w/w of glycerol and 100mL of distilled water. The mixtures were gelatinized under different conditions according to the amylose content. Normal

starch (30% amylose) was partially gelatinized at 90 °C for 10 min on a hot stirring plate; meanwhile, high amylose starches (50 and 70% amylose) were completely and partially gelatinized, respectively, at 121 °C for 30min in an autoclave. The gelatinized solutions were poured into acrylic plates (20x20 cm) and dried at 60 °C for 6 h in a conventional oven (IBTF-050). Finally, the films were peeled and stored until further analysis.

3.2.3 HMDSO plasma treatment on native films

Films from normal and high amylose starch were placed in a cylindrical glass reactor (4 L) that included a vacuum pump and a radio frequency (RF) power generator operating at 13.56 MHz. Initially, the pressure inside the reactor was fixed at 0.4 mbar; afterward, the HMDSO monomer was injected increasing the pressure to 0.45 mbar, which was held constant throughout the treatment with a HMDSO gas flow of 0.35 sccm into the reactor. To achieve a homogeneous coating with no pores or fissures, the films were exposed to the inductive plasma treatment for 30 min at an input power of 70 W.

3.3 Analysis techniques

3.3.1 Film thickness

The thickness (mm) was measured at 6 random points of each film using a micrometer (ET115S, Etari GmbH, Stuttgart, Germany), before characterization tests and mean values were considered for further calculations.

3.3.2 Morphology

3.3.2.1 Scanning electronic microscopy

The morphology of the starch-based films was studied with a scanning electron microscope (SEM) (Phenom-World, model Phenom pro, Eindhoven, Netherlands)

using an acceleration voltage of 5 kV. The samples were placed on an aluminum pin at 45° and 90° angles using a conductive double-sided carbon tape, thus allowing visualizing the cross-section surface of the films. The images were obtained at a magnification of 1500x.

3.3.2.2 Atomic force microscopy

Atomic force microscopy (AFM) was performed to assess the effect of HMDSO plasma treatment on the surface of the corn starch films. A Dimension™ 3100 from Digital Instruments with Pt-coated Si tip with a 15 nm nominal radius (model OSCM-PT Bruker) was employed to obtain the images in the tapping mode at a scanning rate of 1.0 Hz during 256 lines. The morphological images, showing the surface roughness (R_q) given by the root mean square (RMS) average of the height deviation, were taken from the data plane using the Nanoscope IIIa software available in the microscope.

3.3.3 Structural properties

3.3.3.1 FTIR spectroscopy

The Fourier transform infrared (FTIR) spectra of the starches and films were obtained using a spectrophotometer (Nicolet iS5 iD7, Perkin Elmer, Waltham, MA, USA) with an attenuated total reflectance (ATR) attachment. The samples were scanned in the range from 500 to 4000 cm^{-1} with a resolution of 4 cm^{-1} . An averaged spectrum from 20 scans was obtained. The analysis of the spectra was performed using the Thermo Scientific OMNIC software that provided information on the functional groups in the samples. Also, the double helical order of starch samples was estimated using a deconvolution Gaussian function on a specific spectra region (950- 1000 cm^{-1}).

3.3.3.2 X ray diffraction

The X ray diffractograms of the starches and films were obtained using a diffractometer (Siemens D5000, Midland, ON, Canada) equipped with a CuK α radiation line, operated at 40 Kv and a current intensity of 30 mA. The samples were scanned in an angular range of 5–50 degrees (2θ) with an angular pitch of 0.05° in a counting time per angular step of 15 s. The relative crystallinity was calculated as described by Rabek [30] using the Eq. (1).

$$RC (\%) = (A_c)/(A_c+A_a) \times 100 \quad (1)$$

where **A_c** is the crystalline area; **A_a** is the amorphous area on the X-ray diffractograms.

3.3.3.3 X-ray photoelectron spectroscopy

An X-ray photoelectron spectroscopy Versa Probe II, PHI (Massachusetts, USA) with vacuum pump at 2×10^{-8} mTorr was used to analyze the chemical composition of the starches and films. All spectra were collected using Al-K α radiation (1486.6 eV). The alpha hemispherical analyzer was operated in the constant energy mode with survey scan pass energy of 117.4 eV. The high-resolution spectra were obtained using a pass energy of 11.75 eV. XPS was also used to assess the chemical bonding state and the elemental composition of the samples. The C1s and Si 2p peaks were deconvoluted using Gaussian curves with no restriction of the position and area. The full width at half maximum (FWHM) was maintained fixed for each adjusted peak.

3.3.3.4 Differential scanning calorimetry

Gelatinization parameters of the starches and the melting temperature (T_m) of the films were determined using a Mettler Toledo (TC45) calorimeter. For starches: samples of 3 mg were weighed directly into DSC aluminum pans and 7 μ L of

deionized water were added. The pans were sealed and heated from 25 to 110 °C at 10 °C/min in the calorimeter. For films: samples of 5–7 mg were weighted in aluminum pans and hermetically sealed before test. Subsequently, the samples were subjected to a heating cycle from 25 to 220 °C at a heating rate of 10 °C/min. The thermal parameters were calculated using the STARe Version 9.30 program. All measurements were carried out in triplicate.

3.3.3.5 TGA analysis

Thermogravimetric test was performed using a thermal analyzer (TGA Q-50, TA Instruments, New Castle, PA, USA). Data was acquired on samples of 10 mg in a temperature range from 30 to 300 °C at a heating rate of 10 °C/min under a nitrogen flux of 60 ml/min. The percent loss was calculated using the TA Instruments Universal Analysis 2000 software.

3.3.4 Physical properties

3.3.4.1 Wettability

The effect of the HMDSO plasma treatment and the amylose content on the hydrophilicity of native starch-based films was determined by contact angle measurements using a goniometer (Ramé-Hart model 100-0, Succasunna, NJ, USA). The evolution of a 5- μ L water drop on the surface of the film was evaluated. The contact angle was manually recorded every 60 s for 5 min. The shape evolution of the water drop was measured between the baseline of the drop and the tangent at the drop boundary. All measurements were carried out in triplicate.

3.3.4.2 Water vapor permeability

Water vapor permeability test was performed according to the ASTM E96-66 method [31]. A glass cup of 50 mm height and 35 mm in diameter containing a saturated salt

solution (NaCl, 75% HR) was employed as a permeation device. The films were sealed over a circular opening of the cup and the cup was placed inside the permeability chamber containing silica gel (0% HR) at 30 °C to maintain the water vapor pressure gradient through the film. The water vapor permeability was determined from the weight loss of the permeation cup against time. The records were automatically collected every 1 min during 6 h using an analytical balance connected to a computer. The slope of the straight line, obtained by linear regression, was used to calculate the water vapor transmission rate. The water vapor permeability was calculated considering the water vapor pressure gradient, the thickness and the transfer area of the film. All films were conditioned at 57% RH for 72 h before the test and the results were reported as the average of three determinations.

3.3.4.3 Water vapor adsorption isotherms

Adsorption isotherms were obtained following the ASTM E104-02 method. Constant equilibrium relative humidity environments (RH_{eq}) were established inside glass jars using over saturated salt solutions. LiCl, $MgCl_2$, K_2CO_3 , NaBr, NaCl, and $BaCl_2$ salt solutions were used to cover a water activity (a_w) range from 0.11 to 0.90 ($a_w \approx RH_{eq}/100$). All salts were analytical grade (Sigma-Aldrich, St. Louis, MO). Film samples were cut into pieces (2.0 × 1.5 cm) and stored on silica gel for 7 days before performing the test. Samples were weighed, placed inside the glass jars containing the saturated salt solutions, and closed hermetically. The jars were kept in an environmental chamber at 30 °C for 15 days. Results at equilibrium conditions were reported for each equilibrium relative humidity as grams of water/100 g of dry film. Moisture adsorption tests were done in triplicate at each water activity (a_w).

3.3.5 Mechanical properties

Tensile strength (MPa), elongation at break (%) and Young's modulus (MPa) of the films were evaluated. The tensile test was performed according to the ASTM method

D882-02 using a texture analyzer (TA Plus, Lloyd Instruments). The film samples were cut into rectangles (100 × 10 mm) and conditioned at 57% relative humidity (RH) for 72 h before testing. The initial distance between grips was 50 mm and the cross-head speed was set at 1 mm/s. Ten replicates were measured for each treatment. A sample film during the tension test is shown in Fig. 1b. Tensile strength (TS) was calculated as the ratio of the maximum force at the breaking point and the cross-sectional area (thickness by width). Similarly, the percentage of elongation (%E) was calculated dividing the length achieved at breaking by the original length of the film and expressed as the percentage. Young's modulus (YM) was calculated from the slope of the linear region in the stress-strain curve.

3.3.6 Statistical analysis

An analysis of variance (ANOVA) was accomplished using the Sigma-Stat 11.0® software (Fox, Shotton, & Ulrich, 1995). When significant differences between treatment were found, Tukey's comparison test ($\alpha = 0.05$) was applied.

3. RESULTS AND DISCUSSION

The effects of HMDSO plasma treatment on starches and starch films with different amylose content are presented according to the results described in four research articles, written, published (chapters 4, 5 & 6) and submitted to the journals (chapter 7) during the development of this thesis project. The structure of the results and discussion are divided in four chapters according: to the amylose and HMDSO plasma treatment (chapter 4), the influence of the gelatinization and the treatment in the structural and functional properties of starch films (chapter 5). Moreover, the structural changes on starches after plasma treatment (chapter 6) and its performance during the gelatinization process to obtain films (chapter 7) are described and discussed further ahead.

Chapter 4. Hexamethyldisiloxane cold plasma treatment and amylose content determine the structural, barrier and mechanical properties of starch-based films.

Abstract

In this study, the effect of amylose content and cold plasma treatment on starch films properties was investigated. Films from normal (30%) and high amylose (50 and 70%) starches were subjected to hexamethyldisiloxane (HMDSO) cold plasma treatment. Morphological, structural, mechanical and barrier properties of the films were evaluated. The amount of remnant starch granules (RSG) in the films depended on the amylose content and on the gelatinization extent of the starch. This behavior was corroborated on the films from starch with 50% amylose, where the loss of RSG resulted in poor barrier properties and high hydrophilicity. Moreover, HMDSO cold plasma treatment incorporated methyl groups improving the hydrophobic properties and favored the helix ordering of the starch components resulting in a limited water-film interaction. Furthermore, the simultaneous effect of HMDSO coating and the ordering of the structures reinforced the surface of the films, improving the mechanical properties.

4.1 Introduction

This section describes the importance to develop hydrophobic materials making use of eco-friendly materials and technology.

The increasing of plastic pollution has raised the interest to develop alternative materials. Thus, researchers have focused on studying biopolymers to partially or completely replacing the existing plastics. Starch has been considered as an attractive alternative due to its eco- friendly character, abundance, and low-production cost at a large scale. However, starch-based films have limited functional properties (barrier and mechanical) and different strategies such as chemical modification (crosslinking, oxidation, esterification) or the combination with macromolecules (proteins and polysaccharides), and nanoparticles (nanoclays, cellulose and carbon tubes) have been used to improve them (Suárez et al., 2013; Jansson & Järnström, 2005; Romero-Bastida et al., 2015; Sifuentes-Nieves et al., 2015; Wiacek, 2015; Wiacek et al., 2016b) . Nevertheless, starch-based films still cannot mimic the functional properties of films from conventional plastics. Thus, new approaches to overcome the hydrophilicity and fragility of starch-based films are being studied. Cold plasma, a friendly process with no chemical residues, is a feasible alternative to improve or change the film properties as this treatment can modify starch by different mechanisms including crosslinking, reticulation, etching or by the inclusion of functional groups (S, F, Si, O) (Bastos et al., 2009; Bastos et al., 2014; De Albuquerque et al., 2014; Pankaj et al., 2017; Wiacek & Dul, 2015). Bastos et al. (2009) studied the effect of sulfur hexafluoride (SF_6) plasma on the properties of films from normal starch. The authors reported that the plasma treatment promoted a polymerization on the film surface, as well as a starch crosslinking, which resulted in films with improved water vapor barrier properties. Later, Bastos et al. (2013) evaluated the effect of two plasma sources (SF_6 and HMDSO) and their combination, on the properties of normal starch-based films. The authors found that the SF_6 /HMDSO treatment allowed obtaining more hydrophobic films, probably due to the high levels of methyl and methylene groups in the HMDSO chemical structure. Moreover, De Albuquerque et al. (2014) reported that HMDSO plasma treatment

helps to reduce the amount of moisture adsorbed on the surface of starch-based films. Such results suggest that HMDSO coating leads to surface hydrophobization, thereby improving the water vapor barrier properties of starch-based films.

The amylose content is another important factor which determines the properties of starch-based films (Mali et al., 2004). Films prepared from high amylose (>50%) starch are stronger, with higher values of stress to fracture and elastic modulus compared to those films obtained from normal starch (Lawton, 1996; Liu et al., 2013). However, the films from high amylose starch form stronger hydrogen bonds with water resulting in films with limited barrier properties (Muscat et al., 2012). Since amylose content and HMDSO plasma have shown the capability to modify the mechanical and barrier properties of starch-based films, respectively, the aim of this work was to study the effect of amylose content and HMDSO plasma treatment on the structural, mechanical and barrier properties of corn starch-based film.

4.2 Results and discussion

4.2.1 Morphology

The obtained films had a translucent appearance (Figure 21a) with an average thickness of 0.07 mm. Scanning electronic microscopy was used to observe the morphology and differences due to amylose content or plasma treatment. Figure 22a, b, c shows the presence of remnant starch granules (RSG) of different size and shape, dispersed in the continuous amylose matrix in all samples regardless of the amylose content. However, the film made from normal corn starch (F30) exhibited the biggest size and the higher amount of RSG (Figure 22a) due to the partial gelatinization of the starch granules during the elaboration process. In general, the RSG in F30 displayed a circular-like structure with a depletion in the center similar to the remnant granules reported by Garcia- Hernandez et al. (2017) for films from normal corn starch. The 50% amylose starch-based films (F50) showed an important reduction of RSG (Figure 22b) that was not observed on the 70% amylose starch films (F70 – Figure 22c). Such differences are attributed to the disruption of RSG

due to the temperature and time used to gelatinize this starch. These effects were more noticeable in F50 since its gelatinization process involved a higher disruption of starch granules (Ghiasi et al.,1982).

After plasma treatment, all films showed a continuous HMDSO coating with no visible pores or fissures on the surface (Figure 22g–i). According to Batan et al. (2010) and De Albuquerque et al. (2014), this type of coating has hydrophobic properties and a thickness ranging from 40 to 80 nm.

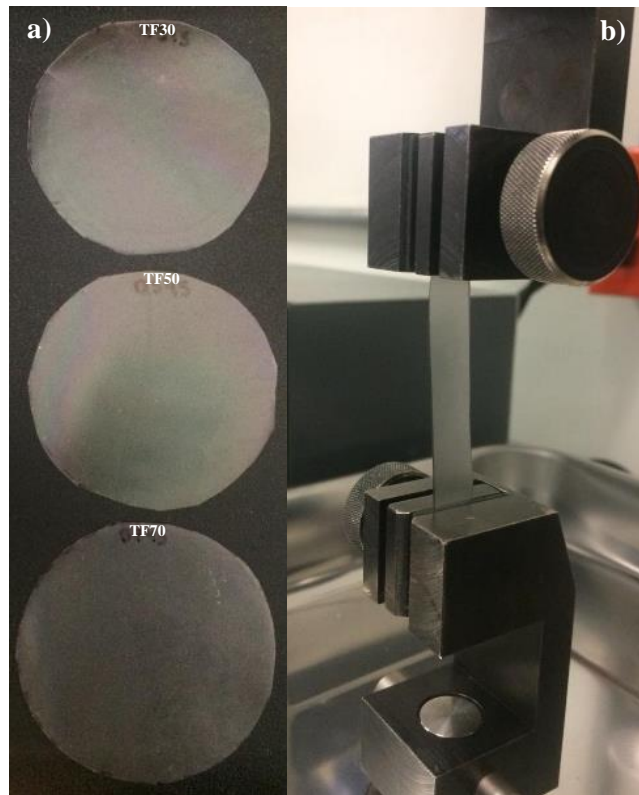


Figure 21. Appearance of the obtained films (a) and a sample of the film fixed with the grips during the tension test (b).

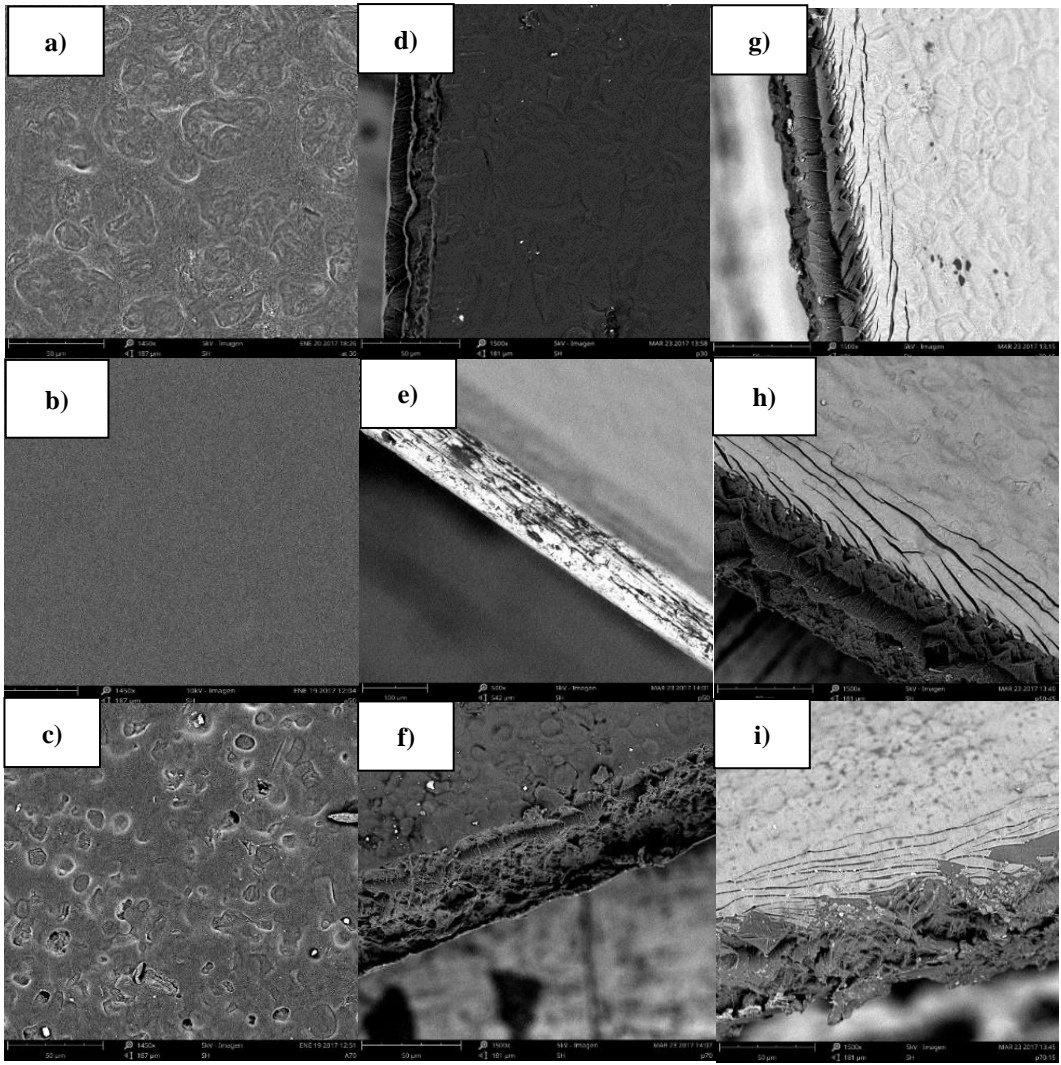


Figure 22. SEM images of films from starch (90° angle), F30: film- 30% amylose a), F50: film- 50% amylose b) and F70: film- 70% amylose c). SEM images of films from starch before and after treatment (45° angle), F30 d), F50 e), F70 f), TF30: treated film- 30% amylose g), TF50: treated film- 50% amylose h) and TF70: treated film- 70% amylose i). All micrographs correspond to 1500x.

4.2.2 FTIR spectroscopy

The FTIR spectra of films before and after plasma treatment are shown in Figure 23. Films with no treatment displayed the characteristic bands of starch at 2936 (C-H vibrations), 1150 (C-O stretching), 1077 (C-O bonding) and 990 cm^{-1} (C-O-C stretching). Also, the wide band centered at 3300 cm^{-1} corresponds to OH groups of the starch molecules that have been related to the hydrophilic behavior of starch-based films (De Albuquerque et al., 2014). In this regard, after normalizing the spectra using the 1082 cm^{-1} band, the band at 3300 cm^{-1} in F50 showed higher intensity ratio than that in F30 and F70, suggesting a higher hydrophilicity. This behavior could be attributed to a loss of RSG, since RSG confer hydrophobic properties to starch films (Garcia-Hernandez et al., 2017); besides, disruption of granules releases amylopectin molecules promoting the interaction with water molecules. After plasma treatment, the band at 3300 cm^{-1} disappeared in all films, suggesting that the reactive species of HMDSO changed the starch film capability to retain water probably due to the barrier effect of the HMDSO coat deposited after plasma treatment. Additionally, the treatment used was a vacuum cold plasma that has been extensively used for material modifications (Sarangapani et al., 2017; Wiacek et al., 2016a; Zhang et al., 2015). The vacuum used during treatment could have also promoted the evaporation of water molecules from the film. Furthermore, bands corresponding to HMDSO functional groups were identified at 840 (Si-C), 1015 (Si-O-Si), and 2965 cm^{-1} (CH_3 stretching) after plasma treatment (Ziari et al., 2013).

The plasma effect on the crystalline order of the starch molecules was studied. Thus, the FTIR spectra in the region from 1100 to 950 cm^{-1} , which corresponds to C-O bond stretching, was explored. According to Van Soest et al. (1995) the bands at 1047 and 1022 cm^{-1} are associated with the ordered and the amorphous structures of starch, respectively. Moreover, the 1047/1022 ratio has been considered as an indicator of the short-range crystalline structure of starch (Agama-Acevedo et al., 2018; Sevenou et al., 2002; Van Soest et al., 1994; Wiacek & Dul, 2015). However, the correct assessment of these intensity ratios is hindered by the overlapping of the

bands of starch and HMDSO. Thus, the computation of individual signal contributions via deconvolution of the absorbance spectrum could be used to obtain precise intensity values (Figure 24). Table 2 shows the intensity variation observed for the 1047/1022 ratio as a function of the amylose content and plasma treatment. In untreated films, the value of 1047/1022 ratio decreased proportionally to the amylopectin content. Thus, F30 showed the highest value associated with a higher proportion and helical order due to the reorganization of the branched chains of amylopectin (Manners, 1989). A similar behavior was reported for gelatinized starch at a lower temperature, where no effect on the hydrogen bonds between the poly (1→4) α glucan chains in the crystallites was found, resulting in higher 1047/1022 ratios [10]. After cold plasma treatment, the 1047/1022 ratio increased in all films. Considering that the band at 1022 cm^{-1} has been associated with the amorphous structure, a low intensity indicates that the proportion of amorphous structures in the starch-based films decreased after plasma treatment suggesting a higher proportion of ordered starch structures. Also, the order level could have been promoted by a lower amount of water molecules (Laovachirasuwan et al., 2010). A similar phenomenon was observed in hydrolyzed starch where the chemical treatment affected the amorphous regions of the starch and increased the ordered structure proportion (Sevenou et al., 2002). This effect is corroborated by the increment on the short-range crystallinity values. Results suggest that the reactive species of plasma and the treatment time promoted a highly ordered structure in the films, which is related to the amylopectin content. In this regard, the 1047/1022 ratio of TF50 had the lowest value, indicating a less ordered structure, which might be due to the loss of RSG. With no presence of RSG, the amylopectin branches are free, and the rearrangement of the molecules takes place in the whole film structure (amylose network). The highest value was observed in TF30 attributed to the higher proportion of amylopectin.

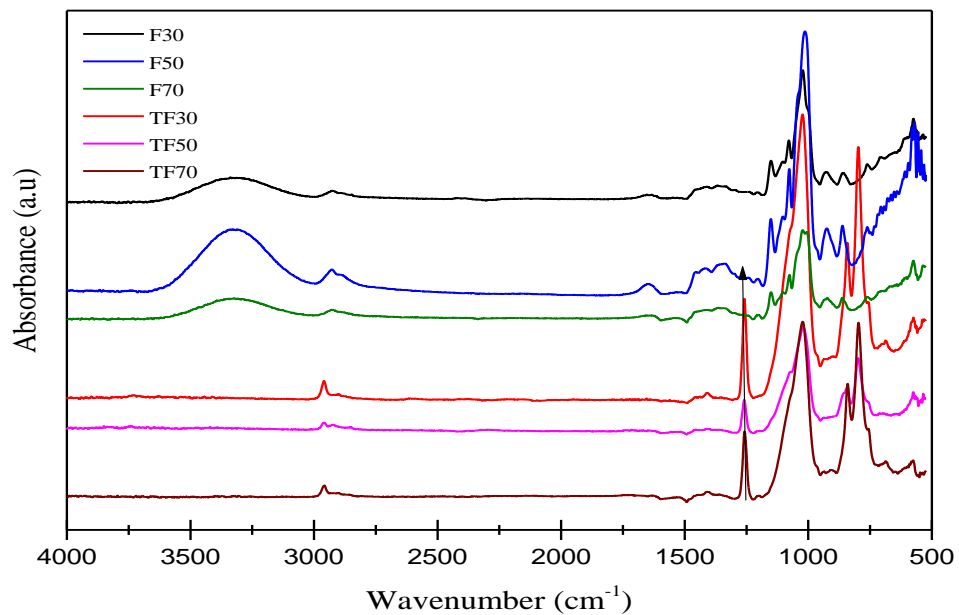


Figure 23. FTIR spectra of starch films from normal and high amylose starches before and after HMDSO plasma treatment. F30: film- 30% amylose, F50: film- 50% amylose, F70: film- 70% amylose, TF30: treated film- 30% amylose, TF50: treated film- 50% amylose and TF70: treated film- 70% amylose.

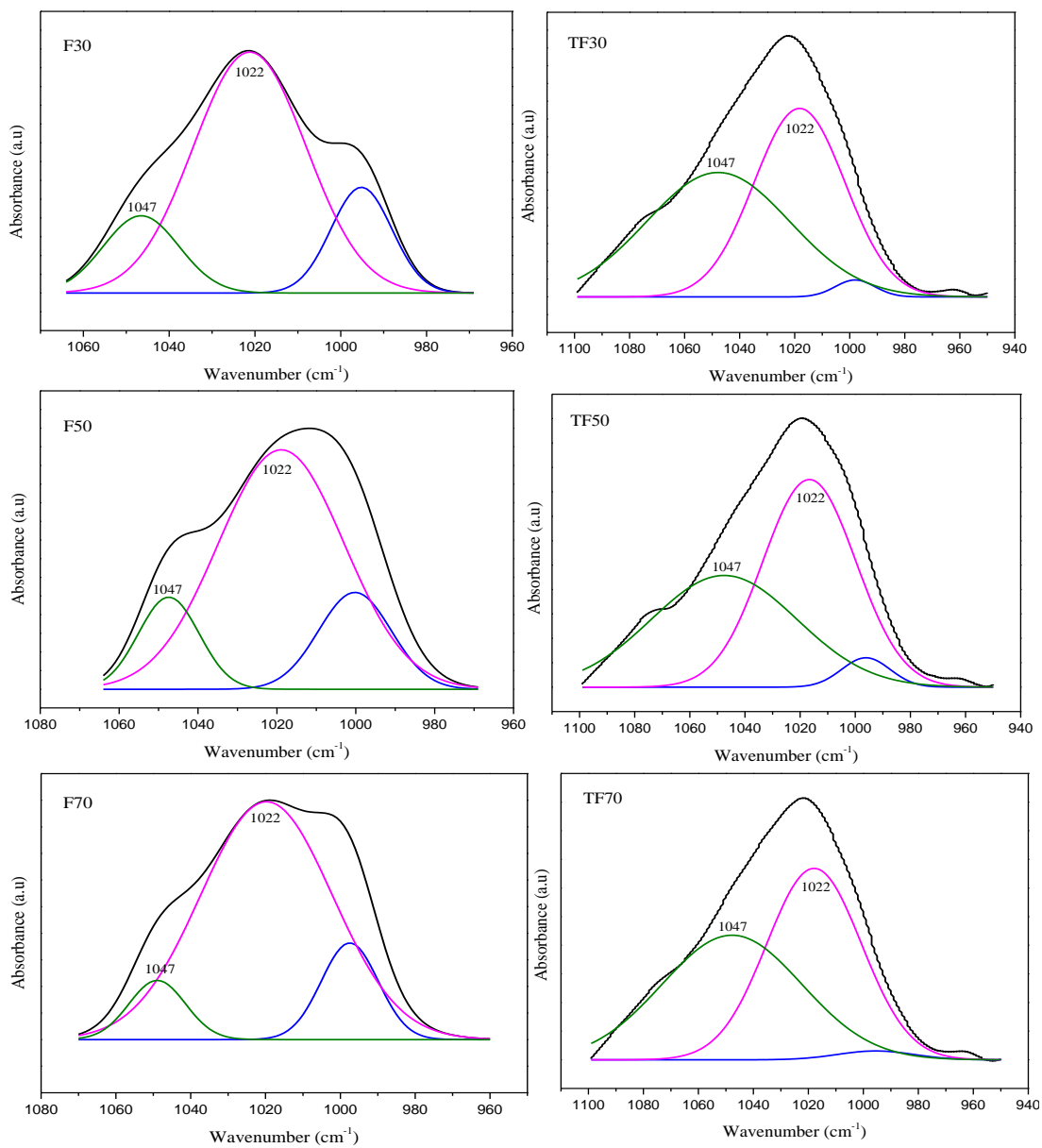


Figure 24. Deconvoluted FTIR peaks of films made of starch with different amylose content before and after HMDSO plasma treatment. F30: film- 30% amylose, F50: film- 50% amylose, F70: film- 70% amylose, TF30: treated film- 30% amylose, TF50: treated film- 50% amylose and TF70: treated film- 70% amylose.

Table 2. Variation of the 1047/1022 ratio of starch films from normal and high amylose starch before and after HMDSO plasma treatment.

Sample	1047/1022
F30	0.20
F50	0.18
F70	0.10
TF30	1.01
TF50	0.82
TF70	0.93

F30= film- 30% amylose; **F50**= film- 50% amylose; **F70**= film- 70% amylose; **TF30**= treated film- 30% amylose; **TF50**= treated film- 50% amylose; **TF70**= treated film- 70% amylose.

4.2.3 Wettability

Wettability was measured to assess the effect of HMDSO plasma treatment on the hydrophilicity of the films. Wettability has been related with the variation in shape and size of a drop of water on the film surface as a function of time and it is usually reported as contact angle; therefore, a hydrophilic or hydrophobic film surface can be inferred depending on the absorption and evaporation phenomena (Karbowski et al., 2006). Figure 25 shows the variation of the contact angle of the films as a function of the amylose content and the HMDSO plasma treatment. Untreated films showed a contact angle value of about 60° and decreased to 45° or 40° after 5 min in F30 or F70, respectively. Meanwhile, F50 completely absorbed the water drop after 3 min, due to the loss of RSG that confers hydrophobicity to the surface of the films (Garcia-Hernandez et al., 2017). These results indicate that the starch disruption before film

formation affected its wettability. The reinforcement effect of the RSG was lost in F50. According to several studies, the water contact angle of normal and high amylose starch-based films is low (40–60°), which allows classifying them as hydrophilic materials (Bastos et al., 2013; De Albuquerque et al., 2014; Romero-Bastida et al., 2016; Wiacek, 2015; Wiacek & Dul, 2015). The wettability of the starch-based films decreased after plasma treatment. All films showed an increase of the contact angle from 60° to higher than 85°, resulting in films with hydrophobic properties. This effect can be attributed to the HMDSO coat and the methyl groups introduced on the films as observed in the FTIR spectra (Bastos et al., 2009). After the HMDSO plasma treatment, the contact angle decreased by 20% in TF30 and TF70, and by 35% in TF50 after 5 min. These results suggest that HMDSO coat maintained stable the hydrophobic properties of the films (Bastos et al., 2013), even on TF50 which lost the RSG.

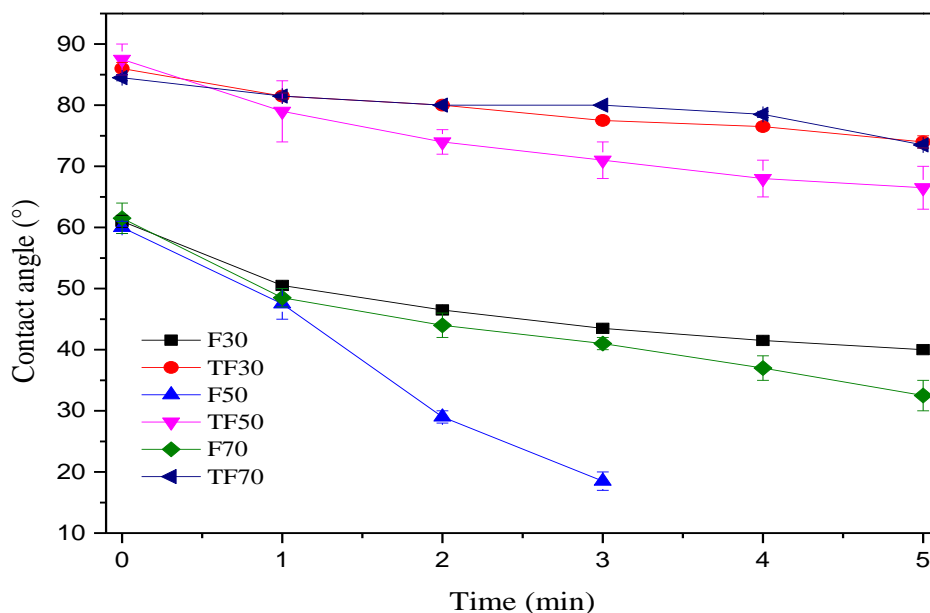


Figure 25. Evolution of water contact angle of films from normal and high amylose starch before and after plasma treatment. F30: film- 30% amylose, F50: film- 50% amylose, F70: film- 70% amylose, TF30: treated film- 30% amylose, TF50: treated film- 50% amylose and TF70: treated film- 70% amylose.

4.2.4 Water vapor adsorption isotherms (WVI)

Figure 26 shows the moisture adsorption isotherms at 30 °C of films made from starch with different amylose content before and after HMDSO plasma treatment as a function of water activity (a_w). Untreated films showed a typical sigmoidal isotherm that has been previously reported for starch-based films (Bertuzzi et al., 2007; Romero-Bastida et al., 2016) and it is characterized by a small slope at $a_w < 0.6$ as the water is adsorbed at the binding sites in the film. However, after the 0.6 value, an increment of moisture as a function of a_w was observed because of the plasticization of the amorphous areas of the starch network in the film (Bertuzzi et al., 2007).

The effect of HMDSO plasma treatment on moisture content at different a_w values is shown in Figure 26. TF30 and TF70 showed an isotherm with a small slope up to $a_w = 0.75$. These results corroborate that the HMDSO coat and the methyl groups observed in the FTIR spectra are responsible for the limited water adsorption on the binding sites in the films. Also, at $a_w > 0.75$, the moisture content was lower than that of the films with no treatment. This effect might be explained by a decrease of the amorphous regions and an increase in the helical order of the films which might be attributed to the reorganization of amylopectin inside de RGS, reducing the plasticization effect of water. Therefore, the number of active sites to bind water molecules was reduced by the restructuring of the starch molecules, thus preventing the moisture adsorption. However, this hydrophobic effect was not that obvious in TF50-based films (Figure 26b). Such difference suggests that the reduction of RSG is responsible for the similarity of the adsorption isotherms compared to that of untreated films. Once the water molecules are absorbed into the HMDSO coat, they interact with a higher amount of amylopectin released from the granules, promoting the plasticization effect of the water molecules. Nevertheless, the presence of HMDSO coating and the reorganized amylopectin into the RSG, are responsible for reducing the number of water molecules interacting with the films.

Moisture adsorption data was satisfactorily fitted by the GAB model ($r^2 > 0.99$) to obtain the moisture content in the monolayer (X_m) (Figure 27), which has been used

to estimate the water adsorption capability of starch films (Muscat et al., 2013). Untreated film from starch with 30% amylose showed a significantly higher X_m value than that of films from starch with high amylose content (50 and 70%). These differences could be associated with the sensibility of the amylopectin chains to plasticizers, increasing the active sites available for water interaction (Muscat et al., 2012).

After plasma treatment, the X_m value of the films decreased. Films from starch with 30 and 70% amylose showed the lowest values, indicating that the HMDSO plasma and the reordered amylopectin in RSG reduced the number of adsorption sites available for water binding, thus decreasing the moisture content of the film. A similar behavior was reported for high amylose starch films, where the addition of a plasticizer resulted in a decrease of X_m , as the number of active sites available for binding water and the moisture content of the film declined (Bertuzzi et al., 2007). Romero et al. (2016), working with starch-based films reinforced with montmorillonite, found lower X_m values than those calculated in this study. The authors reported that the nanoparticles improved the water resistance of the film since the starch can form hydrogen bonds with hydroxyl groups of nanoparticles improving the water vapor barrier capacity. However, films from starch with 50% amylose only decreased by 5%; which may be associated with its RSG loss promoting the water adsorption on the binding sites. The remnant amylopectin, released after granule disruption, increased the capability of the films to interact with water molecules. This behavior is also observed in the adsorption isotherm at $a_w < 0.6$ (Figure 26b).

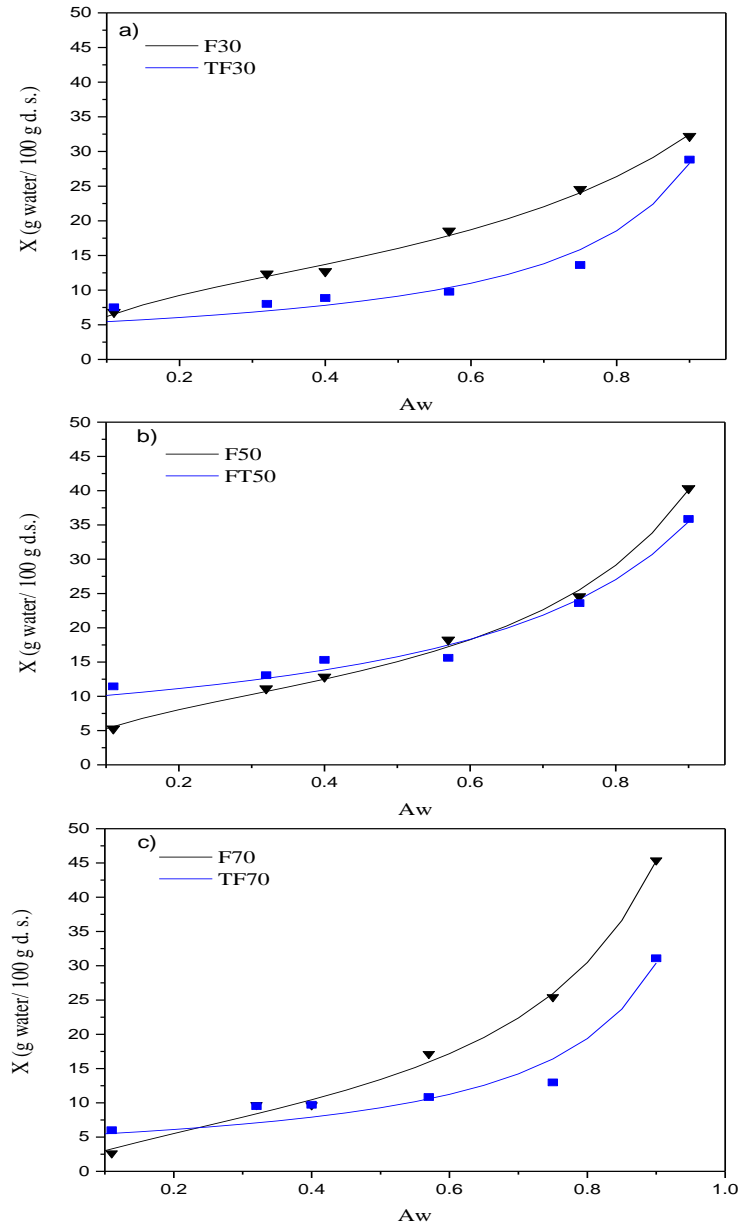


Figure 26. Adsorption isotherms of starch-based films from 30% a), 50% b) and 70% amylose c) before and after plasma treatment. Symbols are experimental data and the solid lines indicate the fitting using the GAB model. F30: film-30% amylose, F50: film- 50% amylose, F70: film- 70% amylose, TF30: treated film- 30% amylose, TF50: treated film- 50% amylose and TF70: treated film- 70% amylose.

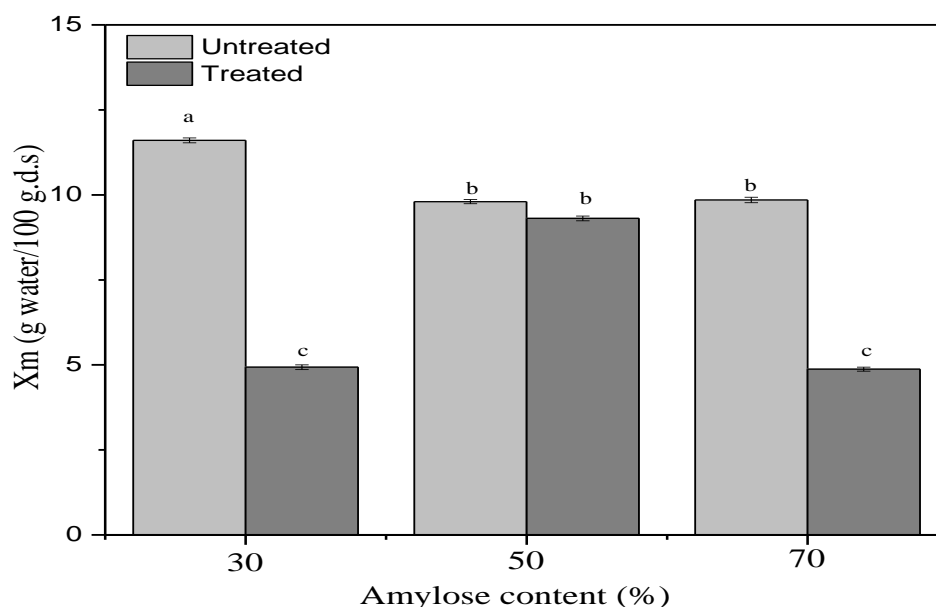


Figure 27. X_m values estimated from GAB model fitted to adsorption isotherms of starch-based films before and after plasma treatment. Error bars with different letters indicate significant differences ($P \leq 0.05$).

4.3.5 Mechanical properties

Tensile strength (TS), Young's modulus (YM) and elongation at break (%E) of the starch-based films before and after plasma treatment are shown in Figure 28a, b, c. Films made from high amylose starches showed the highest values of TS and YM. Several studies have reported this behavior (Rindlav et al., 2002; Romero-Bastida et al., 2015), which has been attributed to the capability of linear amylose chains to interact through hydrogen bonds to a higher extent than the branched amylopectin chains (Muscat et al., 2012). An increase in TS of the films was observed after the HMDSO plasma treatment (Figure 28a), probably caused by the HMDSO coat formed on the surface reinforcing the films and increasing the tensile strength. Furthermore, the changes in the orientation of the helices of starch molecules within the semi crystalline lamellae could have resulted in a compact structure which also increased TS. These results suggest that the simultaneous effect of HMDSO coating and the higher helical organization level observed by FTIR improved the TS of the films. In fact, an increment of 91 and 42% on TS was observed in TF30 and TF70,

respectively. This effect was more noticeable at TF30. However, TF50 only showed an increment of 11% suggesting a lower level of entanglement of amylopectin chains in the RGS as observed in the 1047/1022 ratio, which resulted in a weaker network compared with that of TF30 and F70 films. Young's modulus was also improved by plasma treatment as observed in Figure 28b. Apparently, HMDSO plasma treatment increased the film rigidity as the short-range crystallinity increased resulting in higher YM values.

Elongation at break (%E) showed the opposite behavior of TS and YM in untreated films. %E values decreased when the amylose content increased. Such behavior was expected since amylopectin is more sensitive to plasticizers than amylose (Lourdin et al., 1995). After the HMDSO plasma treatment, the %E value decreased in the starch-based films (Figure 28c). This behavior could be related to the compact rearrangement of starch structures during plasma treatment (Laovachirasuwan et al., 2010) which limits the extensibility of the polymeric chains. In this regard, the structures of TF30 were the most affected due to the lower proportion of linear structures (amylose) and the HMDSO coat resulted in a significant decrease of the %E values from 36 to 9%, providing lower flexibility to these films.

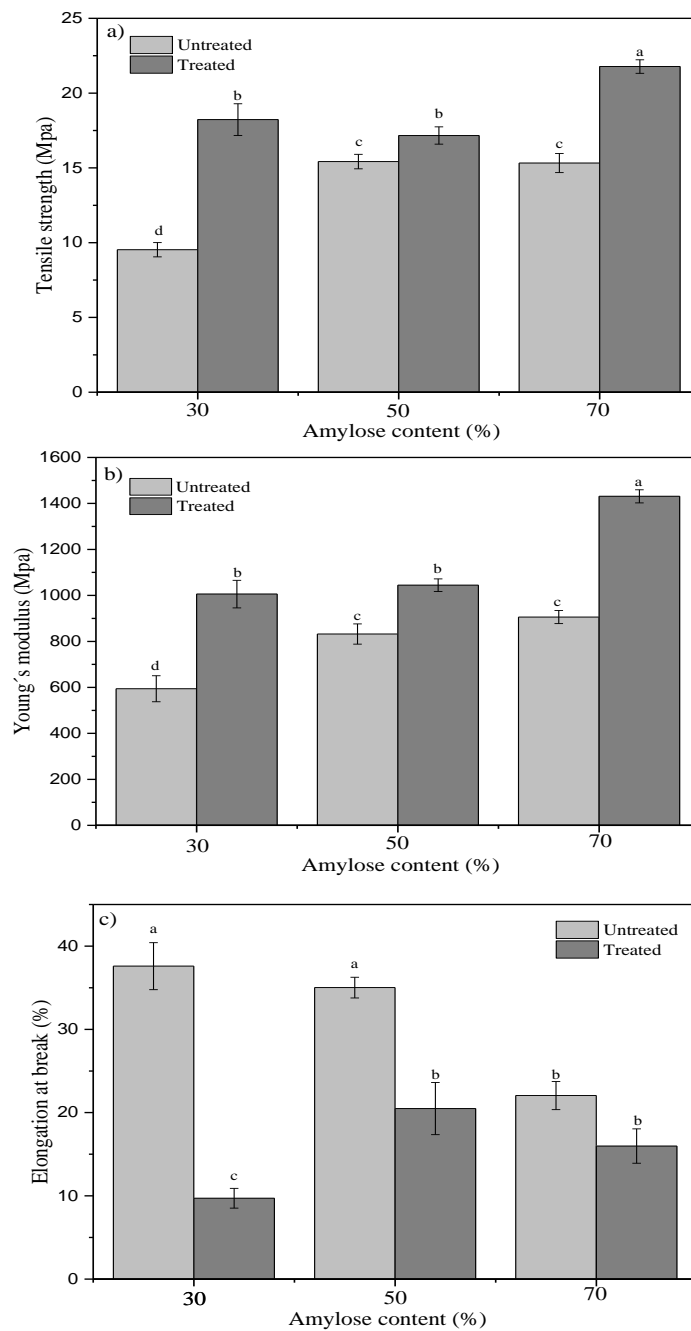


Figure 28. Mechanical properties of 30%, 50%, and 70% amylose starch-based films a) tensile strength, b) Young's modulus, and c) elongation at break. Error bars with different letters indicate significant differences ($P \leq 0.05$).

4.4 Conclusions

Results indicate that the amylose content, the extent of gelatinization, the remnant granules and the HMDSO coat played an important role on the structural, mechanical and barrier properties of the starch films. Films with 50% amylose showed that the disruption of its RSG released a higher amount of remnant amylopectin, which promoted the interaction with water molecules. FTIR analysis suggests a higher helix reorganization after HMDSO plasma treatment in all films, which led to compact structures that reduced water adsorption and increased the hydrophobicity of the films. However, this effect was lower in TF50. Likewise, the ordered structures reinforced the film matrix which, in combination with the HMDSO coating, improved the mechanical properties. The changes were observed in a higher extent in TF70 films. These results suggest that the HMDSO plasma treatment could be used to make starch-based films a suitable packaging material. According to the first objective of this thesis, the use of eco-friendly materials and technology like starch and cold plasma permitted to obtain films with structural, mechanical and barrier properties improved. Also, the obtained results allowed to propose an action mechanism of the species of plasma on the helical configuration of the starch.

Chapter 5. Influence of gelatinization process and HMDSO plasma treatment on the chemical changes and water vapor permeability of corn starch film

Abstract

In this study, surface, chemical, physicochemical and barrier properties of films treated with hexamethyldisiloxane (HMDSO) cold plasma were investigated. Normal and high amylose starches were gelatinized at different level to obtain films with different amount of free amylopectin. The obtained films were subjected to HMDSO plasma treatment. XPS analysis indicated chemical changes including substitution and crosslinking of the starch molecule, as reflected by the C-Si bond increasing and the C-OH bonds reduction on treated films. These changes modified the thermal transitions (T_m and ΔH). The highest amount of C-Si bonds was more noticeable in the TF50 film, suggesting a better interaction between active species of plasma and the free amylopectin released into the continuous phase of the film. Moreover, active species of plasma increased the crystallinity in all films. These results suggested that a higher helical packaging, crosslinking and hydrophobic blocking groups (C-Si) of starch molecules resulted in films with improved barrier performance against water molecules.

5.1 Introduction

This section describes the main mechanisms of cold plasma on the starch and the effect on its functional properties.

The global consumption of synthetic plastics like polyethylene, polypropylene and polystyrene has resulted in residue accumulation. Thus, the use of alternative raw materials like polysaccharides has been investigated to develop biodegradable plastics (Adamu et al., 2017; Paes et al., 2008; Rindlav et al., 2002). Corn starch is a renewable and biodegradable polymer with good film-forming properties (Manoel, et al., 2017). However, corn starch films are brittle, and plasticizers are added aiming to improve its flexibility by reducing the intermolecular bonds in the polymer matrix. Nevertheless, several authors have reported that the addition of plasticizers results in films with some disadvantages including high hydrophilicity and low performance under tensile tests (Edhirej et al., 2017; Sanyang et al., 2015). To overcome such drawbacks, physical modifications like cold plasma have been employed to improve films surface and therefore, barrier properties (Pankaj et al., 2015; Wiacek, 2015; Wiacek & Dul, 2015). Cold plasma includes electrons, free radicals, excited molecules and atoms, which in conjunction can modify chemical bonds on the starch structure promoting changes on the film surface. In this regard, reactive species of air, He, C₂H₂, and SF₆ plasma have shown effect in films made from starch as the plasma treatment forms hydrophobic channels on the surface reducing the hydrophilicity (Bastos et al., 2013). This effect has been more noticeable in films treated with HMDSO plasma mainly due to the formation of a hydrophobic HMDSO coating on the surface (Batan et al., 2010; De Albuquerque et al., 2014). In this regard, in a previous work we reported that the HMDSO coating not only resulted in hydrophobic properties of the films but also improved the mechanical properties (Sifuentes-Nieves et al., 2019). The effect of plasma treatment on the chemical structure of starch films has been investigated elsewhere (Santos et al., 2012). Pankaj et al. (2017) studied the effect of air plasma on films made from starch with different amylose content. The authors found, by XPS analysis, a higher surface

oxygenation after treatment, which derived an increasing of the C-O-H bonds specially in the low-amylose starch films. Bastos et al. (2012) investigated the chemical changes promoted by HMDSO plasma treatment on films made from normal corn starch. The authors reported a higher atomic concentration of Si (%) after treatment, which changed the barrier performance of the films. Recently, our group developed starch-based films, which were subjected to HMDSO plasma treatment. The structural order like short- range crystallinity (crystalline/amorphous ratio), barrier and mechanical properties were studied. However, the elucidation of the main mechanisms of plasma on starch molecules is important to understand the effects of HMDSO plasma treatment on the chemical structure and on the physicochemical properties of starch-based films. Thus, the objective of this study was to determine the effect of HMDSO plasma on the topography, chemical, physicochemical and barrier properties of films from corn starch with low and high amylose content and to inspect the effects due to the gelatinization extent.

5.2 Results and discussion

5.2.1 Topography

Atomic force microscopy (AFM) was used to study the effect of the extent of gelatinization and the HMDSO plasma treatment on the topography and the changes on the surface of the films. Figure 29a–c shows the morphology of untreated films, which exhibited a granular region mainly composed by remnant of amylopectin (RAM) embedded in a continuous matrix of amylose, as already described in similar studies (Bastos et al., 2009; De Albuquerque et al., 2014). The differences of RAM depended on the amylose content and on the extent of gelatinization of the starches, which resulted in different sizes and amount of granules as previously reported (Sifuentes-Nieves et al., 2019). Therefore, the effect of RMA and HMDSO plasma treatment on the surface roughness of the films was explored (Figure 29d–f). The roughness of films from untreated high-amylose starch (F70) was significantly different from that of F50 and F30 films (Figure 30). Such differences could be

attributed to the RAM observed in F70 films, which were dispersed in the continuous matrix (Figure 29a) resulting in a discontinuous surface on the films after the drying process.

Significant variations on the surface morphology of the treated films were observed (Figure 30). After plasma treatment, an increase in roughness from 100, 99 and 179 nm to 306, 532 and 529 nm was observed in TF30, TF50 and TF70 films, respectively. TF50 showed the highest effect promoted by a high amount of amylopectin released from RAM to the continuous matrix after the gelatinization process. The highest roughness values in TF50 suggest that this film was the most susceptible to etching, which is responsible for the increasing of the roughness of the films made from normal and high amylose starches (Pankaj et al., 2017; Santos et al., 2012).

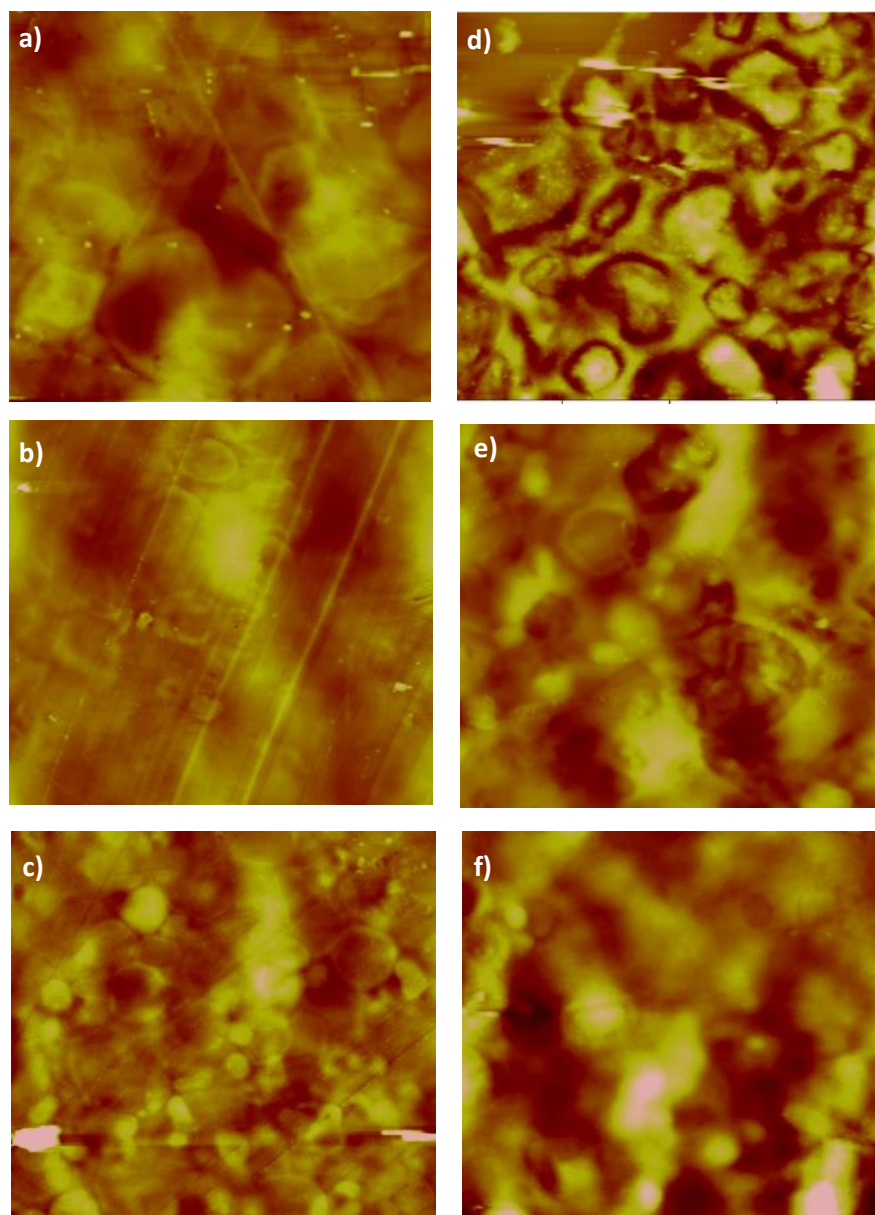


Figure 29.AFM images of starch films before and after treatment F30: film- 30% amylose a), F50: film- 50% amylose b), F70: film- 70% amylose c), TF30: treated film- 30% amylose d), TF50: treated film- 50% amylose e) and TF70: treated film- 70% amylose f).

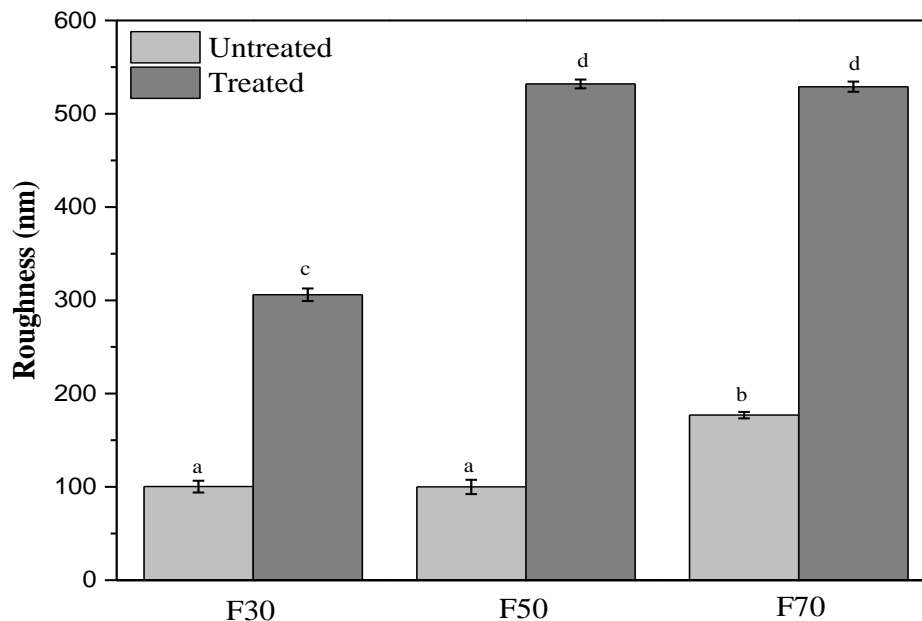


Figure 30. Roughness of starch films made from normal and high amylose starches before and after HMDSO plasma treatment. Error bars with different letters indicate significant differences ($P \leq 0.05$). F30: film- 30% amylose, F50: film- 50% amylose, F70: film- 70% amylose.

5.2.2 X-ray photoelectron spectroscopy

X-ray photoelectron spectroscopy (XPS) was used to study the molecular structure of treated and untreated films made from corn starch with different amylose content (Figure 31). The elemental composition of all films showed peaks corresponding to C1s and O1s, which contained elements of C, O and H (Bastos et al., 2013; Pankaj et al., 2015); additionally, peaks of Si 2s and Si 2p were observed (Bie et al., 2016; Morent et al., 2009).

The C1s peaks of all films were deconvoluted (Figure 32) to identify the chemical bonds between different elements (Table 3). Untreated films showed spectral peaks at 284.6, 286.3 and 288.3 eV corresponding to C-C or C-H, C-O or C-OH and O-C=O bonds, respectively (Santos et al., 2012; Pankaj et al., 2017). HMDSO plasma treatment resulted in a decreasing of the proportions of C-C, C-OH and O-C=O.

These changes could be associated with the breaking and oxidation of starch molecules, resulting in new free radicals, which reacted with the activated HMDSO species forming new chemical bonds like starch molecule substitution. In this regard,

C-Si interactions were observed after treatment. TF50 films showed more C-Si interactions compared with TF30 and TF70 films, suggesting that the high amount of free amylopectin content in the continuous matrix was more susceptible to chemical substitution.

Moreover, a disruption of the C-OH groups was promoted by HMDSO plasma treatment. This behavior suggests a chemical mechanism where the active species of plasma react with two or more hydroxyl groups resulting in a covalent crosslinking of α -D-glucose units (Zou et al., 2004). The highest concentration of C-C and the lowest of C-OH in TF70 films suggest a high crosslinking.

Additionally, the O-C=O peaks disappeared after treatment suggesting that the active species of HMDSO plasma reduced the oxidized species in the films promoting the chemical modification of starch (crosslinking and substitution).

Furthermore, the Si 2p peaks were deconvoluted to identify silicon bindings in the treated films (Table 4). HMDSO plasma-treated films showed four component peaks in the atomic binding states of HMDSO corresponding to $(\text{CH}_3)_3\text{-Si-O}$, $(\text{CH}_3)_2\text{-Si-O}_2$, $\text{CH}_3\text{-Si-O}_3$ and Si-O_4 units (Moon et al., 2009). The major contribution of HMDSO in all treated films was $(\text{CH}_3)_2\text{-Si-O}_2$ units (Table 4), where TF50 and TF70 showed a higher concentration of these silicon bonds than TF30, suggesting that the free amylopectin and large amylose chains in TF50 and TF70 resulted in a different interaction with active species of HMDSO. The same $(\text{CH}_3)_2\text{-Si-O}_2$ units were reported in HMDSO-based coatings on PET, which showed similar characteristics to the deposits obtained by linear polymer of poly-dimethylsiloxane (PDMS). However, HMDSO treatment induced a higher silicon oxidation in TF30 than in high amylose treated films. Such behavior could be attributed to the higher proportion of Si-O_4 units and smaller amount of $(\text{CH}_3)_3\text{-Si-O}$, which suggest that the groups of branched amylopectin in TF30 were more available to react yielding silicon oxidized groups, which have been associated with inorganic character and chemically resemble to SiO_2 (Morent et al., 2009).

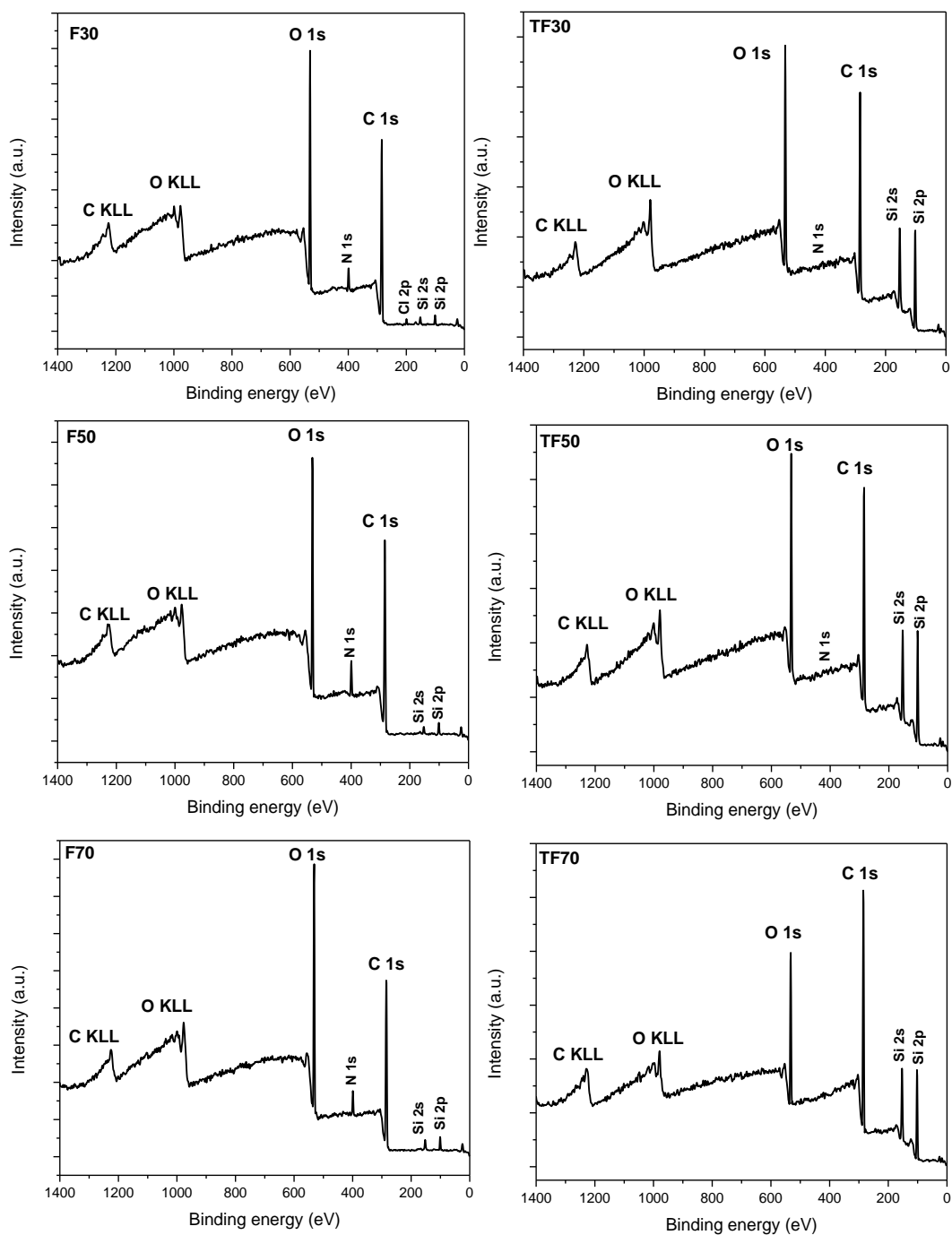


Figure 31. XPS spectra of starch films made from normal and high amylose starches before and after HMDSO plasma treatment. F30: film- 30% amylose, F50: film- 50% amylose, F70: film- 70% amylose, TF30: treated film- 30% amylose, TF50: treated film- 50% amylose and TF70: treated film- 70% amylose.

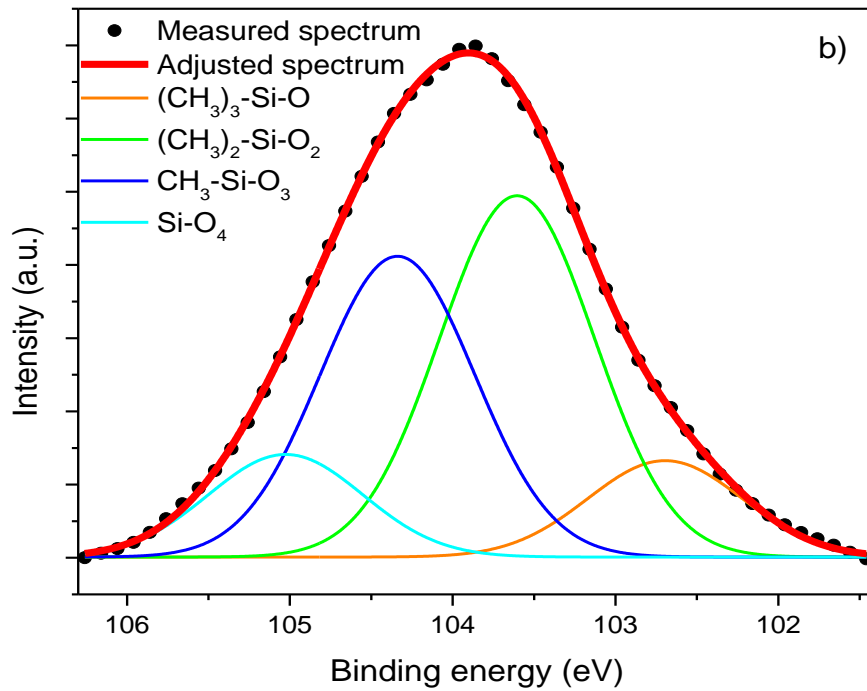
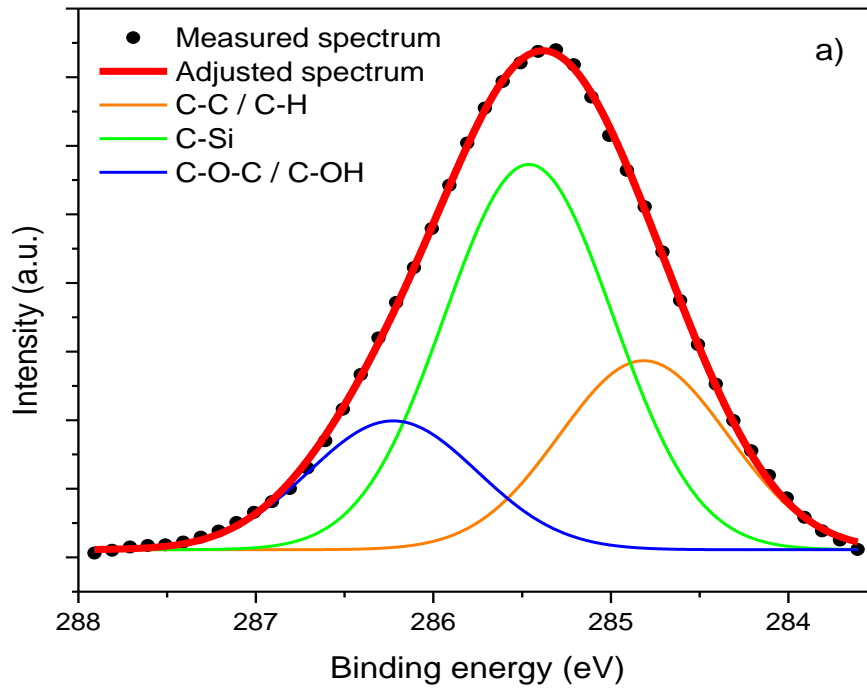


Figure 32. Example of deconvoluted XPS spectrum a) C1s and b) Si 2p

Table 3. C1s peaks of starch films observed before and after plasma treatment.

Sample	C-C or C-H	C-Si	C-O or C-OH	O-C=O
F30	0.55	-----	0.40	0.05
F50	0.47	-----	0.41	0.12
F70	0.41	-----	0.51	0.07
TF30	0.25	0.56	0.18	-----
TF50	0.33	0.60	0.07	-----
TF70	0.55	0.45	-----	-----

F30= film- 30% amylose; **F50**= film- 50% amylose; **F70**= film- 70% amylose; **TF30**= treated film- 30% amylose; **TF50**= treated film- 50% amylose; **TF70**= treated film- 70% amylose.

Table 4. Deconvolution of Si 2p peak for HMDSO plasma-treated films.

Sample	(CH ₃) ₃ -Si-O	(CH ₃) ₂ -Si-O ₂	CH ₃ -Si-O ₃	Si-O ₄
	(%)	(%)	(%)	(%)
TF30	10.5	42.7	35.5	11.2
TF50	15.1	51.4	32.5	1.0
TF70	26.9	48.2	24.8	-----

TF30= treated film- 30% amylose; **TF50**= treated film- 50% amylose; **TF70**= treated film- 70% amylose.

5.2.3 X-ray diffraction

The X ray diffractograms (XRD) of treated and untreated films are shown in Figure 33. Untreated films made from normal corn starch (F30) showed an A-type X-ray diffraction pattern with peaks at 15.1, 16.8, 17.8 and additional peaks at 19.4 and 22.9°. On the other hand, films made from high amylose starches (F50 & F70) displayed a B-type X- ray diffraction pattern with peaks at 5.5, 14, 17, 20, 22 and 24°. However, unlike previous reported results (Pankaj et al., 2015), no changes were observed in the crystal structure of the films after HMDSO plasma treatment. Additionally, the effect of amylose content and HMDSO plasma on the relative crystallinity (RC) of the films was evaluated (Figure 34). Untreated high amylose starch films showed a higher RC value compared with that of films made from a lower amylose content. This behavior could be explained because the amylose chains undergo a faster rearrangement of its helical order than the amylopectin during the drying process (Zhang et al., 2007). The plasma treatment modified the RC values in all films. An increment of 13, 5 and 4% in RC was observed in TF30, TF50 and TF70 films, respectively. These results suggest a modification of the amorphous regions by active species of plasma (Laovachirasuwan et al., 2010), resulting in a better packaging of amylopectin branch chains in double helix form. Similar behavior has been found in the short-range crystallinity of starch- based films after HMDSO plasma treatment (Sifuentes-Nieves et al., 2019). Moreover, the results indicate a better reorganization of amylopectin in the partially gelatinized granules of TF30, which contain more amylopectin than TF50 and TF70 films. The high amount of amylopectin and the extent of gelatinization reached in TF50, prevented the structure reorganization, decreasing the RC; in addition, the available amylopectin reacted with the HMDSO species as shown in XPS.

In addition, the treatment used was a vacuum cold plasma system, which at 70 W of input power could reach a temperature of 40–45 °C in the reactor during the treatment and that could have contributed to minor changes in the films. It has been reported that at a temperature close to 50 °C, the gelatinized and retrograded

amylopectin could disorganize again and decrease the relative crystallinity (Karim, Norziah, & Seow, 2000).

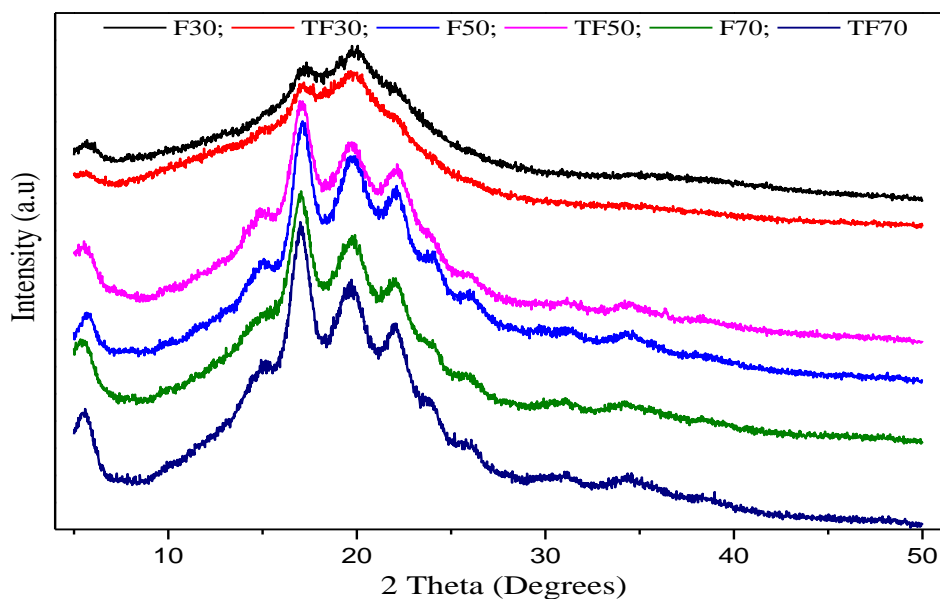


Figure 33. XRD spectra of starch films made from normal and high amylose starches before and after HMDSO plasma treatment. F30: film- 30% amylose, F50: film- 50% amylose, F70: film- 70% amylose, TF30: treated film- 30% amylose, TF50: treated film- 50% amylose and TF70: treated film- 70% amylose.

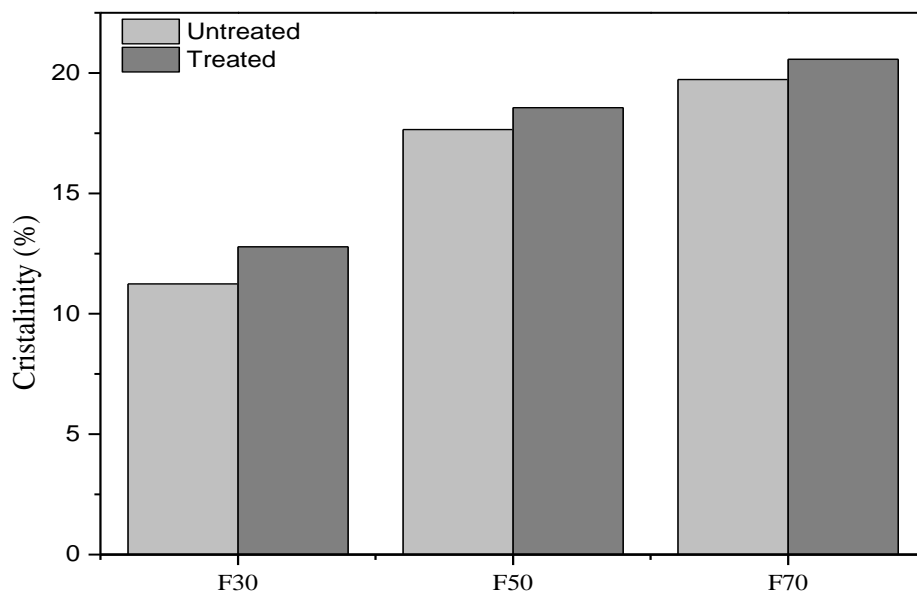


Figure 34. Relative crystallinity of starch films from normal and high amylose starches before and after HMDSO plasma treatment. F30: film- 30% amylose, F50: film- 50% amylose, F70: film- 70% amylose.

5.2.4 Differential scanning calorimetry

Differential scanning calorimetry (DSC) was employed to determine the thermal transitions of starch films before and after HMDSO plasma treatment (Table 5). Untreated films showed a typical endotherm of semi-crystalline materials at 165 and 168 °C in films from normal and high amylose starches, respectively (Figure 35). This behavior has been related with the melting (T_m) of the crystalline structure of starch (Laovachirasuwan et al., 2010; Pankaj et al., 2015). In this regard, the high T_m value observed in F70 could be associated to its high crystallinity as observed in the XRD results.

In general, HMDSO plasma treatment increased the T_m values in the films. This behavior could be attributed to the concomitant increase of crystallinity, chemical substitution (C-Si) and crosslinking of starch matrix as observed by XRD and XPS analysis. These changes restricted the mobility of amylopectin chains due to the rearrangement of the helical order and chemical interactions induced by reactive species of plasma increasing the melting temperature of the treated films. Similar behavior has been observed in HMDSO plasma-treated polymers for fire-retardant purposes (Bardon et al., 2015; Scharrel et al., 2002). Moustapha et al. (2017) studied a polyolefin and polystyrene laminate system covered by an inorganic SiO_2 layer deposited from HMDSO/ O_2 , finding a decrease of weight loss and improvement of the thermal resistivity, which corroborated the high effectivity of silicone and silica-based compounds as fire protection coatings.

Moreover, the effect of amylose content and plasma treatment on the enthalpy (ΔH) was evaluated to determine the stability of the film matrix. Untreated films made from high amylose starch showed the highest values of ΔH , since a high crystallinity has been associated with more energy needed to disassemble the highly-organized structure (Warren et al., 2016). Lower ΔH values were observed in the films after HMDSO plasma treatment (Table 5) suggesting that the new interactions in the starch molecule resulted in more imperfections compared to untreated films. This behavior can be attributed to the C-Si interactions since it has been reported that the chemical modification (substitution) prevents the reassociation of starch molecules

(Senanayake et al., 2014). These changes did not allow the perfection of starch crystals as suggested by the ΔT values for treated films. In this regard, the ΔH values decreased proportionally to the increase of C-Si % and ΔT suggesting a crystalline structure with lower perfection and a more heterogenous structure than that of untreated films. This effect was more noticeable in TF50 because of the high amount of amylopectin lixiviated during the gelatinization.

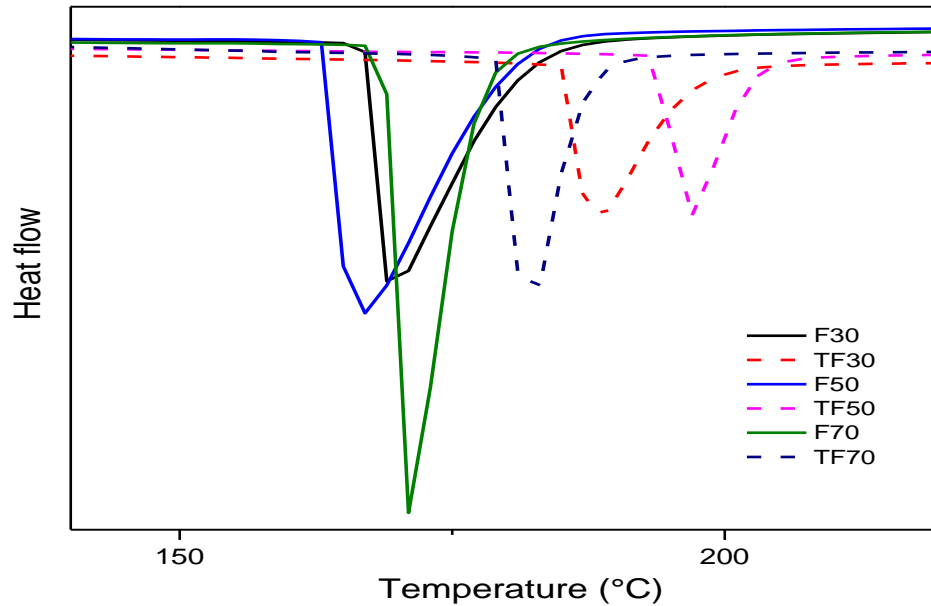


Figure 35. DSC thermograms of starch films from normal and high amylose starches before and after HMDSO plasma treatment. F30: film- 30% amylose, F50: film- 50% amylose, F70: film- 70% amylose, TF30: treated film- 30% amylose, TF50: treated film- 50% amylose and TF70: treated film- 70% amylose.

Table 5. Thermal properties of starch films from normal and high amylose starches before and after HMDSO plasma treatment.

Sample	T _m (°C)	ΔH (J/g)	ΔT (°C)
F30	165.42 ± 2.22 ^a	177.24 ± 3.21 ^a	6.41
F50	168.05 ± 1.18 ^a	180.56 ± 3.51 ^a	10.06
F70	168.70 ± 0.68 ^a	182.07 ± 3.41 ^a	6.80
TF30	189.67 ± 1.75 ^b	86.22 ± 1.33 ^c	8.49
TF50	194.40 ± 1.53 ^b	61.02 ± 0.27 ^b	10.68
TF70	180.92 ± 0.23 ^c	105.13 ± 0.50 ^d	7.13

Values with different letters in the same column indicate significant differences (P ≤ 0.05). **T_m**= melting temperature; **ΔH**= enthalpy; **ΔT**= temperature differential.

F30= film- 30% amylose; **F50**= film- 50% amylose; **F70**= film- 70% amylose; **TF30**= treated film- 30% amylose; **TF50**= treated film- 50% amylose; **TF70**= treated film- 70% amylose.

5.2.5. Water vapor permeability

The water vapor permeability (WVP) of untreated and treated films was evaluated (Figure 36). Untreated F30 film showed lower WVP values compared with those of films made from high amylose starches. This behavior could be explained by the partial gelatinization of this starch that resulted in a higher RAM content with an important amount of amylopectin that confers hydrophobic properties (Garcia-Hernandez et al., 2017; Sifuentes-Nieves et al., 2019a). The HMDSO plasma treatment resulted in films with hydrophobic properties leading to a significant decrease of WVP values. This effect can be attributed to changes in the orientation of double helices (packaging) in the starch crystals and the crosslinking or substitution promoted by the HMDSO plasma treatment. A WVP decrement of 31, 59 and 41% was observed in TF30, TF50 and TF70 films, respectively. In a previous study (Sifuentes-Nieves et al., 2019a), we reported that the TF50 film showed

hydrophilic properties with high water absorption and plasticization effects of the water molecules. In this study we noticed that the TF50 film showed the lowest values of WVP suggesting that the introduction of hydrophobic groups (C-Si) along the amylopectin chains stabilized the starch structure in the film matrix, resulting in reduced diffusion of water molecules. These structural rearrangements lead to a more compact and hydrophobic path for the water vapor molecules, decreasing its adsorption and diffusion throughout the film.

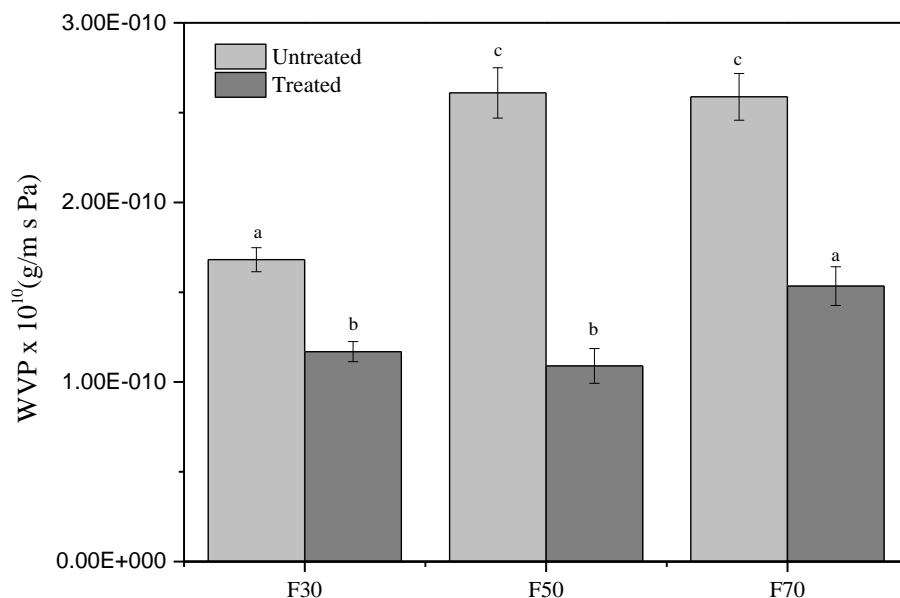


Figure 36. Water vapor permeability of starch films from normal and high amylose starches before and after HMDSO plasma treatment. Error bars with different letters indicate significant differences ($P \leq 0.05$). F30: film- 30% amylose, F50: film- 50% amylose, F70: film- 70% amylose.

5.3. Conclusions

Significant chemical changes were observed in all films after HMDSO plasma treatment. According to XPS analysis the film elaborated from completely gelatinized starch (TF50) was the most reactive to HMDSO plasma which resulted in C-OH and C-Si changes. The results suggest that the lixiviated amylopectin was more susceptible to crosslinking and substitution. Moreover, a higher amount of blocking groups (C-Si) resulted in low diffusion of water vapor molecules throughout the treated films, which in conjunction with the increase on crystallinity, resulted in a significant reduction of water vapor permeability. These results provide value insights of the improvement in the performance of the films after the HMDSO plasma treatment.

According to the second objective of this thesis, it was proposed an action mechanism of specific active species of plasma and its effect on the starch films, which explained the changes in the physicochemical and barrier properties.

Chapter 6. HMDSO plasma treatment as alternative to modify structural properties of granular starch

Abstract

In the present study, the effect of plasma treatment on the structural properties of three granular corn starches (normal, Hylon V and Hylon VII) was investigated. Thermal (TGA/DSC), structural (XRD/FTIR) and chemical (XPS) properties were evaluated. Plasma treatment resulted in partial evaporation of water molecules changing the organization level of the double helices in the crystalline lamellae. Moreover, XRD results suggested a decrease of the long-range crystallinity and suggested changes in amylose chains after treatments. The crosslinking of modified amylose chains measured by XPS analysis resulted in variations in the gelatinization parameters as well as in its heterogeneous crystalline structure. The results indicate that the type and extent of changes in the structure of plasma-treated corn starch depends on the distribution of the water molecules inside the crystalline regions (helical water) and on the amylose content. In addition, the obtained results indicated that plasma treatment is a suitable method to modify starch without any incorporation of new elements from hexamethyldisiloxane (HMDSO), which only promotes stronger interactions between the starch main components.

6.1. Introduction

This section describes the advantages of physical modification of granular starch compared to conventional chemical methods, emphasizing the changes in structural properties.

Starch is one of the most studied biopolymers since it is considered as the major source of energy in the human diet. Over the last century, numerous studies have focused on understanding it and much has been written concerning to the starch structure changes after chemical or physical modifications (Capron et al., 2007; Miles et al., 1985; Pérez & Bertoft, 2010; Pfister & Zeeman, 2016; Tester & Qi, 2004). Starch modifications intended to enhance the functional properties that are relevant to industrial applications usually lead to structural changes affecting its supramolecular structure (Korma et al., 2016). In this regard, differences in amylose content, amylopectin fine structure and the way they are organized within granules, give rise to variability in structure and functionality of starch (Copeland et al., 2009; Wang et al., 2014).

Nowadays, there are four types of starch modifications (chemical, physical, enzymatic and genetic), which change the functionality of the modified starch; among them, chemical modification is the most used (Masina et al., 2017). However, this procedure generates chemical residues during the starch treatment causing environmental concern. Alternative methods like physical modification of starch is attracting attention since they do not generate residuals during the treatment (Thirumdas et al., 2017; Zhu, 2017). Cold plasma treatment has been used as a physical method to modify starch although, the alteration mechanisms are still under study (Thirumdas et al., 2015). Zou et al. (2004) suggested that the active species of argon plasma could collapse the hydroxyl groups of the amylose and amylopectin chains promoting crosslinking. Moreover, Wongsagonsup et al. (2014) reported two competitive reactions (crosslinking and depolymerization) during argon plasma treatment on starch, where the predominant effect was determined by the sample preparation and the input power for the plasma treatment.

The supramolecular changes on the starch after plasma treatment have been also studied. Bie et al. (2016) discovered that the oxygen and helium plasma treatment disorganized the starch crystallites with low perfection and thermal stability, decreasing the double helices alignment within the crystalline lamellae. However, so far there is not a clear understanding of the structural changes taking place due to the physical plasma treatment. Moreover, to our knowledge, the changes in structure and functionality of plasma-treated granules as a function of amylose and amylopectin content and their organization within granules has not been elucidated. Therefore, the aim of this work was to evaluate the effect of the low-pressure HMDSO plasma on the structure of corn starches with different amylose content. The effect of plasma treatment and changes in the structure were assessed using TGA, XRD, FTIR, XPS and DSC techniques.

6.2 Results and discussion

6.2.1 Thermal behavior (TGA)

Figure 37 presents the drying curves of native and modified corn starches. Normal (S30) and high amylose starches (S50 & S70) showed a weight loss (WL) curve associated to water vaporization, which decreased after plasma treatment. Vacuum plasma treatment resulted in water molecules removal thus reducing the WL by 5.24, 23.12 and 15.48 % for treated starches with 30, 50 and 70% amylose (TS30, TS50 and TS70, respectively). The modified high amylose starches were the most affected by HMDSO plasma treatment since they have a B-type arrangement containing more helical water in the crystals resulting in more free radicals during the treatment. Loss of water molecules might result in structural and supramolecular rearrangements in long and short-range crystallinity of the amylose and amylopectin molecules.

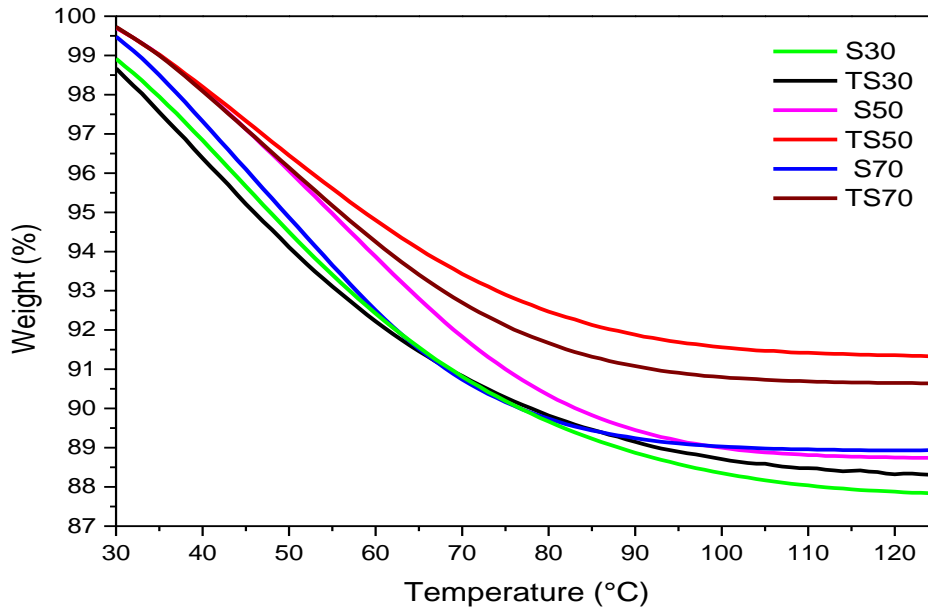


Figure 37. Drying curves from TGA analysis of native and modified corn starches with different amylose content. S30: starch- 30% amylose, S50: starch- 50% amylose, S70: starch- 70% amylose, TS30: treated starch- 30% amylose, TS50: treated starch- 50% amylose and TS70: treated starch- 70% amylose.

6.2.2 Crystalline structure

X-ray diffraction spectra of native and modified corn starches with different amylose content are presented in Figure 38. The crystalline regions consist of double helices of amylopectin, which are arranged in either A or B type unit cells. The characteristic A-type pattern was observed in S30 with peaks located at 15°, 16°, 17° and two additional peaks at 19° and 22°. Different intensity peaks at 5.5°, 14°, 17°, 20°, 22° and 24° were detected in S50 & S70, which corresponds to a B-type diffraction pattern.

The diffraction pattern did not change after HMDSO plasma treatment, but differences in the intensity of some peaks of native and modified starches were identified, resulting in changes in the calculated relative crystallinity (RC). A significant decrement of 12, 43 and 18% in the RC was detected for TS30, TS50 and TS70, respectively. This behavior suggests that the B-type crystals are more

susceptible to free radicals attack than the A- type crystals, due to a more open and hydrated structure, which contains larger amount of inter-helical water (Zhang et al., 2013). In addition, the reduction of crystallinity indicated a decrement in the size and in the amount of crystallites, probably due to the interruption of hydrogen bonds after the treatment, which stabilized the short-range double helices and kept linked the inter-helical water (Bie et al., 2016; Pérez & Bertoft, 2010). Also, Waigh et al. (2000) postulated a self-assembly mechanism for the orientation of amylopectin double helices in presence of water. This orientation could be disturbed due to dehydration of the granules (Waigh et al., 1997), as shown in TGA results. The collapsing of the structure was more notable for TS50 and TS70.

The differences of RC between TS50 and TS30 could be related with the proportion of amylopectin and water molecules in the granule (Hanashiro et al., 1996). The susceptibility of amorphous region to attack by the reactive species of plasma could disrupt the α -1,6 branch linkages in TS50 resulting in a decrease of its crystallinity. Also, most of the branch linkages in B-type crystals of S50 are located in the amorphous regions (Jane et al., 1997), which is most susceptible to plasma treatment (Laovachirasuwan et al., 2010).

Moreover, after normalizing the spectra, the intensity peaks at 14° and 20° decreased in the modified high amylose starches (Figure 38). According to Agama-Acevedo et al. (2018) and Gernat et al. (1993) such peaks are related to amylose helices and complexes. Therefore, its disappearance suggests a modification of single helices of amylose in TS50 & TS70 as a result of the exposition and susceptibility of the molecules to the attack by active species of plasma.

A similar behavior was reported by Zhang et al. (2014); they found that the oxygen plasma treatment decomposed the inter-helical water molecules in the starch crystalline structure resulting in free oxygen, hydroxyl, and hydrogen radicals, which caused damage to the starch crystallinity but also was available to react with the active species of plasma.

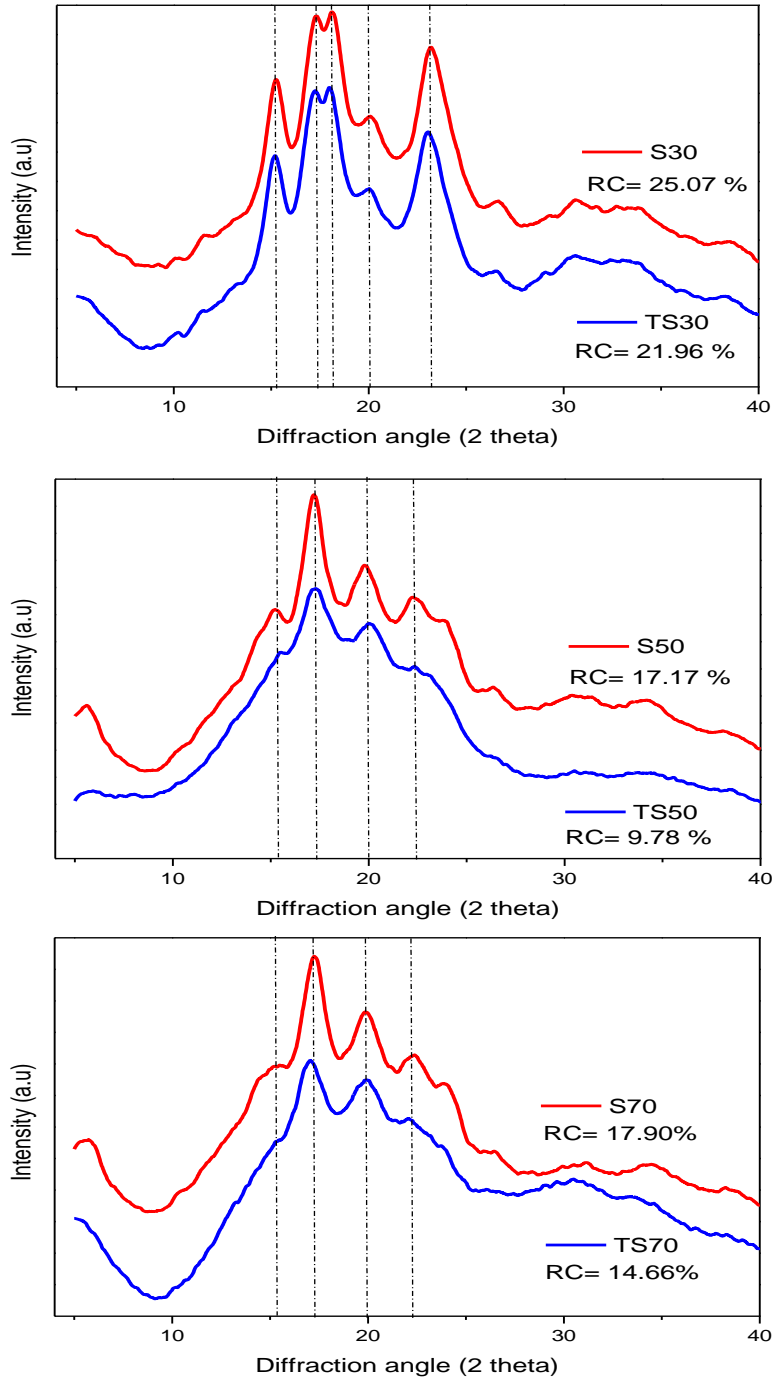


Figure 38. X ray diffraction spectra of native and modified corn starches with different amylose content. RC= Relative crystallinity. S30: starch- 30% amylose, S50: starch- 50% amylose, S70: starch- 70% amylose, TS30: treated starch- 30% amylose, TS50: treated starch- 50% amylose and TS70: treated starch- 70% amylose.

6.2.3 Double helices and order degree

The FTIR spectra of native and modified corn starches are shown in Figure 39. After normalizing the spectra using the 1082 cm^{-1} band, all treated starches showed a remarkable decrease in the intensity of the bands at 3300 cm^{-1} (-OH groups) and 1648 cm^{-1} (water molecules), suggesting that the vacuum used during treatment promoted the removal of some water molecules from the starch (Lii et al., 2002), as observed by TGA and X-ray results. The removal of water resulted in rearrangements at the structural and supramolecular level promoting the collapse of the amylopectin structure. This effect was most noticeable in the modified high amylose starches due to its B-type crystallites which have more structural water molecules than the A-type crystals.

To identify the supramolecular changes after plasma treatment, the FTIR spectrum in the $950\text{--}1100\text{ cm}^{-1}$ region was explored to inspect the short-range crystallinity (Sevenou et al., 2002). The absorption bands at 1047 and 995 cm^{-1} are related with the crystalline region and the hydrated ordered domains, whereas the absorption band at 1022 is linked with the amorphous domains (Capron et al., 2007; Van Soest et al., 1995). The deconvolution of these peaks allowed calculating the intensities and the $995/1022$ and $1047/1022$ ratios (Figure 40). The ratios of those intensities can be used to determine the degree of double helices and the order degree, respectively (Bie et al., 2016). As previously mentioned, the removal of some water molecules in the modified starches influenced the supramolecular structure affecting its order and the double helices degree (Bogracheva et al., 2001). After HMDSO plasma treatment, the $1047/1022$ ratio increased slightly in TS30 and TS50 suggesting its compactness, which is associated with the crystal and amorphous lamellae density of the starch granule, arranged at shorter length scale (Table 6). Apparently, amylopectin chains in TS30 required less amount of water molecules in the crystalline lamellae (Pérez & Bertoft, 2010) to reach a higher ordering of the double helices and the amount of amylopectin in TS50 favored the arrangement compared to TS70, which in conjunction with the single helix disruption, restricted significantly the alignment of the starch molecules.

The B-type crystals like those of TS50 and TS70 contain more water molecules in their structure (Tester et al., 2004). When the moisture is limited, the water molecules are distributed between the crystalline and the amorphous regions and the proportions of double helices are restricted (Bogacheva et al., 2002). In this study, modified high amylose starches showed a low 995/1022 intensity ratio (Table 6), suggesting that the low amount of water molecules in the crystalline lamella and the distribution of amylose in the granule, made it more available to the reactive species of plasma, reducing the amylose segments and limiting the helical interactions. In TS30, the increase in 995/1022 ratio suggests the formation of double helices into crystallites with additional hydrogen bonds, holding the polymeric chains together.

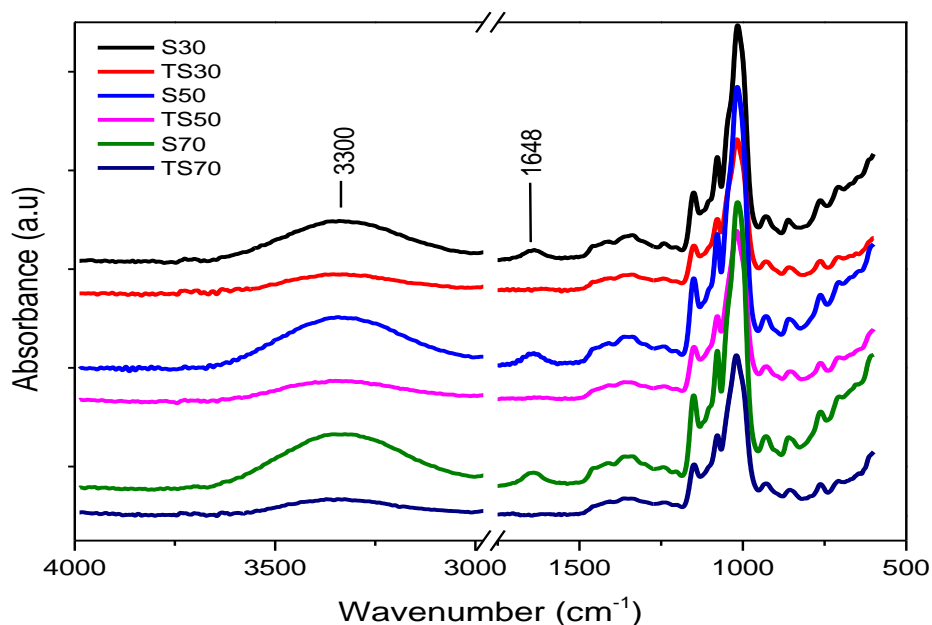


Figure 39. FTIR spectra of native and modified corn starches with different amylose content. S30: starch- 30% amylose, S50: starch- 50% amylose, S70: starch- 70% amylose, TS30: treated starch- 30% amylose, TS50: treated starch- 50% amylose and TS70: treated starch- 70% amylose

Table 6. Intensity 1047/1022 and 995/1022 ratio of native and modified corn starches with different amylose content.

Sample	1047/1022 Ratio	995/1022 Ratio
S30	0.18	0.47
TS30	0.20	0.56
S50	0.17	0.44
TS50	0.19	0.41
S70	0.13	0.35
TS70	0.06	0.25

S30= starch- 30% amylose; **S50**= starch- 50% amylose; **S70**= starch- 70% amylose; **TS30**= treated starch- 30% amylose; **TS50**= treated starch- 50% amylose; **TS70**= treated starch- 70% amylose.

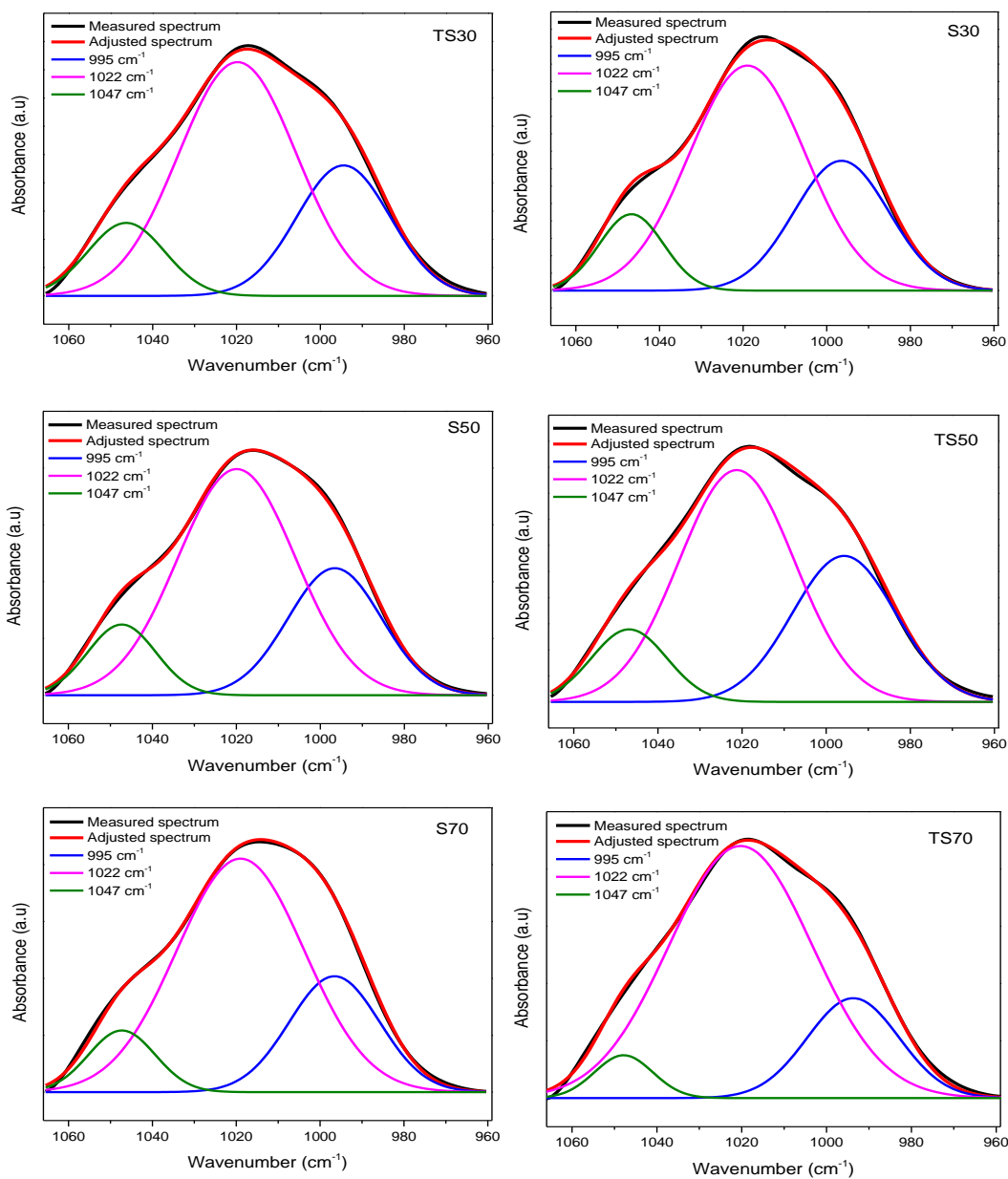


Figure 40. Deconvoluted peaks at 1047, 1022 and 995 cm⁻¹ of native and modified corn starches with different amylose content. S30: starch- 30% amylose, S50: starch- 50% amylose, S70: starch- 70% amylose, TS30: treated starch- 30% amylose, TS50: treated starch- 50% amylose and TS70: treated starch- 70% amylose

5.3.4 XPS analysis

The elemental composition of native and modified corn starches is presented in Table 7. A decrement of O/C atomic ratio was observed after HMDSO plasma treatment suggesting a reduction of oxygenated groups on the starch.

The C1s peaks of all starches were further deconvoluted to identify the chemical groups (Figure 41). The C 1s signal in all starches showed peaks at 284.8, 286.3, 287.6 and 288.9 eV, corresponding to C-C/C-H, C-O/C-OH, O-C-O/C=O and O-C=O, respectively (Saad et al., 2011; Wei et al., 2014). After treatment, no new peaks were observed in the XPS spectra, indicating that the HMDSO plasma did not introduce any new elements into the starch molecule.

However, during the treatment some of the remaining inter-helical water molecules in the crystalline structure could be induced by the active species of HMDSO plasma to lead new

active species, such as free radicals of oxygen, carbon and hydrogen, which promoted the interactions between elements of the starch molecule. The large amount of inter-helical water molecules in each crystal unit of the B-type crystalline structure of S50 and S70 originated more active species than S30, which could be related to the significant decrement of carbon atoms bonded to single hydroxyl groups (C-OH) in TS50 and TS70 (Table 7) or related to water removal during the plasma treatment. Such behavior was also observed in FTIR, where the band associated with OH (3300 cm^{-1}) decreased. In this regard, two possible reactions, oxidation and crosslinking, have been associated to hydroxyl groups reduction. The oxidation was not considered in this study since no signal of carbonyl or carboxyl group was observed in FTIR analysis at 1720 cm^{-1} (Bie et al., 2016). Therefore, the reduction of C-OH indicates the crosslinking of the starch molecule as the plasma treatment is able to collapse hydroxyl groups (Zou et al., 2004) and increase the C-C interactions as observed in all modified starches. TS50 and TS70 were the most affected mainly due to the high proportion and the allocation of amylose, resulting in a higher amount of groups available for crosslinking, increasing the C-C proportions in 66 and 163% and decreasing the C-OH in 31 and 49%, respectively. These results

indicate that the HMDSO plasma treatment could be a good alternative to modify the structural properties of granular starch in the same way as conventional chemical modification methods.

Table 7. O/C atomic ratio and C1s peaks of native and modified maize starches with different amylose content.

Sample	O/C*	C-C/ C-H	C-O/C-OH	O-C-O/ C=O	O-C=O
S30	0.71	0.24	0.64	0.12	---
TS30	0.59	0.34	0.49	0.11	0.06
S50	0.69	0.24	0.65	0.11	---
TS50	0.50	0.40	0.46	0.11	0.03
S70	0.63	0.22	0.66	0.12	---
TS70	0.47	0.58	0.34	0.08	---

*O/C atomic ratio of oxygen to that of carbon element. **S30**= starch- 30% amylose; **S50**= starch- 50% amylose; **S70**= starch- 70% amylose; **TS30**= treated starch- 30% amylose; **TS50**= treated starch- 50% amylose; **TS70**= treated starch- 70% amylose.

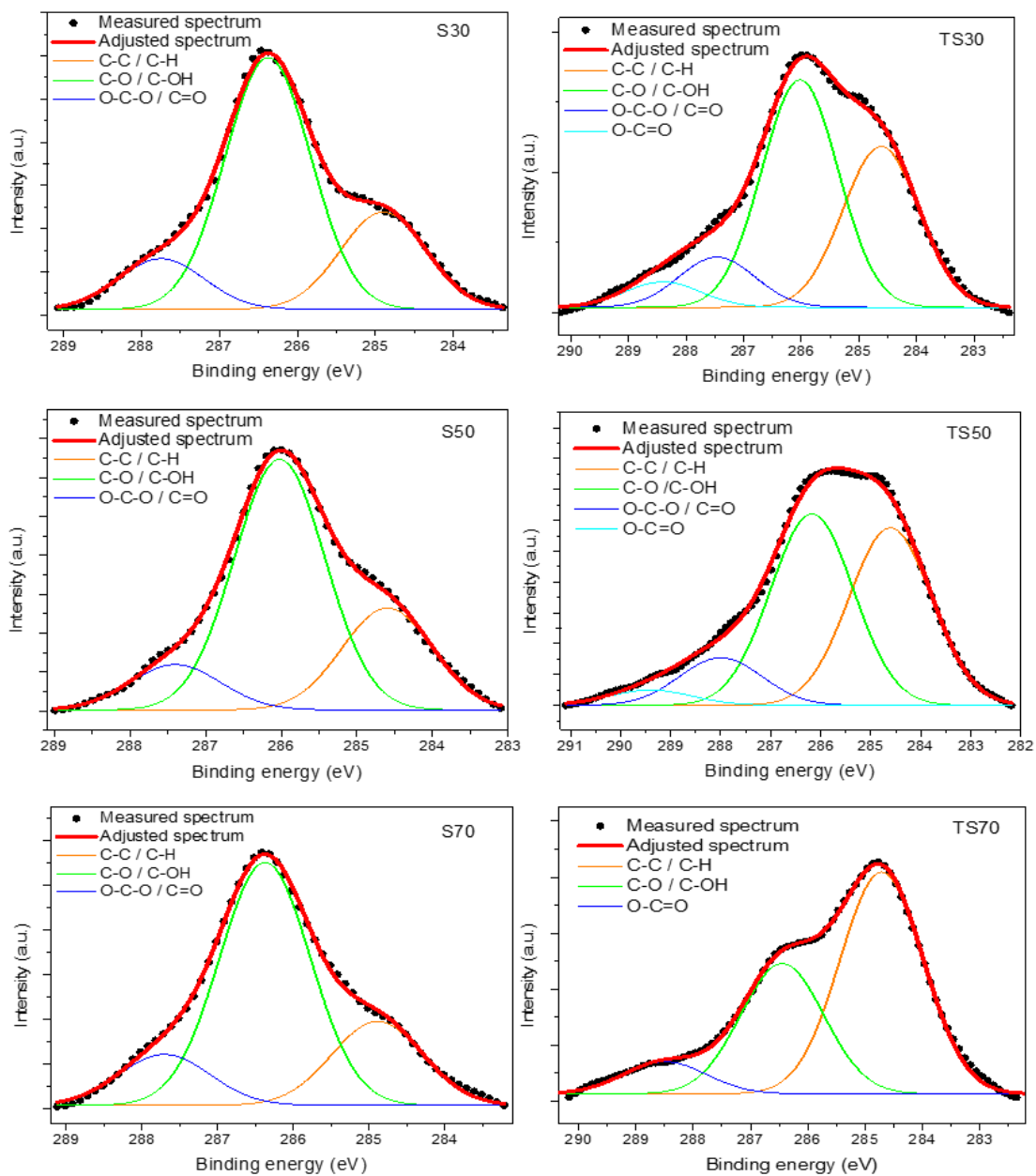


Figure 41. Deconvoluted C1s peaks of native and modified corn starches with different amylose content. S30: starch- 30% amylose, S50: starch- 50% amylose, S70: starch- 70% amylose, TS30: treated starch- 30% amylose, TS50: treated starch- 50% amylose and TS70: treated starch- 70% amylose

6.2.5 Thermal properties (DSC)

The gelatinization parameters obtained by DSC (T_o , T_p , T_f , ΔH and ΔT) of native and modified corn starches are presented in Table 8. HMDSO plasma treatment decreased the onset temperature (T_o) and increased the final temperature (T_f) in comparison to those of native starches. T_o indicates the gelatinization process is initiating in the amorphous region by the weakening of hydrogen bonds (Singh et al., 2003) and final temperature (T_f) is related to the melting temperature of high-perfection crystallites (Luo et al., 2008). The lower T_o values in modified starches suggest that active species of plasma were able to disrupt crystallites of different stabilities regardless of the amylose content; while the higher T_f values suggest that the HMDSO plasma affected the native crystalline structure of starch as observed in the XRD analysis, resulting in a more heterogenous structure. The instability of the crystals rearranged during the plasma modification was corroborated by the ΔT ($T_f - T_o$) values, which increased after HMDSO plasma treatment suggesting a heterogenous order of the starch molecules (Imberty et al., 1988). This effect was more noticeable in TS70 indicating that the susceptibility of amylose chains to the active species of plasma promoted the crosslinking resulting in a better alignment of the polymeric chains. These changes allowed the reordering of amylose chains towards coil-to-helix arrangement after HMDSO treatment. This behavior was not evident in the starches with higher amylopectin content.

Also, TS70 showed a significant increment of T_p , suggesting a crosslinking and the reorganization of amylose chains into heterogenous structures, which is related to an increment of the gelatinization temperature (Pan & Jane, 2000). These results indicate that the treatment promoted the hydrogen bonding between starch molecule reinforcing the granular structure.

Enthalpy of gelatinization (ΔH) indicates the crystallinity in terms of quantity and quality and it is associated to the loss of molecular order within the granule (Tester & Morrison, 1990). According to results shown in Table 8, the high amylose starches increased its ΔH value after treatment. This suggests important changes in the helical configuration restricting the gelatinization by stability of amylose crystals.

Thus, the ΔH found in TS30 could be attributed to a lower effect on the stability of the amylopectin structure as suggested by the ΔT values.

Table 8. Thermal transitions of native and modified corn starches with a different amylose content.

Sample	T_o (°C)	T_p (°C)	T_f (°C)	ΔH (J/g)	ΔT (°C)
S30	66.31± 0.09 ^a	70.24± 0.11 ^a	74.91± 0.53 ^a	13.59± 1.60 ^{ab}	8.60
TS30	65.43± 0.13 ^a	69.53± 0.09 ^a	74.95± 0.37 ^a	12.22± 1.06 ^{ab}	8.82
S50	68.56± 0.11 ^b	76.09± 0.41 ^b	94.64± 2.01 ^b	12.49± 0.64 ^{ab}	26.08
TS50	65.50± 0.11 ^a	75.18± 0.67 ^b	100.75± 1.87 ^{cd}	13.22± 2.60 ^{ab}	35.25
S70	69.62± 0.39 ^c	82.54± 0.30 ^c	96.33± 2.54 ^{bc}	7.84± 1.48 ^c	26.71
TS70	67.71± 0.65 ^b	90.25± 0.36 ^d	105.34± 0.57 ^d	12.27± 2.42 ^{ab}	37.63

Values with different letters in the same column indicate significant differences ($P \leq 0.05$).

T_o = onset temperature; T_p = peak temperature; T_f = final temperature; ΔH = enthalpy; ΔT = temperature differential; $\Delta T (T_f - T_o)$ = temperature differential.

S30= starch- 30% amylose; **S50**= starch- 50% amylose; **S70**= starch- 70% amylose; **TS30**= treated starch- 30% amylose; **TS50**= treated starch- 50% amylose; **TS70**= treated starch- 70% amylose

6.2.6 Final remarks

The results presented suggests that plasma treatment had different effect on the arrangement of the amylose and amylopectin chains in the starch granules. The differences could be explained because S30 has an A-type crystal in which the double-helices are closely packed into a monoclinic unit cell containing 8 water molecules, meanwhile S50 and S70 have a B-type crystal containing double-helices packed in a hexagonal unit cell with 36 water molecules (Bertoft, 2017). TGA analysis confirmed the water removal in the hydrated chains of starch after HMDSO plasma treatment, where the high amylose starches were the most susceptible. This modification resulted in the crosslinking of amylose chains as suggested by XRD, XPS and DSC analysis, , where the covalently bonding crosslinks reinforce the

granule structure of plasma-modified starch, suggesting an application of this starch in processes involving high temperature, high shear and acid conditions. In addition, changes in short-range crystallinity were observed in starch granules, where the normal starch showed better alignment of helices than those with high amylose content (Figure 42).

Another important factor is the distribution of amylose and amylopectin within the granule. Even when the amylose is commonly associated with the amorphous region in the starch granule, Pan & Jane (2000) hypothesized that amylose is located at the peripheral region of the granules rather than in the interior; meanwhile, Glaring et al. (2006) suggest that the amylose is located at the center of the granule. In any case, the way the plasma modified the starch granules correlates with the distribution of the amylose in the starch granule.

Although HMDSO plasma is not yet approved for food industry, the results of FTIR and XPS analysis confirmed that no new elements were incorporated in the starch molecule. Therefore, HDMSO plasma treatment could be consider as a safe and chemical-residue free technique for starch modification since the results showed that the treatment promoted water removal and high reactivity between starch macromolecules. However, more studies on clean technologies such as cold plasma treatment are needed to elucidate the cons and prons of their potential use among the food industry.

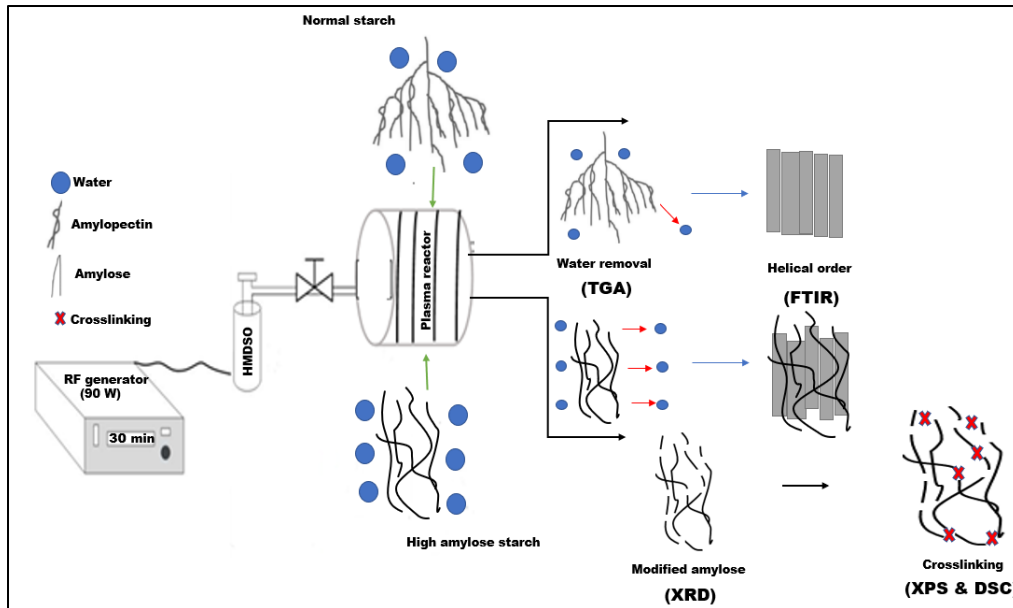


Figure 42. Possible mechanism of starch modification after HMDSO plasma treatment.

6.3. Conclusions

HMDSO plasma treatment resulted in structural, supramolecular and chemical changes on the starch molecule without the incorporation of any functional groups. Hydrated structures of high amylose corn starches and its amylose chains were the most affected by plasma treatment. The modified amylose chains were more susceptible to reactive species of plasma and more available to crosslinking. The removal of water molecules disturbed the structure resulting in heterogeneous crystals as suggested by thermal analysis. The results suggest that the low-pressure HMDSO plasma treatment is a suitable method to produce crosslinked starches, which have shown high thermal resistance and stability, properties needed to elaborate products that require high processing temperature or for developing of biodegradable materials with appropriated mechanical characteristics.

Chapter 7. Films made from plasma-modified corn starch: Chemical, mechanical and barrier properties

Abstract

In this study, the chemical, mechanical and barrier properties of films made from plasma-modified corn starch (MSF) were evaluated as a function of the amylose content (30, 50 and 70 %). XPS analysis was used to identify the oxidation mechanism in all MSF as the atomic proportion of hydroxyl, carbonyl and carboxyl groups changed. Also, the increase of C-C proportions suggested a crosslinking in the MSF70. TGA analysis indicated low interaction between starch and the plasticizer as the tensile strength and elongation at break diminished in the MSF50 and MSF70 due to the low plasticizing effect of glycerol, the oxidation phenomena and the depolymerization of starch chains. However, the crosslinking of MSF70 showed characteristics of rigid films. Moreover, cold plasma acted as a precursor of oxidized and crosslinked starch films reducing the WVP in 47 and 44 % for MSF50 and MSF70, respectively resulting in MSF with good hydrophobic performance.

7.1 Introduction

This section describes the properties of films made from modified starch, highlighting the advantages and disadvantages of these materials.

The introduction of the sustainable concept has led to the development of new packaging materials from biopolymers. Starch is an important raw material to this end as it is easily accessible and of low cost. Chemically, starch consists of two major components: a linear amylose and a highly branched amylopectin (Pérez et al., 2009), which determine its functionality and final applications. However, native starch does not always have appropriated characteristics to produce biodegradable films. Therefore, various starch modifications through chemical and physical methods have been used to enhance the functional properties (BeMiller & Huber, 2015). Chemical modifications consist of derivatization or decomposition of starch molecule mainly by oxidation, crosslinking and esterification (Su & Cheng, 2011). In this regard, the starch molecule could be oxidized using sodium hypochlorite and hydrochloride reagents, where the hydroxyl groups of the starch are oxidized to carbonyl and then to carboxyl groups (Wang & Wang, 2003). The oxidized starch could be used to produce films that show high tensile strength and low water vapor permeability depending on the oxidation extent in the glucan chain (Hu et al., 2009; Zamudio-Flores et al., 2006; Zavareze et al., 2012).

Other chemical reagents like trimetaphosphate and sodium trimetaphosphate have been used to obtain crosslinked starches to produce starch-films, which show high tensile strength as its chains are reinforced by chemical bonds acting as bridges between polymeric chains in the starch (Wurzburg, 1987). However, the use of above-mentioned chemical reagents to obtain oxidized and crosslinked starches implies an environmental issue; thus, the physical treatments are an alternative to modify starch since they are considered safe, cost-effective and environmentally friendly (Zavareze & Dias, 2011).

Cold plasma is a green technology for starch modification, where mainly crosslinking and depolymerization mechanism are usually reported (Banura et al., 2018; Sifuentes-Nieves et al., 2019 a; Zou et al., 2004). In a previous study, our research

group reported the effect of HMDSO plasma on the structural, supramolecular and chemical properties of starch granules with different amylose content, finding an important decrease of long-range crystallinity, fragmentation of amylose chains and its crosslinking after HMDSO plasma treatment of high amylose starches (Sifuentes et al., 2019b).

However, the performance of plasma-modified starch during the gelatinization process applied to obtain films is stills unknow. Thus, the aim of this work was to study the chemical, mechanical and barrier properties of films made from plasma-modified starch with different proportion of amylose.

7.2 Results and discussion

7.2.1 X-ray photoelectron spectroscopy

The chemical composition of the native (SF) and modified starch films (MSF) was studied using XPS analysis. The high-resolution peaks of C 1s were further deconvoluted to obtain chemical bonds present in the MSF (Figure 43). The C 1s signal revealed five peaks at 284.4, 284.9, 286.3, 287.2 and 288.1 eV which correspond to C-C, C-OOH, C-OH, C=O and O-C=O, respectively. In our previous study it was demonstrated that the HMDSO plasma treatment resulted in the crosslinking of MS and the extent of modification depended on the amylose content and structural water (Sifuentes et al., 2019b). However, during the processing of MSF, the granular structure and crystalline arrangement of starch could have been destroyed and modified (Hu et al., 2009). In this regard, the temperature and water used during the gelatinization process could promote the high reactivity of hydroxyl groups in the modified starch resulting in different chemical bonds as it can be observed in the elaborated films (Table 9). All MSF with 30 (MSF30), 50 (MSF50) and 70 % (MSF70) of amylose showed a decrease of C-OH bonds suggesting that the gelatinization process promoted the starch oxidation as indicated by the new carbonyl groups (C=O) in its molecule (Figure 43). The results indicate that the hydroxyl groups on starch were oxidized to carbonyl groups increasing in 0.11, 0.05

and 0.06 % their atomic proportion for MSF30, MSF50 and MSF70, respectively. Moreover, MSF50 showed the highest atomic proportion of carboxyl groups (C-OOH) indicating the highest oxidation of starch molecule (Figure 43). The oxidation has been associated with the depolymerization of the starch chains which promotes the availability of carbon groups for oxidation and the inclusion of functional groups (Halal et al., 2015; Tavares et al., 2010). In addition, the higher oxidation in MSF50 suggests a higher depolymerization in the amylose and amylopectin chains (Hoover, 2000) because of the high gelatinization temperature used.

Similar behavior has been reported in films made from potato starch oxidized with sodium hypochlorite and hydrochloric acid (Fonseca et al., 2015; Hu et al., 2009), where the starches were oxidized at different level to obtain films with different functional properties.

Moreover, MSF70 showed the highest decrease of C-OH groups (Table 9), which could be associated not only to oxidation of starch but also to crosslinking of the starch molecule as indicated by its higher presence of C-C bonds, which affected the mechanical and barrier properties as it will be discussed further ahead.

Table 9. C1s peaks of films made from native and plasma-modified starch containing 30, 50, and 70 % amylose.

Sample	C-C/C-H	C-COOH	C-O/C-OH	O-C-O/C=O	O-C=O
SF30	0.55	----	0.40	----	0.05
SF50	0.47	----	0.41	----	0.12
SF70	0.41	----	0.51	----	0.07
MSF30	0.50	----	0.38	0.11	0.01
MSF50	0.23	0.34	0.30	0.05	0.08
MSF70	0.70	----	0.21	0.06	0.03

SF30= starch film- 30% amylose; **SF50**= starch film- 50% amylose; **SF70**= starch film- 70% amylose; **MSF30**= modified starch film- 30% amylose; **MSF50**= modified starch film- 50% amylose; **MSF70**= modified starch film- 70% amylose.

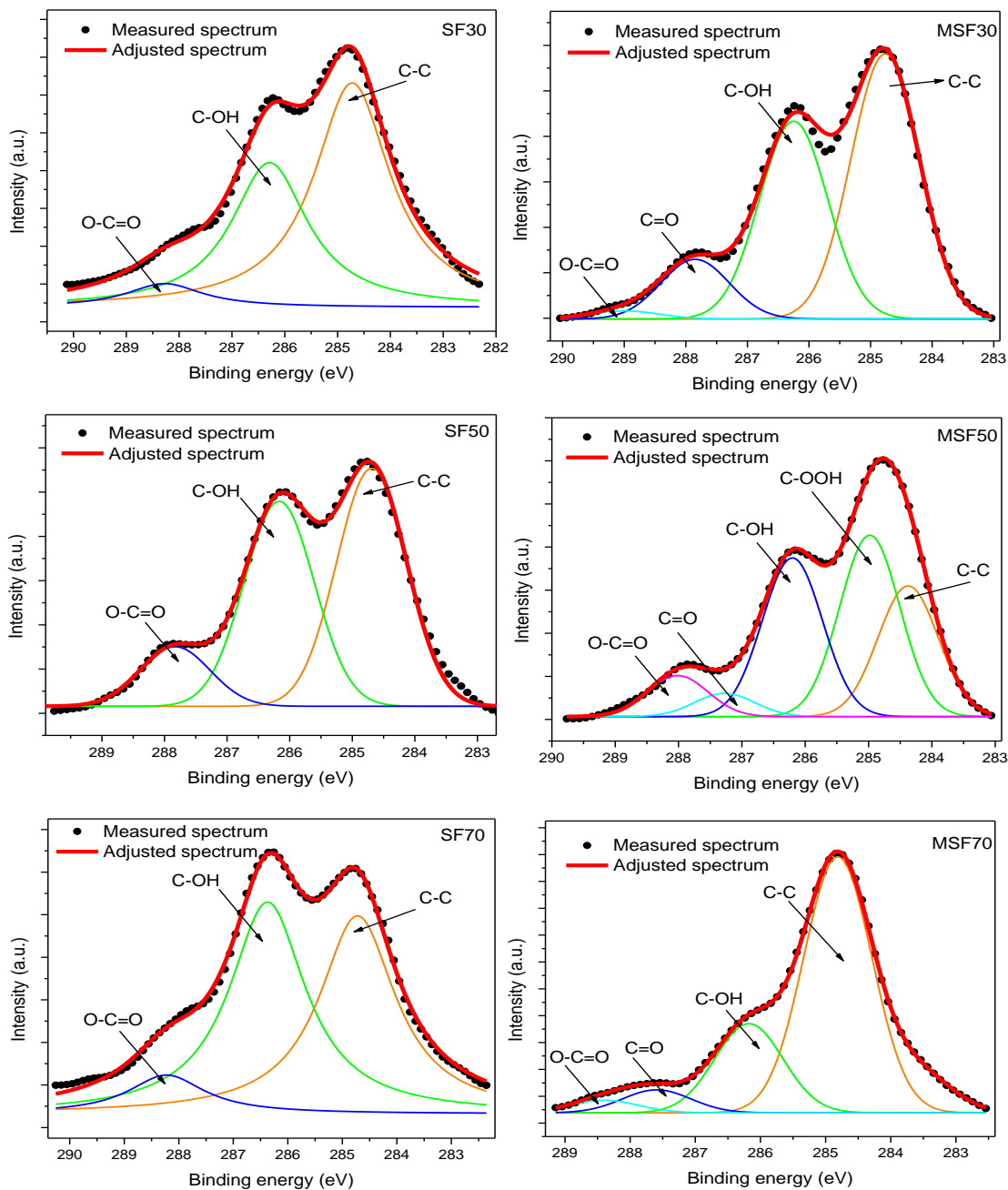


Figure 43. Deconvoluted C1s peaks of films made from native and plasma-modified starch containing 30, 50, and 70 % amylose. SF30: starch film- 30% amylose, SF50: starch film- 50% amylose, SF70: starch film- 70% amylose, MSF30: modified starch film- 30% amylose, MSF50: modified starch film- 50% amylose and MSF70: modified starch film- 70% amylose.

7.2.2 Thermogravimetric analysis

Thermogravimetric weight loss (WL) curves of all films in the region associated to volatilization of plasticizer (30 to 250 °C) was explored (Figure 44). All MSF showed an increase of WL of 25, 11 and 30 % in those films from starch with 30, 50 and 70 % amylose content, respectively. This behavior suggests a modification of intra and intermolecular interactions between starch molecules. According to Hu et al. (2009), the structure of films from oxidized starch is disrupted during its processing favoring the pervasion of the plasticizer into the starch matrix, which resulted in a reduction of intermolecular interactions due to a blocking effect between the starch molecules and the plasticizer (Turhan & Sahbaz, 2004). However, during the MSF elaboration, the amylose and amylopectin chains could suffer depolymerization and limit glycerol interaction as the hydroxyl groups were not available to reduce the intermolecular spaces in the starch molecule.

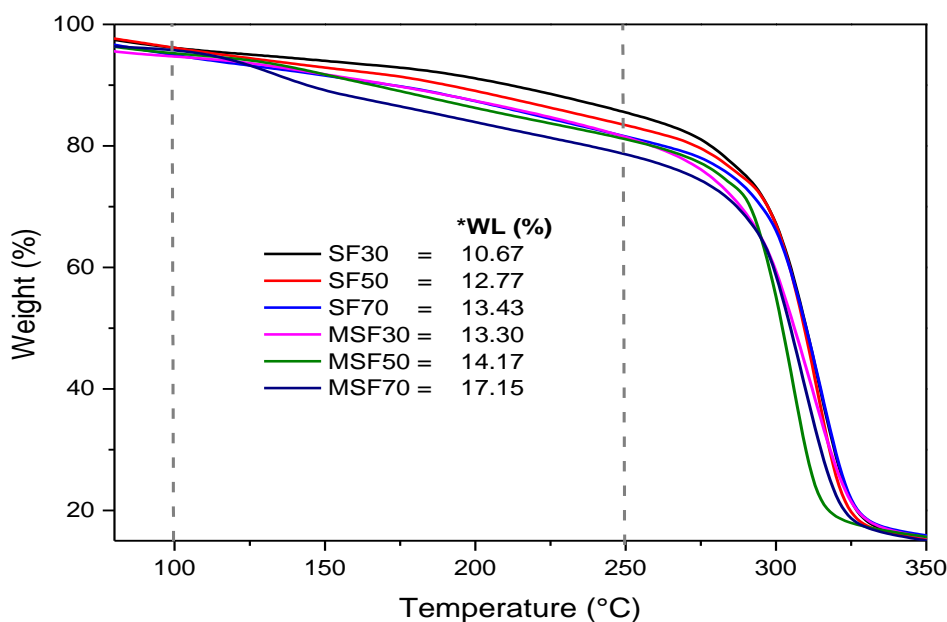


Figure 44. TGA thermograms and % weight loss (WL) of films made from native and plasma-modified starch containing 30, 50, and 70 % amylose. *WL= % W.L at 250 °C – % WL at 100°C. SF30: starch film- 30% amylose, SF50: starch film- 50% amylose, SF70: starch film- 70% amylose, MSF30: modified starch film- 30% amylose, MSF50: modified starch film- 50% amylose and MSF70: modified starch film- 70% amylose.

7.2.3 Mechanical properties

The mechanical properties of SF and MSF films were evaluated. The changes in tensile strength (TS), the Young's modulus (YM) and the elongation percentage (% E) are presented in Figure 45. SF70 showed the highest TS value compared with those made from low amylose content (SF50 & SF30) due to the interactions by hydrogen bonds of the linear amylose chains as already reported (Romero-Bastida et al., 2015; Sifuentes-Nieves et al., 2019 c). However, MSF30 and MSF50 showed a decrease in the TS value (Figure 45a). Similar behavior was reported by Fonseca et al. (2015) in films prepared from oxidized starch, where the highest concentration of chlorine resulted in the lowest tensile strength values. That behavior was attributed to the decreased of hydrogen bonds of starch chains. In this regard, the decrease of TS in MSF with 30 and 50 % amylose content could be related to the extent of oxidation in the starch molecule, where the highest content of carboxylic groups observed in MSF50 resulted in the highest weakening of the hydrogen bonds of OH groups of amylose and amylopectin chains. However, an opposite behavior was observed in MSF70 where the TS increased suggesting that the presence of carbonyl groups in high amylose oxidized starch produced hydrogen bonds, which could provide structural integrity to the matrix (Zhang et al., 2009). Moreover, as XPS analysis indicated, the MSF70 showed an evidence of crosslinking of starch molecule, which also has been related with the increase of tensile strength as the crosslinking stabilizes the starch molecule (Wurzberg, 1987).

Young's modulus (YM) followed the same trend of TS values as MSF50 and MSF30 decreased and MSF70 increased (Figure 45 b); which confirms the rigidity in MSF70 as a result of oxidation and crosslinking of starch molecule.

The elongation at break (% E) decreased in all MSF suggesting that the during the film elaboration the intermolecular interactions between starch and glycerol were lower compared with SF as demonstrated in the TGA analysis, thus, the elongation at break decreased. A high reduction of % E value was observed in MSF50 decreasing its value in 57 %; this decrease could be associated to the oxidation and

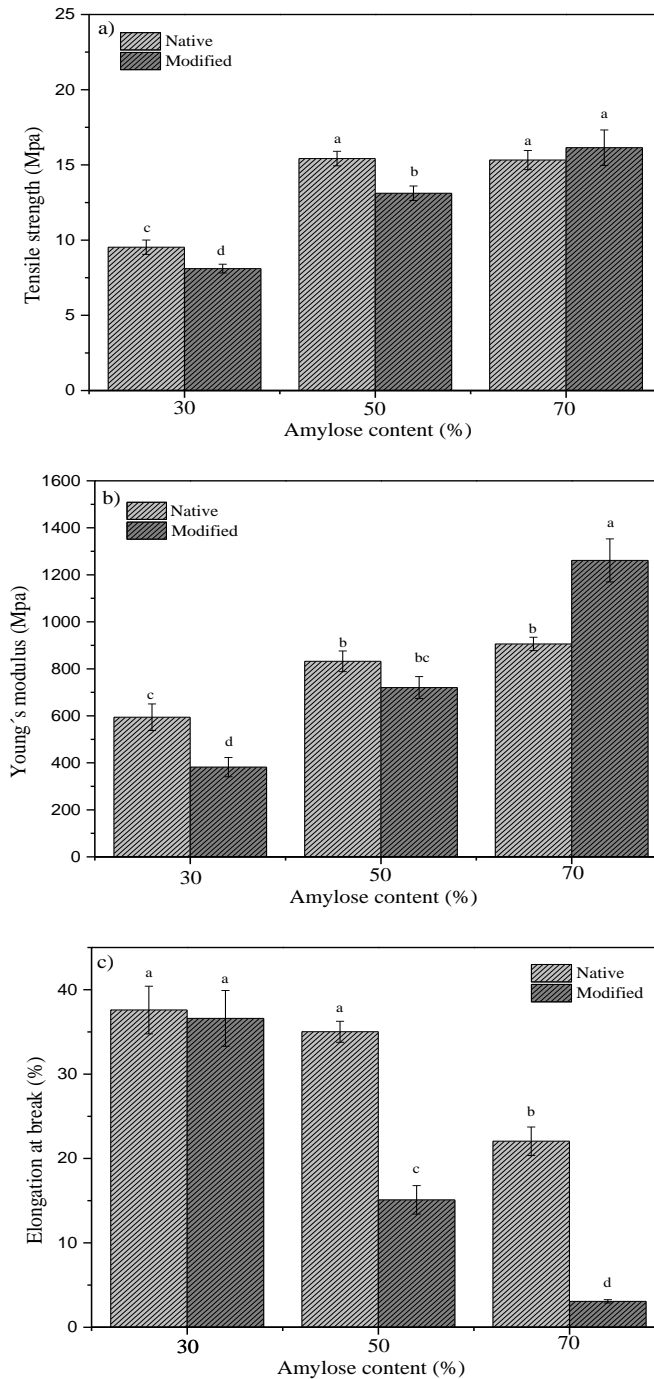


Figure 45. Mechanical properties of films made from native and plasma-modified starch containing 30, 50, and 70% amylose; (a) tensile strength, (b) Young's modulus, and (c) elongation at break. Error bars with different letters indicate significant differences ($P \leq 0.05$).

depolymerization of the starch chains as confirmed by XPS analysis, which limited the interaction with the plasticizer. In addition, the highest reduction of % E (97 %) was observed in MSF70. This behavior is mainly associated to crosslinking of starch molecule, which reinforced its structure and reduced the flexibility of amylose chains (Haq et al., 2019).

7.2.4 Water vapor permeability

The water vapor permeability (WVP) of SF and MSF films are shown in Figure 46. The SF showed higher values of WVP as the glycerol is able to increase intermolecular spaces between biopolymers increasing the water vapor permeability (Sanyang et al., 2015). However, an opposite behavior was observed in those MSF made from 30, 50 and 70 % of amylose content as its WVP value decreased in 41, 53 and 56 %, respectively. According to Zhang et al. (2009) the extent of oxidation of starch decreased the moisture adsorption of the films because during the starch oxidation the addition of hydrophobic aldehyde groups occurs instead of addition of hydrophilic hydroxyl groups. In this regard, the incorporation of aldehyde groups resulted in a low interaction between starch and glycerol restricting the diffusion of water molecules through the films. In addition, the presence of hydrogen bonds because of the starch oxidation could have prevented the migration of water molecules (Yan et al., 2012).

Moreover, the highest reduction in WVP observed in TSF70 suggest that the anchorage of starch molecules due to its crosslinking promoted a stronger structural network, which limited the water vapor migration on the film.

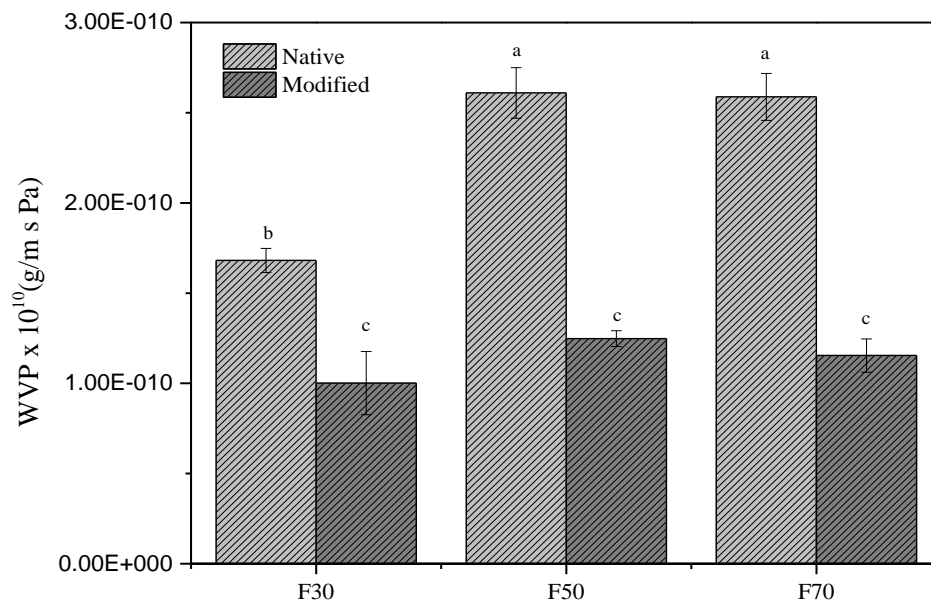


Figure 46. Water vapor permeability of films made from native and plasma-modified starch containing 30, 50, and 70% amylose. Error bars with different letters indicate significant differences ($P \leq 0.05$). F30: starch film- 30% amylose, SF50: starch film- 50% amylose and SF70: starch film- 70% amylose.

7.3 Conclusions

The behavior of films made from plasma-modified starch was investigated. XPS analysis suggested that the hydroxyl groups of starch molecules were oxidized to carbonyl groups during the preparation process in all MSF, and even further oxidized carboxyl groups were observed in MSF50. The highest decrease of C-OH in MSF70 and increase of C-C proportions indicated the crosslinking of starch molecules. The oxidation and low interaction of plasticizer in MSF30 and MSF50 resulted in films with low rigidity as revealed by the tensile strength and elongation at break values. However, the crosslinking in MSF70 showed an opposite trend. Also, all MSF exhibited low water vapor permeability probably due to the oxidation of starch during its elaboration. Plasma-modified starch is promising for biodegradable films production. Depending of its amylose content it could be used for soft or rigid materials with good hydrophobic performance, which are very important characteristics to develop packaging materials.

According to the fourth objective of this thesis, it was possible to develop films made from plasma-modified starch. Also, the results allowed to identify the main chemical groups responsible for improving the mechanical and barrier properties of the films.

8. General conclusions

Results indicated an improvement of the barrier and mechanical properties of films after cold plasma treatment. In this regard, the amylose content and extent of gelatinization determine the amount of remnant starch granules (RSG) on the films. The leached amylopectin from RSG drive the interaction with active species of HMDSO plasma, which promoted structural changes by increasing the helical order, crosslinking and substitution of starch molecules (blocking group (C-Si)) resulting in improved performance of the films against water molecules and reinforced structure as indicated by the tensile test.

HMDSO plasma treatment seems to be a good alternative to modify structural properties of granular starch as observed in the improvement of its structural properties without the incorporation of any functional group of HMDSO. In this regard, the structural water and amylose content determined the starch modification degree. Water molecules reduction disturbed the helical order of starch molecules making the amylose chains more susceptible to plasma modification (crosslinking), which resulted in an increment of gelatinization temperature in high amylose starch, making it as a suitable raw material to elaborate products that require high processing temperature.

Furthermore, the low-pressure HMDSO plasma treatment is an adequate method to produce modified starches compared to conventional chemical methods, which has a great potential to develop biodegradable starch-based films. In this regard, the plasma-modified starches prompted to obtain oxidized and crosslinked starch films; where the amylose content determined the modification degree. The oxidation and crosslinking extent of starch molecule resulted in films with improved barrier and mechanical properties.

According to the fourth objectives developed during this thesis project, it is concluded that the cold plasma treatment has great potential to modify the starch molecule as a granule and as a film. The results allowed to identify the main effect of the treatment and to propose a hypothesis related to the mechanism between starch

and HMDSO cold plasma, which affected the structural, chemical and functional properties of these materials.

9. References

- Adamu, A. D., Jikan, S. S., Talip, B. H. A., Badarulzaman, N. A., & Yahaya, S. (2017). Effect of Glycerol on the Properties of Tapioca Starch Film. *Materials Science Forum*, 888(4), 239–243. <https://doi.org/10.4028/www.scientific.net/MSF.888.239>
- Agama-Acevedo, E., Pacheco-Vargas, G., Bello-Perez, L. A., & Alvarez-Ramirez, J. (2018). Effect of drying method and hydrothermal treatment of pregelatinized Hylon VII starch on resistant starch content. *Food Hydrocolloids*, 77, 817–824. <https://doi.org/10.1016/j.foodhyd.2017.11.025>
- Aila-Suárez, S., Palma-Rodríguez, H. M., Rodríguez-Hernández, A. I., Hernández-Uribe, J. P., Bello-Pérez, L. A., & Vargas-Torres, A. (2013). Characterization of films made with chayote tuber and potato starches blending with cellulose nanoparticles. *Carbohydrate Polymers*, 98(1), 102–107. <https://doi.org/10.1016/j.carbpol.2013.05.022>
- Attri, P., Arora, B., Choi, E.H., 2013. Utility of plasma: a new road from physics to chemistry. *RSC Adv.* 3, 12540–12567.
- Banura, S., Thirumdas, R., Kaur, A., Deshmukh, R. R., & Annapure, U. S. (2018). Modification of starch using low pressure radio frequency air plasma. *LWT - Food Science and Technology*, 89, 719–724. <https://doi.org/10.1016/j.lwt.2017.11.056>
- Bardon, J., Apaydin, K., Laachachi, A., Jimenez, M., Fouquet, T., Hilt, F., ... Ruch, D. (2015). Progress in Organic Coatings Characterization of a plasma polymer coating from an organophosphorus silane deposited at atmospheric pressure for fire-retardant purposes. *Progress in Organic Coatings*, 88, 39–47. <https://doi.org/10.1016/j.porgcoat.2015.06.005>
- Bastos D., Santos, A., Da Fonseca, M. D., & Simao, R. A. (2013). Inducing surface hydrophobization on cornstarch film by SF6 and HMDSO plasma treatment. *Carbohydrate Polymers*, 91(2), 675–681. <https://doi.org/10.1016/j.carbpol.2012.08.031>
- Bastos D., Santos, A., Da Silva, M., & Simao, R. A. (2009). Hydrophobic corn starch thermoplastic films produced by plasma treatment. *Ultramicroscopy*, 109(8), 1089–1093. <https://doi.org/10.1016/j.ultramic.2009.03.031>
- Bastos D., Dos Santos, A., & Simao, R. A. (2014). Acetylene coating on cornstarch plastics produced by cold plasma technology. *Starch/Staerke*, 66(3–4), 267–273. <https://doi.org/10.1002/star.201200219>
- Batan, A., Brusciotti, F., De Graeve, I., Vereecken, J., Wenkin, M., Piens, M., ... Terryn, H. (2010). Comparison between wet deposition and plasma deposition of silane coatings on aluminium. *Progress in Organic Coatings*, 69(2), 126–132. <https://doi.org/10.1016/j.porgcoat.2010.04.009>

- BeMiller, J. N., & Huber, K. C. (2015). Physical Modification of Food Starch Functionalities. *Annu. Rev. Food Sci. Technol.*, 6, 19–69. <https://doi.org/10.1146/annurev-food-022814-015552>
- Bertoft, E., Koch, K., & Åman, P. (2012). Building block organisation of clusters in amylopectin from different structural types. *International Journal of Biological Macromolecules*, 50, 1212–1223.
- Bertuzzi, M. A., Armada, M., & Gottifredi, J. C. (2007). Physicochemical characterization of starch based films. *Journal of Food Engineering*, 82(1), 17–25. <https://doi.org/10.1016/j.jfoodeng.2006.12.016>
- Bie, P., Pu, H., Zhang, B., Su, J., Chen, L., & Li, X. (2016). Structural characteristics and rheological properties of plasma-treated starch. *Innovative Food Science and Emerging Technologies*, 34, 196–204. <https://doi.org/10.1016/j.ifset.2015.11.019>
- De Albuquerque, M., Bastos, D. C., & Simao, R. A. (2014). Surface modification of starch films by plasma. *Macromolecular Symposia*, 343(1), 96–101.
- Deeyai, M. Suphantharika, R. Wongsagonsup, S. Dangtip . (2013). Characterization of modified tapioca starch in atmospheric argon plasma under diverse humidity by FTIR Spectroscopy. *Chin. Phys. Lett.* 30.
- Waigh, T.A., Jenkins, P.J., Gidley, M.J., Debet, M., Smith, A., (1997). Internal structure of starch granules revealed by scattering studies. In: Frazier, P.J., Donald, A.M., Richmond, P. (Eds.), *Starch: Structure and Functionality*, The Royal Society of Chemistry, Cambridge, pp. 172–179.
- Edhirej, A., Sapuan, S. M., Jawaid, M., & Zahari, N. I. (2017). Effect of various plasticizers and concentration on the physical, thermal, mechanical, and structural properties of cassava-starch-based films. *Starch/Staerke*, 69(1–2), 1–11. <https://doi.org/10.1002/star.201500366>
- Flores-Silva, P. C., Roldan-Cruz, C. A., Chavez-Esquivel, G., Vernon-Carter, E. J., Bello-Perez, L. A., & Alvarez-Ramirez, J. (2017). In vitro digestibility of ultrasound-treated corn starch. *Starch/Staerke*, 69(9–10), 1–9. <https://doi.org/10.1002/star.201700040>
- Fonseca, L., Goncalves, R., Halal, S., Pinto, V., Dias, A., Jacques, A., & Zavareze, R. (2015). Oxidation of potato starch with different sodium hypochlorite concentrations and its effect on biodegradable films. *LWT - Food Science and Technology*, 60, 714–720. <https://doi.org/10.1016/j.lwt.2014.10.052>
- Garcia-Hernandez, A., Vernon-Carter, E. J., & Alvarez-Ramirez, J. (2017). Impact of ghosts on the mechanical , optical , and barrier properties of corn starch films. *Starch/Staerke*, 69(10), 1–7. <https://doi.org/10.1002/star.201600308>
- Gernat, C., Radosta, S., Damaschun, G., & Schierbaum, F. (1990). Supramolecular structure of legume starches revealed by X-ray scattering. *Starch-Stärke*, 42, 175–178.

- Ghiasi, K., Hosney, R., & Varriano-Marston, E. (1982). Gelatinization of wheat starch. III. Comparison by differential scanning calorimetry and light microscopy. *Cereal Chemistry*.
- Goesaert, H., Brijs, K., Veraverbeke, W. S., Courtin, C. M., Gebruers, K., Delcour, J. A. (2005). Wheat flour constituents: how they impact bread quality, and how to impact their functionality. *Trends Food Sci. Technol.*, 16(1-3), 12-30.
- Halal, S., Colussi, R., Pinto, V., Bartz, J., Radunz, M., Carreño, V., ... Zavareze, R. (2015). Structure , morphology and functionality of acetylated and oxidised barley starches. *Food Chemistry*, 168, 247–256. <https://doi.org/10.1016/j.foodchem.2014.07.046>
- Haq, F., Yu, H., Wang, L., Teng, L., Haroon, M., Khan, R. U., ... Nazir, A. (2019). Advances in chemical modifications of starches and their applications. *Carbohydrate Research*, 476 12–35. <https://doi.org/10.1016/j.carres.2019.02.007>
- Hu, G., Chen, J., & Gao, J. (2009). Preparation and characteristics of oxidized potato starch films. *Carbohydrate Polymers*, 76(2), 291–298. <https://doi.org/10.1016/j.carbpol.2008.10.032>
- Jovanovich, G., Zamponi, R. A., Lupano, C.E. Aflon, M.C. (1992). Effect of water content on the formation and dissociation of the amylose-lipid complex in wheat flour. *Journal of Agriculture and Food Chemistry*. 40, 1789-93.
- Jansson, A., & Järnström, L. (2005). Barrier and mechanical properties of modified starches. *Cellulose*, 12(4), 423–433. <https://doi.org/10.1007/s10570-004-6092-6>
- Karbowski, T., Debeaufort, F., Champion, D., & Voilley, A. (2006). Wetting properties at the surface of iota-carrageenan-based edible films, 294, 400–410. <https://doi.org/10.1016/j.jcis.2005.07.030>
- Karim, A. A., Norziah, M. H., & Seow, C. C. (2000). Methods for the study of starch retrogradation. *Food Chemistry*, 71, 9–36.
- Laovachirasuwan, P., Peerapattana, J., Srijsdaruk, V., Chitropas, P., & Otsuka, M. (2010). The physicochemical properties of a spray dried glutinous rice starch biopolymer. *Colloids and Surfaces B: Biointerfaces*, 78(1), 30–35. <https://doi.org/10.1016/j.colsurfb.2010.02.004>
- Lawton, J. W. (1996). Effect of starch type on the properties of starch containing films. *Carbohydrate Polymers*, 8617(96), 203–208.
- Le Corre, D., Bras, J., & Dufresne, A. (2010). Starch nanoparticles: A review. *Biomacromolecules*, 11, 1139–1153.
- Lindeboom. N., Chang, P.R., & Tyler, R.T. (2004). Analytical, biochemical and physicochemical aspects of starch granule size, with emphasis on small granule starches: A review. *Starch-Starke*, 56(3-4), 89-99.

- Liu, H., Adhikari, R., Guo, Q., & Adhikari, B. (2013). Preparation and characterization of glycerol plasticized (high-amylose) starch–chitosan films. *Journal of Food Engineering*, 116(2), 588–597. <https://doi.org/10.1016/j.jfoodeng.2012.12.037>
- Lourdin, D., Valle, G. Della, & Colonna, P. (1995). Influence of amylose content on starch films and foams. *Carbohydrate Polymers*, 27(4), 261–270. [https://doi.org/10.1016/0144-8617\(95\)00071-2](https://doi.org/10.1016/0144-8617(95)00071-2)
- Mali, S., Victória, M., Grossmann, E., García, M. A., Martino, M. N., & Zaritzky, N. E. (2004). Barrier, mechanical and optical properties of plasticized yam starch films. <https://doi.org/10.1016/j.carbpol.2004.01.004>
- Manners, D. J. (1989). Recent developments in our understanding of amylopectin structure. *Carbohydrate Polymers*, 11(2), 87–112. [https://doi.org/10.1016/0144-8617\(89\)90018-0](https://doi.org/10.1016/0144-8617(89)90018-0)
- Manoel, A. F., Claro, P. I. C., Mattoso, L. H. C., Marconcini, J. M., & Mantovani, G. L. (2017). Thermoplastic Waxy Starch Films Processed by Extrusion and Pressing: Effect of Glycerol and Water Concentration. *Materials Research*, 2–6. <https://doi.org/10.1590/1980-5373-mr-2016-0881>
- Moon, M. R., Nam, E., Woo, J., Lee, S., Park, K., Jung, D., ... Lee, H. J. (2009). Effects of surface treatments using PECVD-grown hexamethyldisiloxane on the performance of organic thin-film transistor. *Thin Solid Films*, 517(14), 4161–4164. <https://doi.org/10.1016/j.tsf.2009.02.048>
- Morent, R., De Geyter, N., Van Vlierberghe, S., Dubruel, P., Leys, C., Gengembre, L., ... Payen, E. (2009). Deposition of HMDSO-based coatings on PET substrates using an atmospheric pressure dielectric barrier discharge. *Progress in Organic Coatings*, 64(2–3), 304–310. <https://doi.org/10.1016/j.porgcoat.2008.07.030>
- Moustapha, M. E., Friedrich, J. F., Farag, Z. R., Krüger, S., Hidde, G., & Azzam, M. M. (2017). Promotion of Adhesion of Green Flame Retardant Coatings onto Polyolefins by Depositing Ultra-Thin Plasma Polymer Films. *Progress in Adhesion and Adhesives*, 2, 399–427.
- Muscat, D., Adhikari, B., Adhikari, R., & Chaudhary, D. S. (2012). Comparative study of film forming behaviour of low and high amylose starches using glycerol and xylitol as plasticizers. *Journal of Food Engineering*, 109(2), 189–201. <https://doi.org/10.1016/j.jfoodeng.2011.10.019>
- Muscat, D., Adhikari, R., McKnight, S., Guo, Q., & Adhikari, B. (2013). The physicochemical characteristics and hydrophobicity of high amylose starch-glycerol films in the presence of three natural waxes. *Journal of Food Engineering*, 119(2), 205–219. <https://doi.org/10.1016/j.jfoodeng.2013.05.033>
- Naguleswaran, S., Vasanthan, T., Hoover, R., Chen, L., & Bressler, D. (2014). Molecular characterization of waxy corn and barley starches in different solvent systems as revealed by MALLS. *Food Chemistry*, 152, 297–299.

- Paes, S. S., Yakimets, I., & Mitchell, J. R. (2008). Influence of gelatinization process on functional properties of cassava starch films. *Food Hydrocolloids*, 22(5), 788–797. <https://doi.org/10.1016/j.foodhyd.2007.03.008>
- Pankaj, S. K., Bueno-Ferrer, C., Misra, N. N., O'Neill, L., Tiwari, B. K., Bourke, P., & Cullen, P. J. (2015). Dielectric barrier discharge atmospheric air plasma treatment of high amylose corn starch films. *LWT - Food Science and Technology*, 63(2), 1076–1082. <https://doi.org/10.1016/j.lwt.2015.04.027>
- Pankaj, Shashi K, Wan, Z., & Le, J. E. De. (2017). High-voltage atmospheric cold plasma treatment of different types of starch films, *1700009*, 1–7. <https://doi.org/10.1002/star.201700009>
- Pérez, S., Baldwin, P. M., & Gallant, D. J. (2009). *Starch Granules I*. Elsevier Inc. <https://doi.org/10.1016/B978-0-12-746275-2.00005-7>
- Rindlav-Westling, Å., Stading, M., & Gatenholm, P. (2002). Crystallinity and morphology in films of starch, amylose and amylopectin blends. *Biomacromolecules*, 3(1), 84–91. <https://doi.org/10.1021/bm010114i>
- Romero-Bastida, C. A., Bello-Perez, L. A., Velazquez, G., & Alvarez-Ramirez, J. (2015). Effect of the addition order and amylose content on mechanical, barrier and structural properties of films made with starch and montmorillonite. *Carbohydrate Polymers*, 127, 195–201. <https://doi.org/10.1016/j.carbpol.2015.03.074>
- Romero-Bastida, C. A., Tapia-blácido, D. R., Méndez-Montealvo, G., Bello-pérez, L. A., Velázquez, G., & Alvarez Ramirez, J. (2016). Effect of amylose content and nanoclay incorporation order in physicochemical properties of starch / montmorillonite composites. *Carbohydrate Polymers*, 152, 351–360. <https://doi.org/10.1016/j.carbpol.2016.07.009>
- Santos, A., Bastos, D., Da Silva, M., Thiré, R., & Simão, R. A. (2012). Chemical analysis of a cornstarch film surface modified by SF6 plasma treatment. *Carbohydrate Polymers*, 87(3), 2217–2222. <https://doi.org/10.1016/j.carbpol.2011.10.049>
- Sanyang, M. L., Sapuan, S. M., Jawaid, M., Ishak, M. R., Sahari, J., Engineering, G., ... Resources, N. (2015). Effect of Plasticizer Type and Concentration on Tensile, Thermal and Barrier Properties of Biodegradable Films Based on Sugar Palm, 1106–1124. <https://doi.org/10.3390/polym7061106>
- Sarangapani, C., Devi, R. Y., Thirumdas, R., Trimukhe, A. M., Deshmukh, R. R., & Annature, U. S. (2017). Physico-chemical properties of low-pressure plasma treated black gram. *LWT - Food Science and Technology*, 79, 102–110. <https://doi.org/10.1016/j.lwt.2017.01.017>
- Schartel, B., Kühn, G., Mix, R., & Friedrich, J. (2002). Surface Controlled Fire Retardancy of Polymers Using Plasma Polymerisation. *Macromolecular Materials and Engineering*, 579–582.

- Senanayake, S., Gunaratne, A., Ranaweera, K., & Bamunuarachchi, A. (2014). Effect of Hydroxypropylation on Functional Properties of Different Cultivars of Sweet Potato Starch in Sri Lanka. <https://doi.org/10.1155/2014/148982>
- Sevenou, O., Hill, S. E., Farhat, I. A., & Mitchell, J. R. (2002). Organisation of the external region of the starch granule as determined by infrared spectroscopy. *International Journal of Biological Macromolecules*, 31(1–3), 79–85. [https://doi.org/10.1016/S0141-8130\(02\)00067-3](https://doi.org/10.1016/S0141-8130(02)00067-3)
- Sifuentes-Nieves, I., Hernández-Hernández, E., Neira-Velázquez, G., Morales-Sanchez, E., Mendez-Montealvo, G., & Velazquez, G. (2019). Hexamethyldisiloxane cold plasma treatment and amylose content determine the structural, barrier and mechanical properties of starch-based films. *International Journal of Biological Macromolecules*, 124, 651–658. <https://doi.org/10.1016/j.ijbiomac.2018.11.211>
- Sifuentes-Nieves, I., Neira-Velázquez, G., Hernández-Hernández, E., Barriga-Castro, E., Gallardo-Vega, C., Velazquez, G., & Mendez-Montealvo, G. (2019). Influence of gelatinization process and HMDSO plasma treatment on the chemical changes and water vapor permeability of corn starch films. *International Journal of Biological Macromolecules*, 135, 196–202. <https://doi.org/10.1016/j.ijbiomac.2019.05.116>
- Sifuentes-Nieves, I., Rendón-Villalobos, R., Jiménez-Aparicio, A., Camacho-Díaz, B. H., Gutiérrez López, G. F., & Solorza-Feria, J. (2015). Physical, Physicochemical, Mechanical, and Structural Characterization of Films Based on Gelatin/Glycerol and Carbon Nanotubes. *International Journal of Polymer Science*, 2015, 1–8. <https://doi.org/10.1155/2015/763931>
- Su, J. F., & Cheng, J. J. (2011). Modified Methods in Starch-Based Biodegradable Films. *Advanced Materials Research*, 183–185, 1635–1641. <https://doi.org/10.4028/www.scientific.net/amr.183-185.1635>
- Tavares, K., Zanatta, E., Zavareze, R., Helbig, E., & Dias, A. (2010). The effects of acid and oxidative modification on the expansion properties of rice flours with varying levels of amylose. *LWT - Food Science and Technology*, 43(8), 1213–1219. <https://doi.org/10.1016/j.lwt.2010.04.007>
- Turhan, K. N., & Sahbaz, F. (2004). Water vapor permeability, tensile properties and solubility of methylcellulose-based edible films. *Journal of Food Engineering*, 61, 459–466. [https://doi.org/10.1016/S0260-8774\(03\)00155-9](https://doi.org/10.1016/S0260-8774(03)00155-9)
- Van Soest, J. J. G., De Wit, D., Tournois, H., & Vliegthart, J. F. G. (1994). Retrogradation of Potato Starch as Studied by Fourier Transform Infrared Spectroscopy. *Starch - Stärke*. <https://doi.org/10.1002/star.19940461202>
- Van Soest, J. G., Tournois, H., de Wit, D., & Vliegthart, J. F. G. (1995). Short-range structure in (partially) crystalline potato starch determined with attenuated total reflectance Fourier-transform IR spectroscopy. *Carbohydrate Research*, 279(C), 201–214. [https://doi.org/10.1016/0008-6215\(95\)00270-7](https://doi.org/10.1016/0008-6215(95)00270-7)

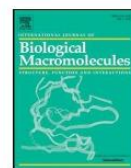
- Vermeylen, R., Goderis, B., Reynaers, H., & Delcour, J. A. (2004). Amylopectin molecular structure reflected in macromolecular organization of granular starch. *Biomacromolecules*, 5, 1775–1786
- Wang, Y., & Wang, L. (2003). Physicochemical properties of common and waxy corn starches oxidized by different levels of sodium hypochlorite, 52, 207–217.
- Warren, F. J., Gidley, M. J., & Flanagan, B. M. (2016). Infrared spectroscopy as a tool to characterise starch ordered structure — a joint FTIR – ATR , NMR , XRD and DSC study. *Carbohydrate Polymers*, 139, 35–42. <https://doi.org/10.1016/j.carbpol.2015.11.066>
- Wiacek, A. E. (2015). Effect of surface modification on starch biopolymer wettability. *Food Hydrocolloids*, 48, 228–237. <https://doi.org/10.1016/j.foodhyd.2015.02.005>
- Wiacek, A. E., & Dul, K. (2015). Effect of surface modification on starch/phospholipid wettability. *Colloids and Surfaces A: Physicochemical and Engineering Aspects*, 480, 351–359. <https://doi.org/10.1016/j.colsurfa.2015.01.085>
- Wiacek, A. E., Terpiłowski, K., Jurak, M., & Worzakowska, M. (2016a). Effect of low-temperature plasma on chitosan-coated PEEK polymer characteristics. *European Polymer Journal*, 78, 1–13. <https://doi.org/10.1016/j.eurpolymj.2016.02.024>
- Wiacek, A. E., Terpiłowski, K., Jurak, M., & Worzakowska, M. (2016b). Low-temperature air plasma modification of chitosan-coated PEEK biomaterials. *Polymer Testing*, 50, 325–334. <https://doi.org/10.1016/j.polymertesting.2016.01.020>
- Yan, Q., Hou, H., Guo, P., & Dong, H. (2012). Effects of extrusion and glycerol content on properties of oxidized and acetylated corn starch-based films. *Carbohydrate Polymers*, 87(1), 707–712. <https://doi.org/10.1016/j.carbpol.2011.08.048>
- Yuan, Y., & Randall, T.L. (2013). Contact angle and wetting properties. Chapter 1. G. Bracco, B. Holst (eds.), *Surface Science Techniques*, Springer Series in Surface Sciences.
- Zamudio-Flores, P. B., Vargas-Torres, A., Bosquez-Molina, E., & Bello-perez, L. A. (2006). Films prepared with oxidized banana starch: mechanical and barrier properties, 274–282. <https://doi.org/10.1002/star.200500474>
- Zavareze, R. E., & Dias, G. R. A. (2011). Impact of heat-moisture treatment and annealing in starches: A review, 83, 317–328. <https://doi.org/10.1016/j.carbpol.2010.08.064>
- Zavareze, R., Zanella, V., Klein, B., Lisie, S., El, M., Cardoso, M., ... Dias, G. (2012). Development of oxidised and heat – moisture treated potato starch film. *Food Chemistry*, 132(1), 344–350. <https://doi.org/10.1016/j.foodchem.2011.10.090>

- Zhang, B., Chen, L., Li, X., Li, L., & Zhang, H. (2015). Food Hydrocolloids Understanding the multi-scale structure and functional properties of starch modulated by glow-plasma: A structure-functionality relationship. *Food Hydrocolloids*, 50, 228–236. <https://doi.org/10.1016/j.foodhyd.2015.05.002>
- Zhang, Q., Yu, Z., Xie, X., Naito, K., & Kagawa, Y. (2007). Preparation and crystalline morphology of biodegradable starch / clay nanocomposites, 48, 7193–7200. <https://doi.org/10.1016/j.polymer.2007.09.051>
- Zhang, S., Zhang, Y., Wang, X., & Wang, Y. (2009). High Carbonyl Content Oxidized Starch Prepared by Hydrogen Peroxide and Its Thermoplastic. *Starch/Staerke*, 61, 646–655. <https://doi.org/10.1002/star.200900130>
- Ziari, Z., Nouicer, I., Sahli, S., Rebiai, S., Bellel, A., Segui, Y., & Raynaud, P. (2013). Chemical and electrical properties of HMDSO plasma coated polyimide. *Vacuum*, 93, 31–36. <https://doi.org/10.1016/j.vacuum.2012.12.009>
- Zia-ud- Din, Hanguo Xiong & Peng Fei (2015): Physical and chemical modification of starches - A Review, *Critical Reviews in Food Science and Nutrition*, DOI: 10.1080/10408398.2015.1087379
- Zou, J. J., Liu, C. J., & Eliasson, B. (2004). Modification of starch by glow discharge plasma. *Carbohydrate Polymers*, 55(1), 23–26. <https://doi.org/10.1016/j.carbpol.2003.06.001>



Contents lists available at ScienceDirect

International Journal of Biological Macromolecules

journal homepage: <http://www.elsevier.com/locate/ijbiomac>

Hexamethyldisiloxane cold plasma treatment and amylose content determine the structural, barrier and mechanical properties of starch-based films

Israel Sifuentes-Nieves^a, Ernesto Hernández-Hernández^b, Guadalupe Neira-Velázquez^b, Eduardo Morales-Sánchez^a, Guadalupe Mendez-Montelvo^a, Gonzalo Velazquez^{a,*}

^a Instituto Politécnico Nacional, Centro de Investigación en Ciencia Aplicada y Tecnología Avanzada, Cerro Blanco No. 141, Col. Colinas del Cimataro, C.P. 76090 Santiago de Querétaro, Querétaro, Mexico

^b Centro de Investigación en Química Aplicada, Blvd. Enrique Reyna No. 140, C.P. 25253 Saltillo, Coahuila, Mexico

ARTICLE INFO

Article history:

Received 23 September 2018

Received in revised form 17 November 2018

Accepted 23 November 2018

Available online 23 November 2018

Keywords:

Starch

Amylose

HMDSO cold plasma

ABSTRACT

In this study, the effect of amylose content and cold plasma treatment on starch films properties was investigated. Films from normal (30%) and high amylose (50 and 70%) starches were subjected to hexamethyldisiloxane (HMDSO) cold plasma treatment. Morphological, structural, mechanical and barrier properties of the films were evaluated. The amount of remnant starch granules (RSG) in the films depended on the amylose content and on the gelatinization extent of the starch. This behavior was corroborated on the films from starch with 50% amylose, where the loss of RSG resulted in poor barrier properties and high hydrophilicity. Moreover, HMDSO cold plasma treatment incorporated methyl groups improving the hydrophobic properties and favored the helix ordering of the starch components resulting in a limited water-film interaction. Furthermore, the simultaneous effect of HMDSO coating and the ordering of the structures reinforced the surface of the films, improving the mechanical properties.

© 2018 Elsevier B.V. All rights reserved.

1. Introduction

The increasing of plastic pollution has raised the interest to develop alternative materials. Thus, researchers have focused on studying biopolymers to partially or completely replacing the existing plastics. Starch has been considered as an attractive alternative due to its eco-friendly character, abundance, and low-production cost at a large scale. However, starch-based films have limited functional properties (barrier and mechanical) and different strategies such as chemical modification (crosslinking, oxidation, esterification) or the combination with macromolecules (proteins and polysaccharides), and nanoparticles (nanoclays, cellulose and carbon tubes) have been used to improve them [1–6]. Nevertheless, starch-based films still cannot mimic the functional properties of films from conventional plastics. Thus, new approaches to overcome the hydrophilicity and fragility of starch-based films are being studied. Cold plasma, a friendly process with no chemical residues, is a feasible alternative to improve or change the film properties as this treatment can modify starch by different mechanisms including crosslinking, reticulation, etching or by the inclusion of

functional groups (S, F, Si, O) [7–11]. Bastos et al. [7] studied the effect of sulfur hexafluoride (SF₆) plasma on the properties of films from normal starch. The authors reported that the plasma treatment promoted a polymerization on the film surface, as well as a starch crosslinking, which resulted in films with improved water vapor barrier properties. Later, Bastos et al. [12] evaluated the effect of two plasma sources (SF₆ and HMDSO) and their combination, on the properties of normal starch-based films. The authors found that the SF₆/HMDSO treatment allowed obtaining more hydrophobic films, probably due to the high levels of methyl and methylene groups in the HMDSO chemical structure. Moreover, De Albuquerque et al. [9] reported that HMDSO plasma treatment helps to reduce the amount of moisture adsorbed on the surface of starch-based films. Such results suggest that HMDSO coating leads to surface hydrophobization, thereby improving the water vapor barrier properties of starch-based films.

The amylose content is another important factor which determines the properties of starch-based films [13]. Films prepared from high amylose (>50%) starch are stronger, with higher values of stress to fracture and elastic modulus compared to those films obtained from normal starch [14,15]. However, the films from high amylose starch form stronger hydrogen bonds with water resulting in films with limited barrier properties [16]. Since amylose content and HMDSO plasma have shown the capability to modify the mechanical and barrier properties

Abbreviations: HMDSO, hexamethyldisiloxane; RSG, remnant starch granules.

* Corresponding author.

E-mail address: gvelazquezd@ipn.mx (G. Velazquez).



Contents lists available at ScienceDirect

International Journal of Biological Macromolecules

journal homepage: <http://www.elsevier.com/locate/ijbiomac>

Influence of gelatinization process and HMDSO plasma treatment on the chemical changes and water vapor permeability of corn starch films



Israel Sifuentes-Nieves^a, Guadalupe Neira-Velázquez^b, Ernesto Hernández-Hernández^b, Enrique Barriga-Castro^b, Carlos Gallardo-Vega^b, Gonzalo Velazquez^a, Guadalupe Mendez-Montealvo^{a,*}

^a Instituto Politécnico Nacional, Centro de Investigación en Ciencia Aplicada y Tecnología Avanzada, Cerro Blanco No. 141, Col. Colinas del Cimatario, C.P. 76090 Santiago de Querétaro, Querétaro, Mexico

^b Centro de Investigación en Química Aplicada, Blvd. Enrique Reyna No. 140, C.P. 25253 Saltillo, Coahuila, Mexico

ARTICLE INFO

Article history:

Received 22 February 2019
Received in revised form 3 May 2019
Accepted 19 May 2019
Available online 20 May 2019

Keywords:

Cold plasma
Chemical bonds
Crosslinking

ABSTRACT

In this study, surface, chemical, physicochemical and barrier properties of films treated with hexamethyldisiloxane (HMDSO) cold plasma were investigated. Normal and high amylose starches were gelatinized at different level to obtain films with different amount of free amylopectin. The obtained films were subjected to HMDSO plasma treatment. XPS analysis indicated chemical changes including substitution and crosslinking of the starch molecule, as reflected by the C—Si bond increasing and the C—OH bonds reduction on treated films. These changes modified the thermal transitions (T_m and ΔH). The highest amount of C—Si bonds was more noticeable in the TF50 film, suggesting a better interaction between active species of plasma and the free amylopectin released into the continuous phase of the film. Moreover, active species of plasma increased the crystallinity in all films. These results suggested that a higher helical packaging, crosslinking and hydrophobic blocking groups (C—Si) of starch molecules resulted in films with improved barrier performance against water molecules.

© 2019 Elsevier B.V. All rights reserved.

1. Introduction

The global consumption of synthetic plastics like polyethylene, polypropylene and polystyrene has resulted in residue accumulation. Thus, the use of alternative raw materials like polysaccharides has been investigated to develop biodegradable plastics [1–3]. Corn starch is a renewable and biodegradable polymer with good film-forming properties [4]. However, corn starch films are brittle, and plasticizers are added aiming to improve its flexibility by reducing the intermolecular bonds in the polymer matrix. Nevertheless, several authors have reported that the addition of plasticizers results in films with some disadvantages including high hydrophilicity and low performance under tensile tests [5,6]. To overcome such drawbacks, physical modifications like cold plasma have been employed to improve films surface and therefore, barrier properties [7–9]. Cold plasma includes electrons, free radicals, excited molecules and atoms, which in conjunction can modify chemical bonds on the starch structure promoting changes on the film surface. In this regard, reactive species of air, He, C₂H₂, and SF₆ plasma have shown effect in films made from starch as the plasma treatment forms hydrophobic channels on the surface reducing the hydrophilicity [10]. This effect has been more noticeable in films treated with HMDSO

plasma mainly due to the formation of a hydrophobic HMDSO coating on the surface [11,12]. In this regard, in a previous work we reported that the HMDSO coating not only resulted in hydrophobic properties of the films but also improved the mechanical properties [13].

The effect of plasma treatment on the chemical structure of starch films has been investigated elsewhere [14]. Pankaj et al. [15] studied the effect of air plasma on films made from starch with different amylose content. The authors found, by XPS analysis, a higher surface oxygenation after treatment, which derived an increasing of the C—O—H bonds specially in the low-amylose starch films. Bastos et al. [14] investigated the chemical changes promoted by HMDSO plasma treatment on films made from normal corn starch. The authors reported a higher atomic concentration of Si (%) after treatment, which changed the barrier performance of the films.

Recently, our group developed starch-based films, which were subjected to HMDSO plasma treatment. The structural order like short-range crystallinity (crystalline/amorphous ratio), barrier and mechanical properties were studied. However, the elucidation of the main mechanisms of plasma on starch molecules is important to understand the effects of HMDSO plasma treatment on the chemical structure and on the physicochemical properties of starch-based films. Thus, the objective of this study was to determine the effect of HMDSO plasma on the topography, chemical, physicochemical and barrier properties of films from corn starch with low and high amylose content and to inspect the effects due to the gelatinization extent.

Abbreviations: HMDSO, hexamethyldisiloxane; RAM, remnant of amylopectin.

* Corresponding author.

E-mail address: cmendez@ipn.mx (G. Mendez-Montealvo).



HMDSO plasma treatment as alternative to modify structural properties of granular starch

Israel Sifuentes-Nieves^{a,*}, Gonzalo Velazquez^a, Pamela C. Flores-Silva^a, Ernesto Hernández-Hernández^b, Guadalupe Neira-Velázquez^b, Carlos Gallardo-Vega^b, Guadalupe Mendez-Montealvo^{a,*}

^a Instituto Politécnico Nacional, Centro de Investigación en Ciencia Aplicada y Tecnología Avanzada, Cerro Blanco No. 141, Col. Colinas del Cimatario, C.P. 76090, Santiago de Querétaro, Querétaro, Mexico

^b Centro de Investigación en Química Aplicada, Blvd. Enrique Reyna No. 140, C.P. 25253, Saltillo, Coahuila, Mexico

ARTICLE INFO

Article history:

Received 20 August 2019

Received in revised form 28 November 2019

Accepted 14 December 2019

Available online xxx

Keywords

Corn starch
Cold plasma
Crosslinking

ABSTRACT

In the present study, the effect of plasma treatment on the structural properties of three granular corn starches (normal, Hylon V and Hylon VII) was investigated. Thermal (TGA/DSC), structural (XRD/FTIR) and chemical (XPS) properties were evaluated. Plasma treatment resulted in partial evaporation of water molecules changing the organization level of the double helices in the crystalline lamellae. Moreover, XRD results suggested a decrease of the long-range crystallinity and suggested changes in amylose chains after treatments. The crosslinking of modified amylose chains measured by XPS analysis resulted in variations in the gelatinization parameters as well as in its heterogeneous crystalline structure. The results indicate that the type and extent of changes in the structure of plasma-treated corn starch depends on the distribution of the water molecules inside the crystalline regions (helical water) and on the amylose content. In addition, the obtained results indicated that plasma treatment is a suitable method to modify starch without any incorporation of new elements from hexamethyldisiloxane (HMDSO), which only promotes stronger interactions between the starch main components.

© 2018

1. Introduction

Starch is one of the most studied biopolymers since it is considered as the major source of energy in the human diet. Over the last century, numerous studies have focused on understanding it and much has been written concerning to the starch structure changes after chemical or physical modifications [1–5]. Starch modifications intended to enhance the functional properties that are relevant to industrial applications usually lead to structural changes affecting its supramolecular structure [6]. In this regard, differences in amylose content, amylopectin fine structure and the way they are organized within granules, give rise to variability in structure and functionality of starch [7,8].

Nowadays, there are four types of starch modifications (chemical, physical, enzymatic and genetic), which change the functionality of the modified starch; among them, chemical modification is the most used [9]. However, this procedure generates chemical residues during the starch treatment causing environmental concern. Alternative methods like physical modification of starch are attracting attention since they do not generate residuals during the treatment [10,11]. Cold plasma treatment has been used as a physical method to modify starch although, the alteration mechanisms are still under study [12]. Zou, Liu, and Eliasson [13] suggested that the active species of argon plasma could collapse the hydroxyl groups of the amylose and amylopectin chains promot-

ing crosslinking. Moreover, Wongsagonsup et al. [14] reported two competitive reactions (crosslinking and depolymerization) during argon plasma treatment on starch, where the predominant effect was determined by the sample preparation and the input power for the plasma treatment.

The supramolecular changes on the starch after plasma treatment have been also studied. Bie et al. [15] discovered that the oxygen and helium plasma treatment disorganized the starch crystallites with low perfection and thermal stability, decreasing the double helices alignment within the crystalline lamellae. However, so far there is not a clear understanding of the structural changes taking place due to the physical plasma treatment. Moreover, to our knowledge, the changes in structure and functionality of plasma-treated granules as a function of amylose and amylopectin content and their organization within granules have not been elucidated.

Therefore, the aim of this work was to evaluate the effect of the low-pressure HMDSO plasma on the structure of corn starches with different amylose content. The effect of plasma treatment and changes in the structure were assessed using TGA, XRD, FTIR, XPS and DSC techniques.

2. Materials and methods

2.1. Materials

Corn starch with 30% (normal — S30), 50% (Hylon V — S50) and 70% (Hylon VII — S70) amylose content were acquired from Ingredion (formerly, Corn Products and National Starch at Bridgewater, NJ). HMDSO (205389) was purchased from Sigma-Aldrich (Saint Louis, MO, USA).

Abbreviation: HMDSO, hexamethyldisiloxane.

* Corresponding authors.

E-mail addresses: sifuentes_01@hotmail.com (I. Sifuentes-Nieves); cmendez@ipn.mx (G. Mendez-Montealvo)